

# **Blood Glucose Level Prediction: A Graph-based Explainable Method with Federated Learning**

*Chengzhe Piao, Ken Li*

A dissertation submitted in partial fulfillment  
of the requirements for the degree of  
**Master of Research**  
of  
**University College London.**

Institute of Health Informatics  
University College London

December 21, 2023

---

I, Chengzhe Piao, Ken Li, confirm that the work presented in this thesis is my own. Where information has been derived from other sources, I confirm that this has been indicated in the work.

# Abstract

Around 400 thousand people in the UK have type 1 diabetes (T1D). They cannot maintain their normal blood glucose (BG) levels without the help of insulin delivery because their pancreas cannot produce enough insulin. Some appropriate precautions, e.g., insulin delivery and carbohydrate intake, can help them avoid complications caused by unstable BG levels. Blood glucose level prediction (BGLP) based on the BG time series collected by continuous glucose monitoring (CGM) enables them to take suitable precautions, where CGM tracks the BG levels every 5 minutes.

Numerous researchers focus on modeling complex and dynamic temporal features by proposing novel sequential models based on historical BG time series, and they also consider extra attributes, e.g., carbohydrate intake, insulin delivery, and time, as the input. These methods achieved excellent performance in BGLP; some are explainable from a temporal perspective. However, they cannot provide clinicians with clear correlations among the considered attributes, presenting how much importance each attribute has in BGLP. Besides, some of these methods try to learn population patterns by merging the training data of all participants, which is an invasion of privacy.

Based on the limitations, we proposed a graph attentive memory (GAM), consisting of a graph attention network (GAT) and a gated recurrent unit (GRU). GAT utilizes graph attention to model the correlations of multiple attributes, and the dynamic graph structure can present transparent relationships among these attributes. The attention weights can be used to dynamically measure the importance of the attributes at different time slots. Moreover, federated learning (FL) is introduced to learn population patterns safely, protecting participants' privacy.

Our proposed method is evaluated by OhioT1DM'18 [Marling and Bunescu, 2018] and OhioT1DM'20 [Marling and Bunescu, 2020], containing 12 participants in total, where the data includes multiple attributes. We designed experiments to select 6 valuable attributes, and we proved the stability of our model by exploring the impact of hyperparameters. Finally, our model got the root mean squared error (RMSE) as 18.753 mg/dL or 31.275 mg/dL when the prediction horizon (PH) is 30 or 60 minutes, and it got the mean absolute relative difference (MARD) as 8.893% or 15.903% when PH is 30 or 60 minutes. Compared with the methods of the BGLP 2020 Challenge, our model achieved third place when training without FL. We also use two examples to visualize our GAM, presenting the dynamic correlations among the active attributes in different time slots.

**Keywords:** *type 1 diabetes; blood glucose level prediction; graph attention network; gated recurrent unit; federated learning*

# Contents

<b>1</b>	<b>Introduction</b>	<b>7</b>
1.1	Background . . . . .	7
1.2	Related work . . . . .	8
1.2.1	Methods for Blood Glucose Level Prediction (BGLP) . . . . .	8
1.2.2	Multi-Variate Time Series and Graph Neural Networks . . . . .	10
1.2.3	Training and Deployment of the BGLP Methods . . . . .	13
1.2.4	Federated Learning (FL) . . . . .	14
1.3	Objectives . . . . .	15
1.4	Contributions . . . . .	15
<b>2</b>	<b>Method</b>	<b>17</b>
2.1	Problem Definition . . . . .	17
2.2	Setting and Dataset . . . . .	18
2.3	Ethics . . . . .	18
2.4	Data Preprocessing . . . . .	19
2.5	Data Analysis . . . . .	23
2.5.1	Impact of “meal” and “bolus” . . . . .	23
2.5.2	Impact of Temporal Features . . . . .	26
2.6	Proposed method . . . . .	27
2.6.1	Overview . . . . .	27
2.6.2	Graph Attention Networks (GATs) . . . . .	30
2.6.3	Gated Recurrent Units (GRU) based Memory . . . . .	32
2.6.4	Training without FL . . . . .	33

---

2.6.5	Training with FL . . . . .	34
2.6.6	Metrics . . . . .	35
<b>3</b>	<b>Results</b>	<b>39</b>
3.1	Impact of Attributes . . . . .	39
3.1.1	Experiment Settings . . . . .	39
3.1.2	Result Analysis . . . . .	40
3.2	Impact of Hyperparameters . . . . .	44
3.2.1	Experiment Settings . . . . .	47
3.2.2	Result Analysis . . . . .	47
3.3	Impact of FL . . . . .	50
3.3.1	Experiment Settings . . . . .	50
3.3.2	Result Analysis . . . . .	52
3.4	Impact of Time-Aware Attention . . . . .	53
3.4.1	Experiment Settings . . . . .	53
3.4.2	Result Analysis . . . . .	55
3.5	Answers to the Research Questions . . . . .	57
<b>4</b>	<b>Discussion</b>	<b>59</b>
4.1	Compare with Other Methods . . . . .	59
4.2	Discussion of selected attributes . . . . .	63
4.3	Visualization . . . . .	65
4.4	Convergence and Training Time . . . . .	69
4.5	Conclusion and Future Work . . . . .	71

# Chapter 1

## Introduction

### 1.1 Background

T1D<sup>1</sup>, whose ICD-10 is E10, happens when the pancreas cannot produce enough insulin, leading to high BG levels ( $> 180$  mg/dL, hyperglycemia). People with T1D need insulin to maintain their everyday life by insulin pumps and bolus stabilizing their BG levels in a normal range (70-180 mg/dL). Otherwise, they are highly likely to get hypoglycemia ( $< 70$  mg/dL) or hyperglycemia ( $> 180$  mg/dL), contributing to some serious complications<sup>2</sup>, e.g., kidney problems, sight problems, blindness, and so forth. However, there are many precautions to avoid these complications, and one effective prevention is to monitor and manage BG levels actively.

Currently, people with T1D often use CGM to monitor their BG levels, where CGM can track the variations of BG levels per 5 minutes. Based on the nearly continuous BG time series, a lot of researchers successfully proposed all kinds of methods to do the BGLP for people with T1D. Even though these approaches achieve excellent performance, they still have some non-ignorable limitations (see section 1.2). This paper is aiming at solving these problems by proposing novel methods and algorithms (see section 1.3), where the proposed methods are evaluated in OhioT1DM'18 [Marling and Bunescu, 2018] and OhioT1DM'20 [Marling and Bunescu, 2020], and the contributions are briefly mentioned in sec-

---

<sup>1</sup><https://www.nhs.uk/conditions/type-1-diabetes/>

<sup>2</sup><https://www.nhs.uk/conditions/type-1-diabetes/living-with-type-1-diabetes/avoiding-complications/>

tion 1.4.

## 1.2 Related work

### 1.2.1 Methods for Blood Glucose Level Prediction (BGLP)

In BGLP, the historical data can be organized as multivariate time series (MTS) when considering multiple attributes. Since 2020, methods based on neural networks (NNs) have achieved outstanding performance, exceeding non-NN approaches, especially in the BGLP 2020 Challenge [Bach et al., 2020].

Rubin-Falcone et al. [2020] introduced N-BEATS [Oreshkin et al., 2020] to model MTS, where N-BEATS is the state-of-the-art method dealing with time series around 2020, and the proposed method based on N-BEATS achieved first place in the BGLP 2020 Challenge. N-BEATS utilizes residual structure and forecast and backcast mechanisms to make the sequential model very deep, modeling complex temporal dependencies. Besides, it has trend stacks and seasonal stacks, making the whole structure temporally explainable to some degree. However, it is far from enough because this approach cannot explain the importance of attributes, i.e., feature importance, during the prediction. For example, Rubin-Falcone *et al.* considered glucose levels, bolus, finger sticks, etc., as the input of their NNs. However, they cannot explain each attribute's importance during the prediction. Nevertheless, many clinicians care more about how a model makes predictions rather than only getting an estimation from a black box.

Similarly, recent approaches in BGLP primarily focus on modeling temporal dependencies based on RNN-like structures, e.g., long short-term memory (LSTM, Yang et al. [2020]), BiLSTM [Schuster and Paliwal, 1997] and gated recurrent unit (GRU, Cho et al. [2014]) rather than explicitly modeling the correlations of attributes in an explainable way. Hence, we first discuss how these works focus on modeling temporal features. Iacono et al. [2022] utilized the original LSTM to model the historical CGM data. There are fewer innovations in the methods in their work. Comparably, some researchers try to introduce other algorithms to make the recurrent model more powerful in learning complex temporal correla-



tions. Bhimireddy et al. [2020] proposed a BiLSTM-based model trained with a sequence-to-sequence framework [Sutskever et al., 2014], because they believe this framework can predict continuous future time series of CGM data, enabling users to have a complete changing curve of the future BG levels. Nemat et al. [2022] proposed an ensemble deep learning model, where it uses some deep sequential models, e.g., LSTM, BiLSTM, etc., as weak learners, and the output of the weak learner is collected by a meta-learner which generates final estimations by fusing the collected predictions.

The above methods achieved satisfying performance in BGLP, but they are not explainable. Meanwhile, many researchers focus on revising the recurrent structure by adding attention mechanisms to make the model explainable from a temporal view. Bevan and Coenen [2020] proposed a model based on temporal attention and LSTM, only using the historical BG levels collected by CGM as the input. It achieved good performance in OhioT1DM. Zhu et al. [2022a,b] proposed an attention-based sequential model which leverages GRU layers to model MTS, including historical BG levels, meal intake, insulin delivery, etc., followed by temporal attention to integrate the output of GRU layers. Instead of using recurrent structure, Cui et al. [2021] introduced self-attention [Vaswani et al., 2017] to model temporal dependencies and achieved excellent performance in OhioT1DM. One of the advantages of using self-attention is that the temporal dependencies are explainable. However, the computation resources are higher than RNN-based structures, which need more time to converge during the training process.

Nevertheless, even though the above methods contribute to modeling temporal dependencies, they ignore explicitly modeling correlations of various attributes. Some researchers tend to add special modules to extract features from different attributes. Yang et al. [2020] proposed a multi-scale and multi-lag LSTM to model different attributes explicitly. The multi-scale LSTM models the CGM data with different sampling granularity, and each attribute has a special LSTM to model its temporal variations. Li et al. [2020] proposed a convolution recurrent neural network (CRNN), where CNN layers are used to extract features from MTS, and a

modified LSTM is utilized to model temporal correlations, where the LSTM is revised in a residual way, adding the input to the hidden state. Zhu et al. [2020b] proposed a particular generative adversarial network (GAN), using a gated recurrent unit (GRU, Cho et al. [2014]) as a generator and convolution neural networks (CNN) as a discriminator, where the generator generates the future estimations of BG levels. The discriminator distinguishes the actual data from the predicted data, and the whole structure is trained in an adversarial algorithm [Goodfellow et al., 2014], making it possible to utilize complex features from different attributes.

Then, also as for the feature extraction, Yang et al. [2022b] proposed a channel deep learning framework based on LSTM. They hold the view that different attributes have various time dependencies. For example, BG levels change for several hours after a meal, while BG levels might be affected for the whole day after receiving some long-term insulin. Hence, they leverage special channel-wise gates to control the feature extraction from different attributes, where only conducive features are leveraged. They use LSTM to model temporal dependencies of the MTS. Rabby et al. [2021] proposed a stacked LSTM aided by a Kalman smoothing approach leveraged to deal with the inaccuracy of CGM data. They believe the stacked LSTM can further improve prediction accuracy. Furthermore, CGM data is processed by a Kalman smoother filter and other attributes, i.e., meal, insulin, and so forth, are processed by a feature extraction module. The output of these two modules is fused and acts as the input of the stacked LSTM.

Even if the above methods can model complex temporal dependencies and can also model correlations of attributes, the correlations are not explainable. The NNs can achieve excellent performance in BGLP, but they are still black boxes.

### 1.2.2 Multi-Variate Time Series and Graph Neural Networks

Recently, there have been some general models for MTS, but they have not been used in BGLP. Schirmer et al. [2022] proposed a continuous recurrent unit (CRU), given that the observation times of samples are irregular in MTS in some scenarios. The model is able to deal directly with MTS via a continuous-discrete Kalman filter. The model interpolates MTS according to neural ordinary differential equations,

achieving better performance than other methods. Given that different time series in MTS have various temporal granularity, Hou et al. [2022] proposed a multi-granularity residual learning framework (MRLF), where the multi-granularity can extract features from different temporal perspectives, and residual learning framework make the NNs deeper. Hence, this structure can extract more complex temporal features.

Similar to the methods in the previous subsection, even though these two methods can extract complex temporal features from MTS, they do not model the correlations among the attributes in MTS. Some researchers leverage graph neural networks (GNNs) or graph convolutional networks (GCNs) to model the relationships among the attributes in MTS because graph-based methods can clearly describe the relationships. In order to explicitly and flexibly model the correlations among the attributes in MTS in an explainable manner, we need graph-based methods.

Recently, GNNs are very popular in all kinds of applications, and GNNs are the combination of graph and neural networks. In MTS, specific attributes may collect valid samples at each time slot. After embedding these samples separately, the generated tensors can be treated as graph node tensors, where each tensor relates to a node in a graph. Then, we assume that each active node connects to all nodes, including itself, and we want to introduce a GNN method to model the correlations of the graph node tensors dynamically. This is because graphs can clearly represent the correlations among these attributes.

A classic GNN is proposed by Kipf and Welling [2017], where the concept of GCN is similar to CNN. GCN is the convolution for graph node tensors, and the convolution is along the edges, where the weights of the edges coming to a node can be seen as a filter. After a GCN layer, each node tensor will be replaced by the weighted summation of all the adjacent node tensors. This process can be seen as the neural message passing and aggregation, and the adjacent node tensors are neural messages in GCN. In this case, nodes' messages are merged based on the graph's structure, i.e., edges and weights of the edges. The size of a weight of a coming edge decides how crucial the adjacent node tensor is. The higher the

weight, the more critical the adjacent node tensor. Hence, the size of the weights can be used to calculate the ranking of attribute importance. Then, simplifying graph convolutional networks (SGC) is proposed by Wu et al. [2019]. SGC is a simplified version of GCN so as to reduce complexity and computation by removing unnecessary activation functions. Besides, as for modeling complicated graph relationships, Morris et al. [2019] proposed a k-dimensional GNN (k-GNN) containing higher-order graph structures at various scales.

However, these GNNs are based on static graphs, where the structure, including the edges and the weights of the edges, are unchangeable. Such graphs are not suitable in our scenario, as they cause unnecessary computations when most attributes do not have valid samples at specific time slots.

In terms of GNNs based on dynamic graphs, where the weights of the edges are learnable, Velickovic et al. [2018] proposed graph attention networks (GAT), where each weight of an edge is based on the node tensors that are adjacent, and the weights are learnable. Then, Brody et al. [2022] proposed a GATv2 which is more expressive using a more dynamic attention mechanism.

In this paper, our proposed model is based on GAT. This is because we can build dynamic graphs for active nodes at each time slot with the help of changing and learnable weights of edges. Note that we do not use GATv2, because we did not get more benefits when using it.

On the other hand, many researchers also proposed GNN-based sequential models. Chen et al. [2022] proposed a variational graph convolutional recurrent network (VGCRN) for MTS, consisting of GCNs and LSTM. Then, VGCRN is extended to a deep variational network, and it is more potent in modeling complex correlations of the attributes in MTS, especially when facing noisy MTS. However, GCNs is based on static graphs, which is unsuitable for this paper, as in specific time slots, only part of the nodes in the graph are activated (the values of attributes are not none). Using static graphs in this scenario is a waste of computation resources.

When modeling complex correlations among the attributes in MTS, multi-graph-based NNs are also considered. Shao et al. [2022] proposed a multi-graph

neural network (MGNN) so as to extract complex graph features from long-term MTS. They built multiple graph models to respectively learn the contextual correlations of the attributes in MTS, followed by a dynamic multi-graph fusion module to aggregate the extracted features. The actual number of conducive attributes in this scenario is limited, and there are not very complicated correlations among the attributes. This view has also been confirmed in our experiments, so we do not need such complex multi-graph-based structures.

Zhang et al. [2022] proposed a graph-based sequential NN, consisting of dynamic GNN layers and self-attention layers, where the structure and the weights of the graph are learnable, and the self-attention models the temporal dependencies. This is a precisely perfect model that we really need, as the graph is explainable, and the weights of edges in the graphs are also changeable, and the temporal correlations are also explainable by self-attention. However, the official code<sup>3</sup>, where the link of the code is also given in their paper, is not consistent with the methods proposed in their paper. There is a super massive gap between their imagined model and their actually implemented model. Furthermore, we carefully debug their published code and test the actual performance, confirming that their imagination is totally different from their implementation.

Therefore, the latest methods for MTS in top conferences cannot satisfy our expectations, i.e., dynamically building explainable correlations for the attributes. This is why we propose novel methods instead of introducing popular MTS models.

### 1.2.3 Training and Deployment of the BGLP Methods

In terms of the training and deployment of these NNs, Daniels et al. [2020, 2022] introduced multi-task learning to train personalized models, where it does not need to mix the personalized data to pretrain a population model, followed by fine-tuning in personalized data separately. This is because multi-task learning enables concurrently leveraging population patterns and keeping personal specialties, generating multiple personalized models at a time without too much fine-tuning. Zhu et al. [2021] applied a well-trained LSTM-based model in a microcontroller unit to pre-

---

<sup>3</sup>[https://github.com/mims-harvard/Raindrop/blob/main/code/Ob\\_propagation.py](https://github.com/mims-harvard/Raindrop/blob/main/code/Ob_propagation.py)

dict future BG levels for people with T1D. Then, Zhu et al. [2022a] successfully utilized an Internet of Medical Things (IoMT) enabled wearable device to implement a temporal attention-based GRU model, where the device contains a low-cost chip to run the trained model, and desktops and cloud platform are leveraged to backup data and fine-tuning models. D’Antoni et al. [2022] also successfully leveraged the API tools of TensorFlow and Keras to implement their well-trained LSTM-based model on edge, sacrificing some prediction accuracy, which is tolerable.

However, the above methods neglect to protect the participants’ privacy when mixing all the data to learn population patterns, which restricts the number of participants, and the amount of available training data is also limited.

#### 1.2.4 Federated Learning (FL)

Nowadays, most people have smartphones, and they regard these smart devices as an indispensable part of their lives. With the rapidly developing of technology, smart devices have more and more powerful computing hardware, supporting more sophisticated computations.

Then, FL appears, and the target of FL is to fully leverage the computing resources of these intelligent devices to do the training tasks of artificial intelligence, using the data generated by the smart devices, and keeping the data safely in the place where the data is generated. Meanwhile, the learnable parameters from personal devices are sent to a central server periodically, and a population model is generated by averaging the learnable parameters from these personal devices. When the population model is updated, smart devices update the local learnable parameters by copying the learnable parameters of the population model in the server. This is the classic FedAvg algorithm proposed by McMahan et al. [2017].

Recently, FL has been developing towards being decentralized, personalized and asynchronous. Jiang and Hu [2020] proposed a decentralized FL, fully leveraging node-to-node bandwidth and removing the center server. T Dinh et al. [2020] proposed a personalized FL called “pFedMe”. It utilizes Moreau envelopes as regularized loss in smart devices, decoupling the local models of smart devices from the population model in the server. Shamsian et al. [2021] proposed a personalized

federated hypernetworks, called “pFedHN”. These hypernetworks make the learnable parameters be shared effectively across smart devices. Marfoq et al. [2022] also proposed a personalized FL based on local memorization, fully utilizing local images and text to generate compact representation tensors. Yang et al. [2022a] proposed an anarchic federated learning (AFL). It enables the smart devices flexibly join or leave the training, and the smart devices asynchronously communicate with the server.

However, in this work, we only use the classic FL, i.e., FedAvg, and the advanced FL will be considered in our future work.

### 1.3 Objectives

Based on the limitations of the recent work in sections 1.2.1-1.2.2, we have the following targets in this paper.

Recent Models generally focus on modeling complex temporal dependencies and extracting features from different attributes, e.g., BG time series collected by CGM, carbohydrate and insulin intake. Some of these methods explain temporal dependencies by leveraging temporal attention or self-attention mechanisms. However, they do not explain how important each attribute is in BGLP. Hence, we aim to leverage the GAT (see section 1.2.2) to propose a novel sequential model in order to dynamically present clear explanations for the correlations and the importance of these attributes.

Furthermore, recent work does not consider privacy protection when training population models. Given that FL can well protect the participants’ privacy when learning population patterns, we try to introduce FL (see section 1.2.4) to train the proposed model, in order to figure out whether FL can be leveraged in BGLP.

### 1.4 Contributions

First of all, we proposed a graph attentive memory, called “GAM”, based on GAT and GRU. The model is an explainable sequential NN for dealing with MTS, clearly presenting the correlations of the attributes by graph attention. In GAM, the graph structure, i.e., edges and weights of the edges, is dynamically changing based on

which attributes are activated (the collected values are not none), where each attribute is a node of the graph, and the node can generate and send neural messages to the adjacent nodes. The graph features extracted by GAT are aggregated by GRU sequentially, generating a compact tensor for predicting BG levels. Besides, we introduced FL to train our proposed model (see chapter 2).

Secondly, we designed four experiments in OhioT1DM'18 and OhioT1DM'20. The first experiment proved the conducive attributes are “glucose\_level”, “meal”, “bolus”, “finger\_stick”, “sleep” and “exercise”. The second experiment showed the impact of different hyperparameters of our proposed model, presenting the stability in different settings. The third experiment showed the influence of FL, confirming that FL decreased some prediction accuracy when being used with our model. The final experiment proved that our model cannot be used with a time-aware attention because it cannot further improve the performance (see chapter 3).

Finally, we compared our proposed model (training without FL) with the top 8 methods in BGLP 2020 Challenge, showing a satisfying performance of our model. Our model got the root mean squared error (RMSE) as 18.753 mg/dL or 31.275 mg/dL when the prediction horizon (PH) is 30 or 60 minutes, and it got the mean absolute relative difference (MARD) as 8.893% or 15.903% when PH is 30 or 60 minutes. We visualized our proposed model in order to present the explainable graph-based correlations of attributes in BGLP (see chapter 4).



## Chapter 2

# Method

In this chapter, the problem is defined in section 2.1, and the setting and description of the dataset are in section 2.2. Then, ethical concerns are mentioned in section 2.3. Next, data preprocessing and data analysis are respectively in sections 2.4 and 2.5. Finally, the proposed model is depicted in section 2.6 in great detail, starting with an overview and followed by details of each module.

### 2.1 Problem Definition

**Blood glucose level prediction based on regular multivariate time series (BGLP-RMTS):** given  $N$  attributes from historical  $T$  time slots, denoted as  $\mathbf{X} = [\mathbf{x}_1 \dots \mathbf{x}_t \dots \mathbf{x}_T] \in \mathbb{R}^{N \times T}$ , where  $\mathbf{x}_t \in \mathbb{R}^N$  contains  $N$  attributes, predict the BG level  $y_{T+W}$  in 30 minutes ( $W = 6$ ) or in 60 minutes ( $W = 12$ ). As for  $\mathcal{T} \triangleq \{1, \dots, t, \dots, T\}$ , the adjacent pair equals 5 minutes, which is the same as the sampling frequency of CGM since the BG levels are recorded every 5 minutes by CGM.

Usually, the attributes are historical BG levels, carbohydrate intake, insulin delivery, etc., and these attributes are self-reported or collected by all kinds of sensors. Initially, these attributes are organized as irregular multivariate time series (IMTS). Specifically, the values of each attribute may be collected or reported with various frequencies, and even the adjacent values of the same attributes may have different time intervals. Besides, the values may be missing for many reasons, e.g., forgetting to report carbohydrate intake after a meal. Therefore, IMTS is padded with zero in this work. This is because the current sequential neural network, such as LSTM,

**Table 2.1:** Basic information of the OhioT1DM’18 and OhioT1DM’20.

Patient ID (PID)	BGLP challenge	Gender	Age	#Training_examples	#Test_examples
559	2018	female	40–60	10796	2514
563	2018	male	40–60	12124	2570
570	2018	male	40–60	10982	2745
575	2018	female	40–60	11866	2590
588	2018	female	40–60	12640	2791
591	2018	female	40–60	10847	2760
540	2020	male	20–40	11947	2884
544	2020	male	40–60	10623	2704
552	2020	male	20–40	9080	2352
567	2020	female	20–40	10858	2377
584	2020	male	40–60	12150	2653
596	2020	male	60–80	10877	2731

multi-head attention, etc., are good at dealing with RMTS rather than IMTS.

## 2.2 Setting and Dataset

OhioT1DM’18 [Marling and Bunescu, 2018] and OhioT1DM’20 [Marling and Bunescu, 2020] are the two datasets considered in this work. They consist of 12 participants (6 of each), and all these 12 participants have T1D. The statistics of these two datasets can be seen in Table 2.1. We have the following observations.

- There are 5 female and 7 male participants, meaning that the data is nearly balanced in gender.
- Most participants are middle-aged, as 8 participants belong to 40-60 in terms of age.
- For most participants, the proportion between the number of training and testing examples is around 5:1.

## 2.3 Ethics

According to Marling and Bunescu [2020], there are more than 50 anonymous contributors, and they provide their daily events and data. These people signed consent documents, enabling these data to be available to researchers for only research usage after de-identification. Hence, the data were totally de-identified based on

the Safe Harbor method. On the other hand, researchers must sign a data use agreement (DUA) before they get access to the data. Hence, OhioT1DM'18 and OhioT1DM'20 are public as long as signing the DUA, so there are no ethical problems with the datasets, and ethical approval is not needed.

## 2.4 Data Preprocessing

The data is preprocessed based on the following steps.

- **Loading data.** The original data is saved individually in “PID-ws-training.xml” and “PID-ws-testing.xml” files, e.g., “540-ws-training.xml” and “540-ws-testing.xml files”. Then, the data is extracted from these .xml files and separately saved by the pandas data frame.
- **Removing attributes.** “stressors”, “illness” and “hypo\_event” are removed from all attributes, as they are incredibly sparse. For example, in terms of “illness”, each person only has around 1 samples, so it is removed because the quantity is far from enough.
- **Reorganising attributes.** Some attributes that can last for specific periods are discretized. For example, if “sleep” happens over the period between `ts_begin` and `ts_end`, it is re-sampled every 5 minutes for discretization. The attributes generating values multiple times within 5 minutes are averaged by 5 minutes, e.g., “basis\_heart\_rate”. More details of processing these attributes will be explained later in this section, and the statistics of these attributes can be seen in Tables 2.2 and 2.3.
- **Splitting, normalizing and padding.** The training data extracted from “PID-ws-training.xml” files are split into training data (80%) and validation data (20%) for early stopping and avoiding overfitting. Testing data from “PID-ws-testing.xml” are all leverage to evaluation of the well trained methods. All training data, validation data and testing data are normalized with the mean and standard derivation of the attributes in the training data through standard

**Table 2.2:** Statistics of self-reported attributes in OhioT1DM'18 and OhioT1DM'20.

PID	finger_stick (mg/dL)	meal (g)	bolus (U)	sleep	work	exercise
559	185.70±100.95	35.93±15.99	3.66±1.83	2.25±0.56	4.48±0.79	5.17±0.99
563	165.39±64.00	29.90±16.31	7.96±4.10	2.60±0.49	3.11±0.56	4.52±1.23
570	199.21±68.74	105.25±42.16	7.58±3.75	2.13±0.51	1.85±0.55	5.02±0.74
575	157.99±82.20	40.57±22.96	4.83±2.56	2.71±0.53	4.27±0.99	5.53±1.05
588	153.66±54.96	32.52±31.00	4.27±2.31	2.78±0.41	4.82±0.53	5.22±0.46
591	163.10±68.40	31.43±14.01	3.16±1.76	2.71±0.49	None	4.96±1.48
540	155.22±72.45	55.50±29.03	3.93±2.47	None	None	None
544	140.70±56.89	70.94±36.87	12.19±5.21	1.94±0.45	3.43±0.85	None
552	152.42±60.72	54.00±32.15	3.82±3.22	2.64±0.65	2.03±0.67	7.52±1.02
567	185.79±65.34	75.44±20.40	11.93±5.66	2.01±0.77	None	None
584	205.34±63.76	54.79±12.38	7.19±3.08	2.97±0.18	5.05±0.22	10.00±0.00
596	140.58±42.15	25.15±13.29	3.01±1.44	2.82±0.46	None	5.04±1.08

normalization, Then, all attributes are collected as RMTS by padding with zeros, where time interval between the adjacent tensors in RMTS is 5 minutes.

- **Generating training samples.** For the participant  $p \in \mathcal{P}$ , training samples extracted from training data are organized as  $(\mathbf{X}^p, y_{T+W}^p) \in \mathcal{D}_{Training}^p, \forall p$  which is obtained by a sliding window ( $W = 6$  or  $W = 12$ ), where  $\mathcal{P} \triangleq \{1, \dots, p, \dots, P\}$  is the participants. Note that  $y_{T+W}^p$  is not the padding value, i.e., zero.
- **Generating validation and testing samples.** Similarly, for the participant  $p \in \mathcal{P}$ , validation samples  $\mathcal{D}_{Validation}^p$  and testing samples  $\mathcal{D}_{Testing}^p$  are respectively extracted from the validation data and testing data. The general process is also similar to generating training samples. In order to ensure the number of testing samples is the same as the one in Table 2.1, when generating testing samples, several data from the last validation data are leveraged.

Note that neither interpolation nor extrapolation is introduced in the data processing, considering both Rubin-Falcone et al. [2020] and Bevan and Coenen [2020] find that using zero padding can lead to more stable methods and more accurate predictions. This is because padding IMTS with zeros after standard normalization is equivalent to padding IMTS with the mean value.

The brief introduction of selected attributes and the preprocessing details are as follows.

- **glucose\_level:** the BG levels (mg/dL) are collected by CGM per 5 minutes.

**Table 2.3:** Statistics of attributes collected by sensors in OhioT1DM'18 and OhioT1DM'20.

PID	glucose_level (mg/dL)	basal (U/h)	basis_gsr ( $\mu$ S)	basis_skin_temperature ( $^{\circ}$ F)	acceleration ( $m/s^2$ )	basis_sleep	basis_air_temperature ( $^{\circ}$ F)	basis_steps	basis_heart_rate (BPM)
559	167.23±69.91	0.96±0.32	0.40±2.04	87.65±3.43	None	1.00±0.00	84.27±4.37	3.65±15.05	73.99±16.04
563	149.80±49.75	0.83±0.24	0.41±1.68	87.94±2.71	None	1.00±0.00	84.02±3.60	4.85±11.33	96.45±13.89
570	192.95±64.10	0.93±0.19	0.55±2.61	86.42±3.66	None	1.00±0.00	82.52±4.13	2.73±8.30	83.49±11.88
575	143.34±60.40	0.74±0.12	0.29±1.53	87.31±3.10	None	1.00±0.00	83.76±3.87	2.81±7.07	81.12±11.51
588	166.82±50.33	1.20±0.20	0.06±0.79	90.18±4.08	None	1.00±0.00	87.76±5.33	2.23±10.74	76.89±14.28
591	153.75±56.94	0.96±0.17	2.27±5.07	87.86±2.99	None	1.00±0.00	84.97±3.78	3.15±10.15	66.86±11.69
540	141.35±58.21	0.48±0.33	1.16±5.22	86.95±4.17	1.02±0.07	1.00±0.00	None	None	None
544	163.44±58.87	1.46±0.25	1.70±4.58	87.91±3.10	1.73±3.18	1.00±0.00	None	None	None
552	145.47±54.23	1.22±0.24	0.29±0.90	84.15±3.21	1.03±0.08	1.00±0.00	None	None	None
567	152.46±59.97	1.07±0.28	1.14±3.23	89.61±3.40	1.00±0.06	1.00±0.00	None	None	None
584	188.50±65.19	1.66±0.22	4.03±8.56	84.66±3.09	0.97±0.06	1.00±0.00	None	None	None
596	147.33±49.52	0.47±0.07	0.25±1.44	87.12±2.73	1.04±0.03	1.00±0.00	None	None	None

In this paper, after preprocessing, by padding missing values with zeros, the time interval between the adjacent points is 5 minutes.

- **finger\_stick:** the BG levels (mg/dL) are obtained by finger stick, a self-monitoring method.
- **basal:** the rate (U/h) of insulin delivery of pump. The rate is fixed from a particular timestamp “ts”, and it is changed to another value at the next timestamp. “temp\_basal” is the temporary rate of insulin delivery between “ts\_begin” and “ts\_end”, when the normal basal is suspended. Hence, “basal” and “temp\_basal” are merged as “basal”. Then, the basal is re-sampled every 5 minutes.
- **bolus:** it is a kind of insulin dose (U), including two types. The first type is to deliver all insulin at a time. The second type is to extend insulin delivery within a period from “ts\_begin” to “ts\_end”. Then, the second type of bolus is re-sampled every 5 minutes.
- **meal:** it is the carbohydrate intake (g) of a meal self-reported by the participants. The type of meal, i.e., breakfast, lunch, dinner, snacks, etc., is also recorded but ignored in this paper. This is because the type of meal can be regarded as a piece of redundant information when considering temporal features, i.e., time of a day, in the input.
- **sleep:** a participant falls asleep between “ts\_begin” and “ts\_end”, and “sleep” is a self-reported attribute. The participant also estimates the sleep quality from 1 to 3, where 3 means good sleep, 1 is poor sleep, and 2 is in the middle.

- work: a participant works between “ts\_begin” and “ts\_end”, and “work” is a self-reported attribute. The intensity of the work is estimated by the participant from 1 to 10, where 10 means working in extremely high intensity.
- exercise: a participant exercises between “ts\_begin” and “ts\_end”, and “exercises” is a self-reported attribute. The intensity of the exercise is estimated by the participant from 1 to 10, where 10 means exercising at extremely high intensity.
- basis\_heart\_rate: it is the heart rate (BPM) of the participants, and it is collected by Basis Peak per 1 minute. Then, it is aggregated per 5 minutes by averaging all values within the 5 minutes.
- basis\_gsr: it is the galvanic skin response ( $\mu\text{S}$ ) of the participants, and it is collected by Basis Peak per 5 minutes or Empatica Embrace per 1 minute. Then, the values collected per 1 minute are aggregated per 5 minutes by averaging all values within the 5 minutes.
- basis\_skin\_temperature: it is the skin temperature ( $^{\circ}\text{F}$ ) of the participants, and it is collected by Basis Peak per 5 minutes or Empatica Embrace per 1 minute. Then, the values collected per 1 minute are aggregated per 5 minutes by averaging all values within the 5 minutes.
- basis\_air\_temperature: it is the air temperature ( $^{\circ}\text{F}$ ) of the participants, and it is collected by Basis Peak per 1 minute. Then, it is aggregated per 5 minutes by averaging all values within the 5 minutes.
- basis\_steps: it is the step count of the participants every 5 minutes, and it is collected by Basis Peak.
- acceleration: it is the magnitude of acceleration ( $m/s^2$ ) of the participants, and it is collected by Empatica Embrace per 1 minute. Then, it is aggregated per 5 minutes by averaging all values within the 5 minutes.

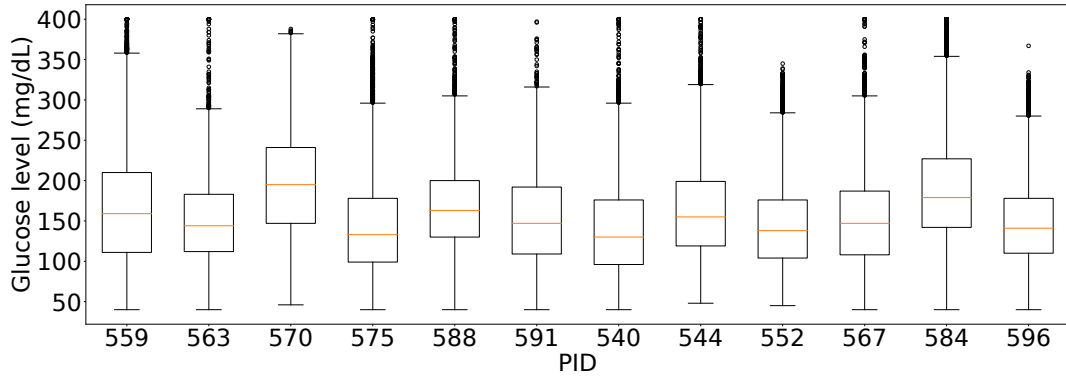


**Figure 2.1:** Distributions of “glucose\_level” in terms of all participants.

In terms of the way of collecting values, the attributes can be divided into two categories: 1) attributes that are self-reported (see Table 2.2); 2) attributes that are collected by sensors (see Table 2.3). From Tables 2.2 and 2.3, we can have the following observations.

- For each attribute, the distributions are different among various participants. For example, patient 584 tends to have worse BG management, as the mean “glucose\_level” is hyperglycemia ( $>180$  mg/dL). Patient 544 has the best BG management since the mean “glucose\_level” is the lowest and within a normal range (70-180 mg/dL).
- Participants (559-591) from OhioT1DM’18 do not have “acceleration”, while participants (540-596) from OhioT1DM’20 do not have “basis\_air\_temperature”, “basis\_steps”, “basis\_heart\_rate”.

## 2.5 Data Analysis

### 2.5.1 Impact of “meal” and “bolus”

In this section, we first visualize the distribution of “glucose\_level” (Figure 2.1), “meal” (Figure 2.2) and “bolus” (Figure 2.3).

Overall, we can observe that some participants have severe hyperglycemia. For example, 58.02% of the samples of participant 570 are hyperglycemia (see Table 2.4). This is because participant 570 has the highest carbohydrate intake (see Figure 2.2) but relatively lower bolus delivery compared with other participants.

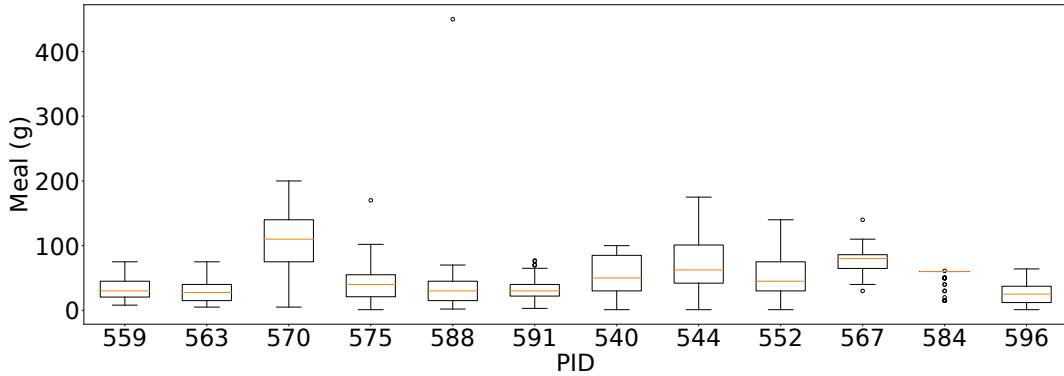


**Figure 2.2:** Distributions of “meal” in terms of all participants.

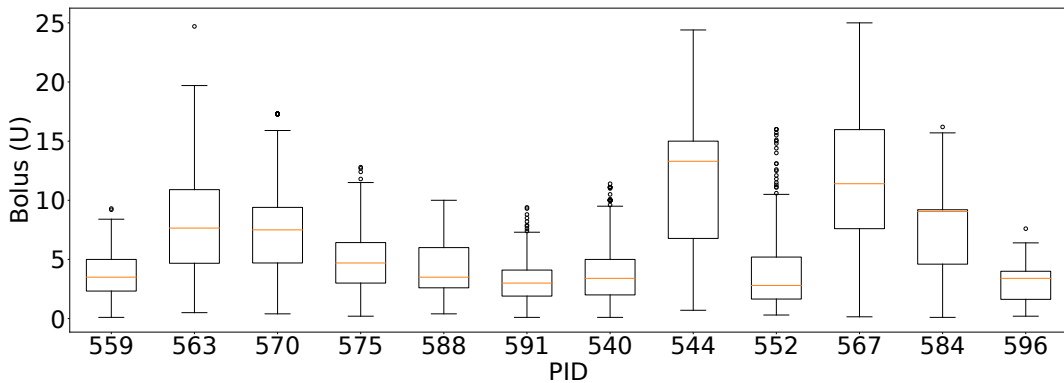


**Figure 2.3:** Distributions of “bolus” in terms of all participants.

Comparably, we can also find that even though participants 544 and 567 have high carbohydrate intake (see Figure 2.2), their BG levels can maintain relatively normal (see Figure 2.1). Only 33.97% and 28.60% of the samples of participant 544 and 567 are hyperglycemia, respectively (see Table 2.4). This is because they have high insulin delivery (see Figure 2.3), enabling them to reduce their BG levels

**Table 2.4:** Proportions of Hypoglycemia, Normal and Hyperglycemia for each participant.

PID	Hypoglycemia	Normal	Hyperglycemia
559	3.61%	56.71%	39.68%
563	1.99%	71.79%	26.21%
570	1.49%	40.49%	58.02%
575	7.60%	68.21%	24.18%
588	0.80%	61.98%	37.22%
591	3.93%	64.89%	31.18%
540	6.02%	71.00%	22.98%
544	1.30%	64.73%	33.97%
552	3.28%	73.56%	23.16%
567	6.67%	64.72%	28.60%
584	0.90%	50.04%	49.06%
596	1.99%	74.32%	23.69%



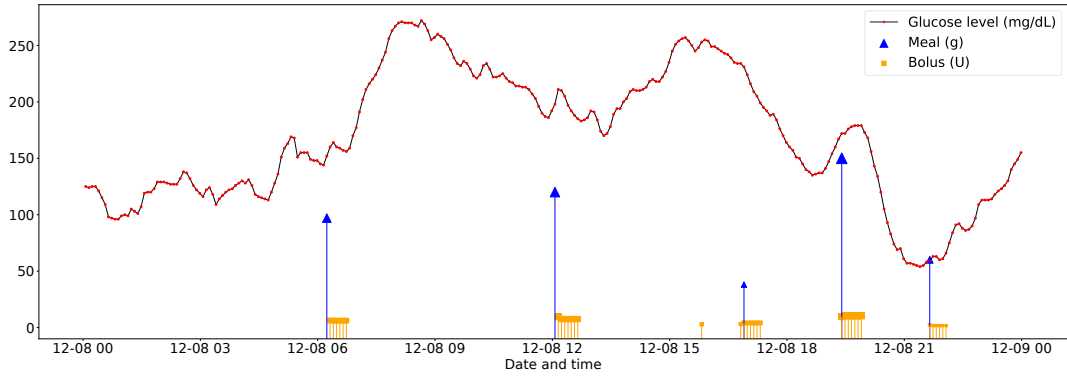


**Figure 2.4:** Visualizing “glucose\_level”, “bolus” and “meal” of a day for participant 570.

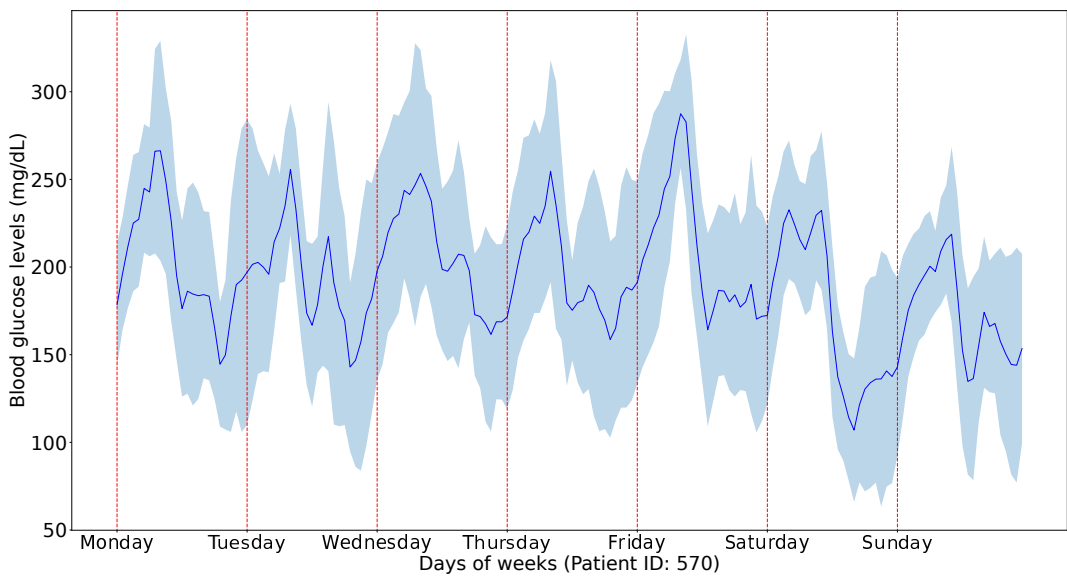


**Figure 2.5:** Visualizing “glucose\_level” for participant 570 in terms of days of weeks.

even if they have high carbohydrate intake.

Furthermore, for participant 570, we visualize the variations of “glucose\_level”, “meal” and “bolus” of a day (see Figure 2.4). We can observe that, in most cases, insulin is delivered after having a meal. Besides, BG levels tend to increase in the next few hours after a meal. With the help of insulin, there is always a downtrend following the uptrend of the BG levels.

In summary, both “meal” and “insulin” have a significant influence on the “glucose\_level”. Hence, we can guess that maybe “meal” and “insulin” are helpful for the prediction of future BG levels.

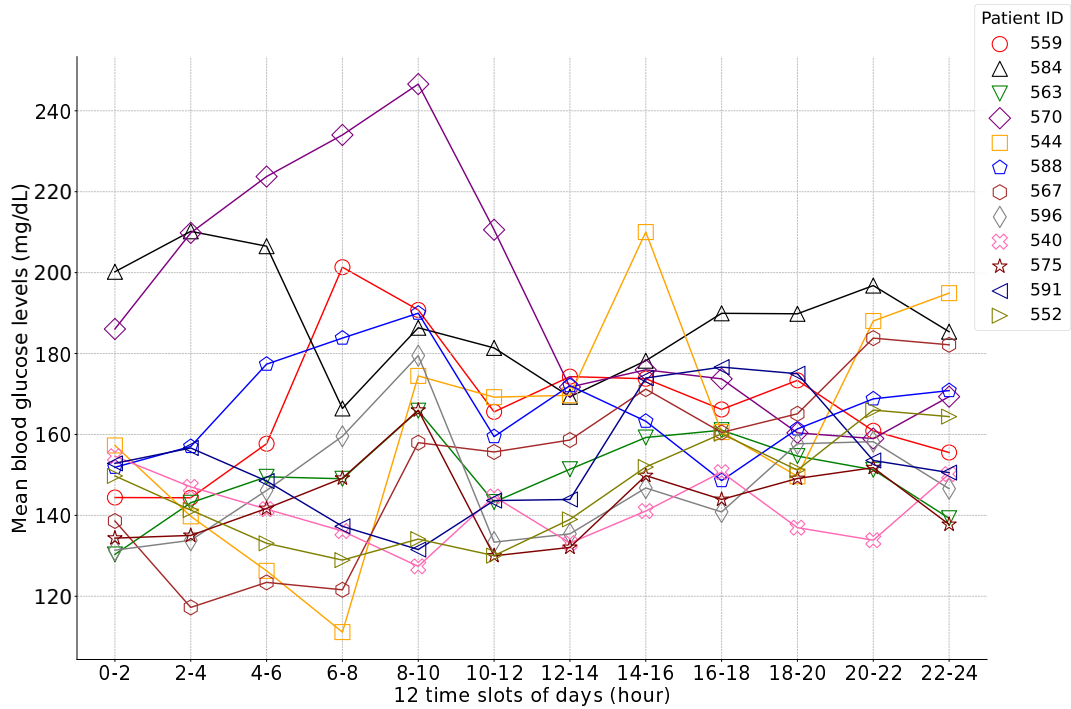


**Figure 2.6:** Visualizing “glucose\_level” for all participant in terms of time slots of days.

## 2.5.2 Impact of Temporal Features

In order to figure out the temporal features of “glucose\_levels”, we visualize the variations of “glucose\_level” from different temporal granularity. We find that most participants have interesting and special temporal features. For example, Figure 2.5 contains all “glucose\_level” samples of patient 570, organized sequentially by time. The darker blue line is the mean value of “glucose\_level”.

We can find that for each day, the BG levels tend to be high in the first half and low in the second half. It is obviously a daily pattern. On the other hand, we can find that the participant tends to have higher BG levels during weekdays compared with weekends. It is a weekly pattern.

Moreover, we visualize the variations in the “glucose\_level” of all participants in terms of time slots of days (see Figure 2.6) and days of weeks (see Figure 2.7). People have daily and weekly patterns, which different lifestyles and body conditions may cause.

Finally, according to the observations above, temporal features, i.e., times of days and days of weeks, are also considered in the following experiments. More

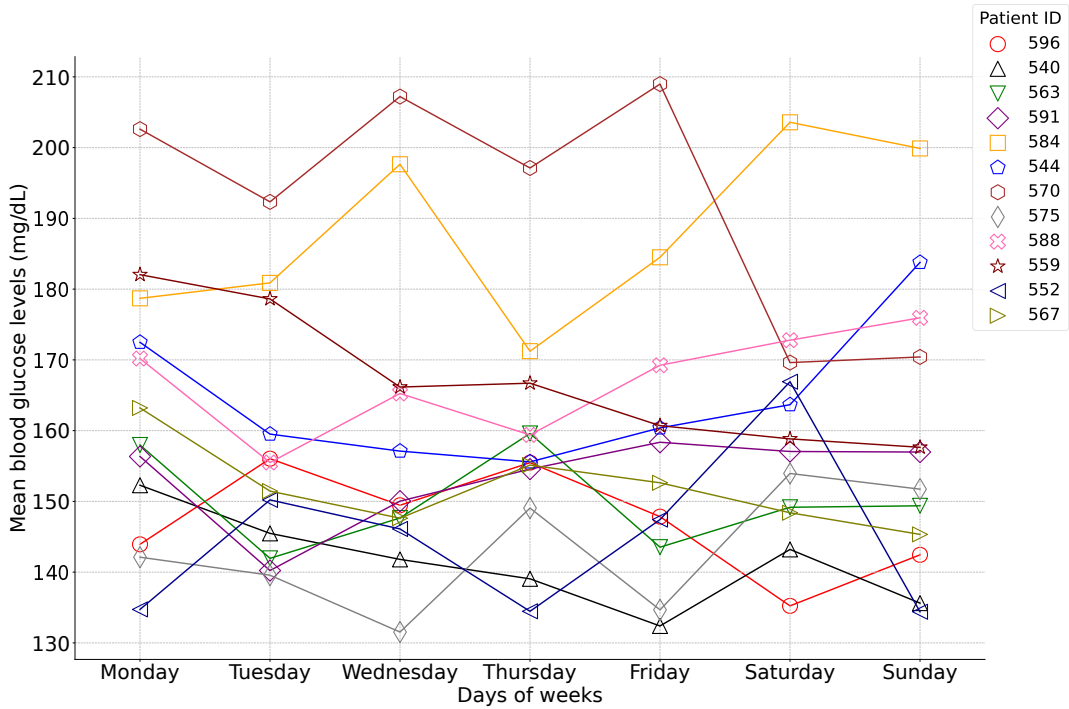


**Figure 2.7:** Visualizing “glucose\_level” for all participant in terms of days of weeks.

relevant experiments will show whether temporal features help predict future BG levels. Given that each person has his or her BG changing styles, personalized model will be designed in the following sections.

## 2.6 Proposed method

### 2.6.1 Overview

In this paper, we proposed a graph attentive memory neural network, called “GAM” and trained by FL. It can be seen in Figure 2.8, consisting of a graph attention network (GAT, Velickovic et al. [2018]) and a gated recurrent unit (GRU, Cho et al. [2014]). GAT is leveraged to explicitly model correlations among various attributes in an RMTS generated from IMTS padded with zeros. Each valid value of an attribute, excluding zeros, can be seen as a node of a dynamic graph, and the value is mapped to a tensor by fully connected layers, denoted as graph embeddings. Then, at each time slot, graph features are gotten from GAT via graph convolutions on graph embeddings given an adjacent matrix. These graph features are sequentially aggregated by GRU, generating a compact vector containing temporal graph fea-

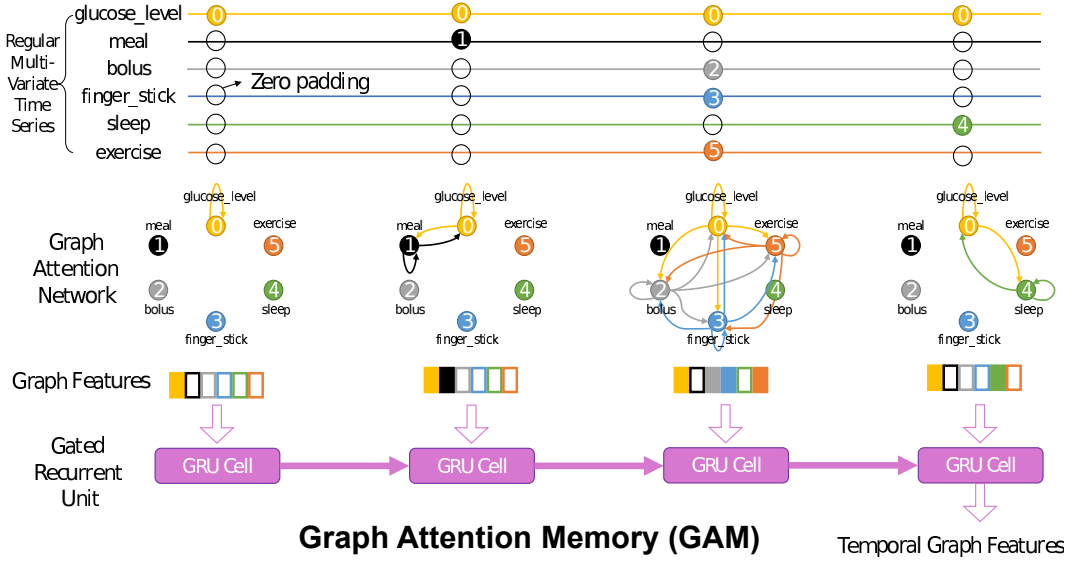


Figure 2.8: Graph attention memory (GAM).

tures. The temporal graph features will be used for the estimation of BG levels.

On the other hand, the overview of  $\hat{y}_{T+W} = \text{GAM}(\mathbf{X}; \theta)$  are as follows ( $\forall t \in \mathcal{T}, \forall n \in \mathcal{N}$ ):

$$\mathbf{e}_t^n = f_n(x_t^n), \quad (2.1a)$$

$$\mathbf{E}_t = [\mathbf{e}_t^1 \dots \mathbf{e}_t^n \dots \mathbf{e}_t^N], \quad (2.1b)$$

$$\mathbf{G}_t = \text{GATs}(\mathbf{E}_t, \mathbf{A}), \quad (2.1c)$$

$$\mathbf{h}_t = \text{GRU}(\phi(\mathbf{G}_t), \mathbf{h}_{t-1}), \quad (2.1d)$$

$$\hat{y}_{T+W} = f_{out}(\mathbf{h}_T), \quad (2.1e)$$

where  $\mathcal{T} \triangleq \{1, \dots, t, \dots, T\}$  and  $\mathcal{N} \triangleq \{1, \dots, n, \dots, N\}$ ;  $x_t^n$  is the item in the  $n$ -th row  $t$ -th column of  $\mathbf{X} \in \mathbb{R}^{N \times T}$  which is the RMTS defined in Section 2.1;  $f_n(\cdot)$  and  $f_{out}(\cdot)$  are fully connected layers;  $\mathbf{A} \in \mathbb{R}^{N \times N}$  is the adjacent matrix of a graph;  $\mathbf{h}_t$  is the hidden state of GRU, and  $\mathbf{h}_0$  is a zero tensor;  $\hat{y}_{T+W}$  is the estimation of  $y_{T+W}$ .

Firstly, in Equation (2.1a), each item  $x_t^n$ , excluding zeros, of RMTS  $\mathbf{X}$  is individually embedded by fully connected layers  $f_n(\cdot)$ , where each attribute  $n \in \mathcal{N}$  has its own  $f_n(\cdot)$ . The embedding  $\mathbf{e}_t^n \in \mathbb{R}^E$  is a tensor representation of  $x_t^n$ , and it is collected by  $\mathbf{E}_t \in \mathbb{R}^{E \times N}$  in Equation (2.1b). Then, for each time slot  $t$ , in

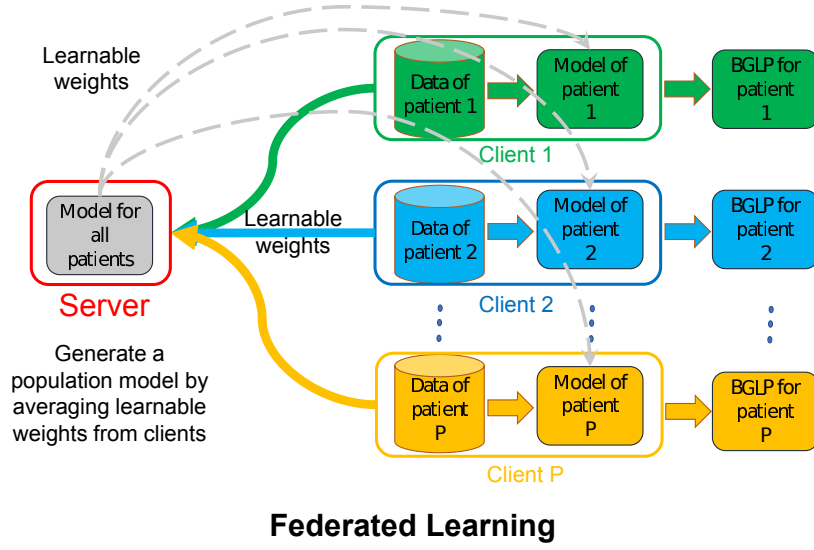


**Figure 2.9:** Federated learning (FL).

Equation (2.1c), GATs are leveraged to do the graph convolution for  $\mathbf{E}_t$  when given the adjacent matrix  $\mathbf{A}$ . More details are explained in section 2.6.2. After graph convolutions,  $\mathbf{G}_t \in \mathbb{R}^{E' \times N}$  is generated, containing correlations among all the attributes. Next,  $\mathbf{G}_t$  is flattened to a tensor by  $\phi(\cdot)$ , as  $\phi(\mathbf{G}_t) \in \mathbb{R}^{E'N \times 1}$ . Then,  $\{\phi(\mathbf{G}_1), \dots, \phi(\mathbf{G}_t), \dots, \phi(\mathbf{G}_T)\}$  aggregated by GRU in Equation (2.6.3), and more details are explained in section 2.6.3, generating a compact tensor  $\mathbf{h}_T$  which contains temporal information. Finally, the estimated glucose level  $\hat{y}_{T+W}$  is generated from  $\mathbf{h}_T$  through fully connected layers  $f_{out}(\cdot)$ .

The above structure has the following advantages.

- Graph convolutions by GAT can model complex correlations among attributes, focusing on more valuable attributes and ignoring noises.
- GRU-based memory can further aggregate temporal information, reducing irrelevant information by a self-gated mechanism.
- GAM fully leverages attribute and temporal information by combining GAT and GRU in the BGLP.

Mean square error (MSE) loss is leveraged in the following training process,

as:

$$\mathbf{L}(y_{T+W,b}, \hat{y}_{T+W,b}; \boldsymbol{\theta}) = \frac{1}{B} \sum_b (y_{T+W,b} - \hat{y}_{T+W,b})^2, \quad (2.2)$$

where  $B$  is the batch size,  $\boldsymbol{\theta}$  is the learnable weights of the proposed model. Then, Adam [Kingma and Ba, 2015] optimizer is introduced to update learnable weights.

The training of the GAM is explained in section 2.6.4 and section 2.6.5. Especially federated learning (FL) is generally depicted in Figure 2.9. In FL, personal data can only be accessed by the related personalized model in the clients. After training for certain epochs in the clients, the learnable weights of the personal model are sent to a server, and a population model is calculated by averaging the latest personal learnable weights. Then, personalized models of clients copy the latest learnable weights of the population model, and each client replaces the personalized learnable weights with the population learnable weights. The above process is repeated until the convergence. In this case, the participant privacy is well protected by the clients, as the personal data is only kept by the clients separately. Meanwhile, population patterns are also learned in the server without invasion of privacy. Note that we leverage multi-process to simulate FL in this paper, where each client or the server is an independent process.

## 2.6.2 Graph Attention Networks (GATs)

For each time slot  $t$ , node embedding  $\mathbf{E}_t$  can be gotten from Equation (2.1b). Then, each attribute  $n \in \mathcal{N}$  has its own embedding  $\mathbf{e}_t^n$ , and all attribute embedding tensors can be treated as a tensor graph  $\langle \mathbf{E}_t, \mathbf{A} \rangle$ , where  $\mathbf{A}$  is the adjacent matrix. In this case, each valid attribute connects all other valid attributes. For example, when  $i, j \in \mathcal{N}$ , if  $\mathbf{e}_t^i$  and  $\mathbf{e}_t^j$  are not null, both  $\mathbf{A}[i, j]$  and  $\mathbf{A}[j, i]$  are equal to 1. That is to say. There are directed edges, respectively, from node  $j$  to node  $i$  and from  $i$  to node  $j$ . Otherwise, when any tensor of  $\mathbf{e}_t^i$  and  $\mathbf{e}_t^j$  is null, both  $\mathbf{A}[i, j]$  and  $\mathbf{A}[j, i]$  are equal to 0. It means that there are no directed edges between node  $i$  and node  $j$ . Note that all valid attributes connect to themselves. In other words,  $\mathbf{A}[i, i] = 1$  when  $\mathbf{e}_t^i$  is not null.

Then, GAT is introduced to this work, and it can be represented as follows

( $\forall t \in \mathcal{T}, \forall i \in \mathcal{N}$ ):

$$\alpha_t^{i,j} = \frac{\exp\left(\text{LeakyReLU}\left(\mathbf{a}^\top[\mathbf{W}\mathbf{e}_t^i; \mathbf{W}\mathbf{e}_t^j]\right)\right)}{\sum_{k \in \mathcal{N}_i} \exp\left(\text{LeakyReLU}\left(\mathbf{a}^\top[\mathbf{W}\mathbf{e}_t^i; \mathbf{W}\mathbf{e}_t^k]\right)\right)}, \quad (2.3a)$$

$$\mathbf{g}_t^i = \sigma\left(\sum_{j \in \mathcal{N}_i} \alpha_t^{i,j} \mathbf{W}\mathbf{e}_t^j\right), \quad (2.3b)$$

$$\mathbf{G}_t = [\mathbf{g}_t^1 \dots \mathbf{g}_t^i \dots \mathbf{g}_t^N], \quad (2.3c)$$

where  $\mathbf{W} \in \mathbb{R}^{E' \times E}$  and  $\mathbf{a} \in \mathbb{R}^{2E'}$  contains learnable parameters;  $[\cdot]$  means the concatenation of two tensors;  $\mathcal{N}_i$  contains all adjacent nodes of the node  $i$ .

Each node tensor  $\mathbf{e}_t^j$  can generate a neural message  $\mathbf{W}\mathbf{e}_t^j$  which can be passed along the edges to the adjacent nodes. For example, when  $\mathbf{A}[i, j] = 1$ , neural message  $\mathbf{W}\mathbf{e}_t^j$  can be passed to node  $i$ . Meanwhile, if  $\mathbf{A}[i, j] = 0$ , neural message  $\mathbf{W}\mathbf{e}_t^j$  cannot be passed to node  $i$ . Only when the node tensor  $\mathbf{e}_t^j$  is not null can the node tensor be transformed into a neural message by  $\mathbf{W}$ .

Hence, at the end of time slot  $t$ , each node might receive several neural messages from the adjacent nodes. For example, in Equation (2.3b), the adjacent nodes of node  $i$  are denoted as  $\mathcal{N}_i$ , then the neural messages  $\mathbf{W}\mathbf{e}_t^j$  from the adjacent nodes ( $j \in \mathcal{N}_i$ ) are weighted and summarized by the attention weights  $\{\alpha_t^{i,j} | j \in \mathcal{N}_i\}$  which are generated in Equation (2.3a).

Specifically, in Equation (2.3a), a similarity score between the neural messages  $\mathbf{W}\mathbf{e}_t^i$  and  $\mathbf{W}\mathbf{e}_t^j$  are calculated by  $\text{LeakyReLU}\left(\mathbf{a}^\top[\mathbf{W}\mathbf{e}_t^i; \mathbf{W}\mathbf{e}_t^j]\right)$ . The edge weight from node  $j$  to node  $i$ , i.e., attention weight  $\alpha_t^{i,j}$ , is calculated by normalizing the similarity score through ‘‘softmax’’.

Finally, after Equation (2.3a) and Equation (2.3b), each node  $i$  has a new tensor  $\mathbf{g}_t^i$  which is a substitute for  $\mathbf{e}_t^i$ , and the new tensor contains all information of the previous tensor  $\mathbf{e}_t^i$  and the adjacent node tensors  $\{\mathbf{e}_t^j | j \in \mathcal{N}_i\}$ . Then,  $\{\mathbf{g}_t^i | i \in \mathcal{N}\}$  are collected and reorganised as new graph node embedding  $\mathbf{G}_t$  as Equation (2.3c). When there are multiple GATs layers ( $\{1, \dots, l, \dots, L\}$ ), the input  $\mathbf{E}_t^l$  of the current GAT layer  $l$  is the output  $\mathbf{G}_t^{l-1}$  of the previous layer  $l-1$ , where  $\mathbf{E}_t^1 = \mathbf{E}_t$ ,  $\mathbf{E}_t^l = \mathbf{G}_t^{l-1}$ ,  $l > 1$ .

On the other hand, for the neural message generating, multi-head attention is also introduced as follows:

$$\mathbf{g}_t^i = \sigma \left( \frac{1}{M} \sum_m \mathbf{g}_t^{i,m} \right) = \sigma \left( \frac{1}{M} \sum_m \sum_{j \in \mathcal{N}_i^m} \alpha_t^{i,j,m} \mathbf{W}^m \mathbf{e}_t^j \right). \quad (2.4)$$

Each node  $j$  can generate multiple neural messages  $\{\mathbf{W}^1 \mathbf{e}_t^j, \dots, \mathbf{W}^m \mathbf{e}_t^j, \dots, \mathbf{W}^M \mathbf{e}_t^j\}$ , where  $M$  is the number of heads. Each head  $m$  has its own new neural tensor  $\mathbf{g}_t^{i,m}$ , and the final new neural tensor  $\mathbf{g}_t^i$  is calculated by averaging  $\mathbf{g}_t^{i,m}$  along  $m$ .

GAT has the following advantages.

- The attention weights in the graph edges are flexible and change according to the comparison between the neural messages. It is able to focus/ignore different attributes in different time slots dynamically. Compared with GCN, whose edge weights are fixed, GAT-based methods are more robust and flexible.
- Similar to CNN, when controlling the number of GAT layers  $L$ , the granularity of features can be selected. When being given larger  $L$ , features with more details are extracted. On the other hand, when  $L$  is small, general features are captured by GATs.
- By leveraging graph-based structure, the method becomes explainable, as it is obvious to observe how different attributes affect each other and how much the impact is through visualizing attention weights and graph structures. Besides, only the valid attributes (not null) can generate and pass neural messages to the valid adjacent tensor nodes (not null), so this method effectively deals with RMTS.

### 2.6.3 Gated Recurrent Units (GRU) based Memory

After passing through GATs in all historical time slots  $\mathcal{T}$ , a set of new graph node tensors are generated, as  $\{\mathbf{G}_t | t \in \mathcal{T}\}$ . The graph tensors  $\mathbf{G}_t \in \mathbb{R}^{E' \times T}$  are reshaped to  $\phi(\mathbf{G}_t) \in \mathbb{R}^{E'T \times 1}$  by flattening  $\phi(\cdot)$ . GRU-based memorization is introduced to



deal with  $\{\phi(\mathbf{G}_t)|t \in \mathcal{T}\}$ , as:

$$\mathbf{r}_t = \sigma(\mathbf{W}_1\phi(\mathbf{G}_t) + b_1 + \mathbf{W}_2\mathbf{h}_{t-1} + b_2), \quad (2.5a)$$

$$\mathbf{z}_t = \sigma(\mathbf{W}_3\phi(\mathbf{G}_t) + b_3 + \mathbf{W}_4\mathbf{h}_{t-1} + b_4), \quad (2.5b)$$

$$\mathbf{q}_t = \tanh(\mathbf{W}_5\phi(\mathbf{G}_t) + b_5 + \mathbf{r}_t * (\mathbf{W}_6\mathbf{h}_{t-1} + b_6)), \quad (2.5c)$$

$$\mathbf{h}_t = (1 - \mathbf{z}_t) * \mathbf{q}_t + \mathbf{z}_t * \mathbf{h}_{t-1}, \quad (2.5d)$$

where  $\mathbf{W}$  and  $b$  are learnable parameters;  $*$  is Hadamard product;  $\mathbf{h}_t \in \mathbb{R}^{H \times 1}$  is a hidden state, where  $\mathbf{h}_0$  is initialized with  $\mathbf{0}$ , and  $H$  is the hidden size.

GRU is one of the self-gated recurrent neural networks, and it is designed to avoid vanishing gradient problems, especially when dealing with long-term series. It contains a reset gate  $\mathbf{r}_t$  and an update gate  $\mathbf{z}_t$ , and they are separately generated from the combination of the current input  $\phi(\mathbf{G}_t)$  and previous history  $\mathbf{h}_{t-1}$ , as Equation (2.5a) and Equation (2.5b). Then, in Equation (2.5c), reset gate  $\mathbf{r}_t$  can decide how much previous history information from  $\mathbf{h}_{t-1}$  will be forgotten. When  $\mathbf{r}_t$  is close to  $\mathbf{1}$ , nearly all historical information is kept. Otherwise, when  $\mathbf{r}_t$  is close to  $\mathbf{0}$ , almost all history is forgotten. Similarly, in Equation (2.5d), the update gate can decide how much history from  $\mathbf{h}_{t-1}$  can be passed to the output  $\mathbf{h}_t$ .

The above structure has the following advantages.

- GRU-based memory can generate a compact tensor from  $\{\phi(\mathbf{G}_t)|t \in \mathcal{T}\}$ , remaining useful information but forgetting irrelevant information and noises. It makes the whole model deal with long-term RMTS.
- Compared with other self-gated methods (LSTM), GRU only leverages one memory state ( $\mathbf{h}_t$ ), while LSTM leverages two memory states ( $\mathbf{h}_t$  and  $\mathbf{c}_t$ ). Hence, GRU needs fewer computation resources and is more effective.

#### 2.6.4 Training without FL

A two-step training algorithm (Algorithm 1) is introduced from Zhu et al. [2020a] since it can not only leverage population patterns across different personal data but also keep personal characteristics via individual fine-tuning based on personal data.

Specifically, in Algorithm 1, the input of the algorithm contains training datasets  $\{\mathcal{D}_{Training}^p | p \in \mathcal{P}\}$  and validation datasets  $\{\mathcal{D}_{Validation}^p | p \in \mathcal{P}\}$  of all participants  $\mathcal{P}$  and initialized parameters  $\theta_0^{global}$  (line 1). Firstly, according to Equation (2.1), a population model  $\text{GAM}(\mathbf{X}; \theta_0^{global})$  is built with  $\theta_0^{global}$  (line 2). The first step of this algorithm is global training. It mixes the personal training data from all participants (line 4). Then, initialize the training epoch  $\tau$  with 0 (line 5), and the global training is started (line 6). In the training loop, a batch of samples is randomly selected from the mixing training dataset  $\mathcal{D}_{Training}$  (line 7). Equation (2.2) is utilized to calculate gradients, and learnable weights  $\theta_\tau^{global}$  are updated by the Adam optimizer (lines 8-10). In certain training epochs (line 11), GAM is evaluated by the validation datasets  $\{\mathcal{D}_{Validation}^p | p \in \mathcal{P}\}$  (lines 12-13). Based on the validation results, if the performance is improved, the best learnable global parameters are saved as  $\theta^{global\_best}$  (lines 14-15).

The second training step, personalized fine-tuning, begins with turning down the learning rate (line 17), followed by the loop of participants (line 18). For each participant  $p$ , a personalized model is built based on Equation (2.1), and it is initialized by the best global parameters  $\theta^{global\_best}$  (lines 19-20). Then, the training epoch  $\tau$  is initialized with 0 (line 21). In the loop of fine-tuning for the personalized model (line 22), a batch of samples are randomly selected from the personal training dataset  $\mathcal{D}_{Training}^p$  (line 23). Equation (2.2) is also utilized to calculate gradients, and learnable weights  $\theta_\tau^{global}$  are updated by the Adam optimizer (lines 24-26). GAM is evaluated by the validation datasets  $\{\mathcal{D}_{Validation}^p | p \in \mathcal{P}\}$  in certain training epochs (lines 27-29). Similarly, if the performance is improved, the best personal learnable personal parameters are saved as  $\theta^{best,p}$  (lines 30-32).

### 2.6.5 Training with FL

As we mentioned in the previous subsection, two-step training can currently keep population patterns and personal characteristics. Nevertheless, it leaks participant privacy by mixing personal data. Hence, if it is possible to sacrifice some performance, privacy may be well protected by introducing FL [McMahan et al., 2017]. In FL, personal data is only stored in the place where it is generated rather than

being sent to a center and mixed with other data.

The details of FL are in Algorithm 2. The input of the algorithm includes training datasets  $\{\mathcal{D}_{Training}^p | p \in \mathcal{P}\}$  and validation datasets  $\{\mathcal{D}_{Validation}^p | p \in \mathcal{P}\}$  of all participants  $\mathcal{P}$  and initialized parameters  $\theta_0^{global}$  (line 1). There are  $T^{total}$  of training epochs for FL (line 4). In each epoch  $\tau_1$ , each client has a participant  $p$ , and a personalized model is built based on Equation (2.1) (lines 5-8). The server sends the population parameters  $\theta_{\tau_1}^{global}$  to the client, and the personalized model is initialized by the population parameters (lines 9-10). Then, the client trains the personalized model by batch learning using Equation (2.2) and Adam optimizer for  $T^{client}$  epochs (lines 11-15). When all clients finish the personalized training, the server collects parameters from all clients and generates population parameters  $\theta_{\tau_1}^{global}$  by averaging (lines 16-18). Next, in certain epochs (line 19), the personalized model is evaluated by personal validation data in each client (lines 20-21). If the total performance is improved, the current population parameters will be saved as the best population parameters  $\theta^{best-global}$  (lines 22-23).

The second step of Algorithm 2, personalized fine-tuning, is the same as the one in Algorithm 1. The only difference between Algorithm 1 and Algorithm 2 is in the first training step since Algorithm 1 mixes all training data to generate a population model, while Algorithm 2 utilizes FL to generate a population model, keeping the personal data in privacy.

### 2.6.6 Metrics

Root mean square error (RMSE) is introduced to evaluate the performance of models comprehensively, and it is utilized to select the best learnable parameters and the best combination of attributes. Mean absolute relative difference (MARD) is sensitive to small values, so it is used to evaluate the prediction of small values. Besides, mean absolute error (MAE) is also introduced to conveniently compare the proposed model with other methods, as all methods in Ohio 2020 challenge [Bach et al., 2020] use MAE as one of the metrics. The above metrics are defined

as follows:

$$RMSE = \sqrt{\frac{1}{I} \sum_i (y_{T+W,i} - \hat{y}_{T+W,i})^2}; \quad (2.6)$$

$$MARD = \frac{1}{I} \sum_i \frac{|y_{T+W,i} - \hat{y}_{T+W,i}|}{y_{T+W,i}} \times 100\%; \quad (2.7)$$

$$MAE = \frac{1}{I} \sum_i |y_{T+W,i} - \hat{y}_{T+W,i}|; \quad (2.8)$$

where  $I$  is the number of test samples of a participant. In the selection of best parameters during validation, only RMSE is referred to, as it can be seen as overall performance.

**Algorithm 1:** Training without FL

---

```

1 Input: Training datasets  $\{\mathcal{D}_{Training}^p | p \in \mathcal{P}\}$  and validation datasets
    $\{\mathcal{D}_{Validation}^p | p \in \mathcal{P}\}$  of all participants  $\mathcal{P}$ , initialized parameters  $\theta_0^{global}$  ;
2 Build a global function  $GAM(\mathbf{X}; \theta_0^{global})$  based on Equation (2.1);
3 # Step 1: global training
4  $\mathcal{D}_{Training} = \mathcal{D}_{Training}^1 \cup \dots \cup \mathcal{D}_{Training}^p \cup \dots \cup \mathcal{D}_{Training}^P$  ;
5  $\tau \leftarrow 0$ ;
6 while  $\tau < T^{global}$  do
7   Randomly select a batch of samples from mixed training data
      $\mathcal{D}_{Training}$ ;
8   Use Equation (2.2) to calculate loss with a batch of samples;
9   Use Adam optimizer to update  $\theta_\tau^{global}$  as  $\theta_{\tau+1}^{global}$  ;
10   $\tau \leftarrow \tau + 1$ ;
11  if  $\tau \% T^{eval1} == 0$  then
12    for  $p$  in  $\mathcal{P}$  do
13      Use validation data  $\mathcal{D}_{Validation}^p$  to evaluate  $GAM(\mathbf{X}; \theta_\tau^{global})$ ;
14      if performance improved in the validation results then
15         $\theta^{global\_best} \leftarrow \theta_\tau^{global}$  ;
16 # Step 2: personalized fine tuning
17 Turn down learning rate;
18 for  $p$  in  $\mathcal{P}$  do
19   Build a personal model  $GAM(\mathbf{X}; \theta_0^p)$  based on Equation (2.1) ;
20    $\theta_0^p \leftarrow \theta_{\tau_1}^{global\_best}$  ;
21    $\tau \leftarrow 0$ ;
22   while  $\tau < T^{person}$  do
23     Randomly select a batch of samples from the personal training
       dataset  $\mathcal{D}_{Training}^p$ ;
24     Use Equation (2.2) to calculate loss with a batch of samples;
25     Use Adam optimizer to update  $\theta_\tau^p$  as  $\theta_{\tau+1}^p$ ;
26      $\tau \leftarrow \tau + 1$ ;
27     if  $\tau \% T^{eval2} == 0$  then
28       for  $p$  in  $\mathcal{P}$  do
29         Use validation data  $\mathcal{D}_{Validation}^p$  to evaluate  $GAM(\mathbf{X}; \theta_\tau^p)$ ;
30         if performance improved in the validation results then
31            $\theta^{best,p} \leftarrow \theta_\tau^p$  ;
32   Save  $\theta^{best,p}$  ;

```

---

**Algorithm 2:** Training with FL

---

```

1 Input: Training datasets  $\{\mathcal{D}_{Training}^p | p \in \mathcal{P}\}$  and validation datasets
    $\{\mathcal{D}_{Validation}^p | p \in \mathcal{P}\}$  of all participants  $\mathcal{P}$ , initialized parameters  $\theta_0^{global}$  ;

2 # Step 1: federated learning
3  $\tau_1 \leftarrow 0$ ;
4 while  $\tau_1 < T^{total}$  do
5   for  $p$  in  $\mathcal{P}$  do
6     # each participant is in a client
7      $\tau_2 \leftarrow 0$ ;
8     Build a personal model  $\text{GAM}(\mathbf{X}; \theta_{\tau_2}^p)$  based on (2.1) ;
9     # send population parameters from the server to the client
10     $\theta_{\tau_2}^p \leftarrow \theta_{\tau_1}^{global}$  ;
11    while  $\tau_2 < T^{client}$  do
12      Randomly select a batch of samples from the personal training
13      dataset  $\mathcal{D}_{Training}^p$ ;
14      Use Equation (2.2) to calculate loss with a batch of samples;
15      Use Adam optimizer to update  $\theta_{\tau_2}^p$  as  $\theta_{\tau_2+1}^p$ ;
16       $\tau_2 \leftarrow \tau_2 + 1$ ;
17    # collect personal parameters from all clients
18     $\theta_{\tau_1+1}^{global} \leftarrow \frac{1}{P} \sum_p \theta_{\tau_2}^p$ ;
19     $\tau_1 \leftarrow \tau_1 + 1$ ;
20    if  $\tau_1 \% T^{eval1} == 0$  then
21      for  $p$  in  $\mathcal{P}$  do
22        Use validation data  $\mathcal{D}_{Validation}^p$  to evaluate  $\text{GAM}(\mathbf{X}; \theta_{\tau_1}^{global})$ ;
23        if performance improved in the validation results then
24           $\theta^{best\_global} \leftarrow \theta_{\tau_1}^{global}$  ;

24 # Step 2: personalized fine tuning
25 Turn down learning rate;
26 for  $p$  in  $\mathcal{P}$  do
27   Build a personal model  $\text{GAM}(\mathbf{X}; \theta_0^p)$  based on (2.1) ;
28    $\theta_0^p \leftarrow \theta^{global\_best}$  ;
29    $\tau \leftarrow 0$ ;
30   while  $\tau < T^{person}$  do
31     Randomly select a batch of samples from the personal training
32     dataset  $\mathcal{D}_{Training}^p$ ;
33     Use Equation (2.2) to calculate loss with a batch of samples;
34     Use Adam optimizer to update  $\theta_{\tau}^p$  as  $\theta_{\tau+1}^p$ ;
35      $\tau \leftarrow \tau + 1$ ;
36     if  $\tau \% T^{eval2} == 0$  then
37       for  $p$  in  $\mathcal{P}$  do
38         Use validation data  $\mathcal{D}_{Validation}^p$  to evaluate  $\text{GAM}(\mathbf{X}; \theta_{\tau}^p)$ ;
39         if performance improved in the validation results then
40            $\theta^{best,p} \leftarrow \theta_{\tau}^p$  ;

40 Save  $\theta^{best,p}$  ;

```

---

## Chapter 3

# Results

In this chapter, we discuss the experiment settings and result analysis of the impact of attributes (see section 3.1), the impact of hyperparameters (see section 3.2), the impact of FL (see section 3.3) and the impact of time-aware attention (see section 3.4). Then, we answer the research questions raised in the research proposal in section 3.5 according to the observations and conclusions of these experiments.

### 3.1 Impact of Attributes

#### 3.1.1 Experiment Settings

In order to well exploit different attributes in OhioT1DM'20 and OhioT1DM'18, considering the experimental consumption, we tried limited combinations of attributes. Surprisingly, we still find that using 6 attributes, i.e., “glucose\_level”, “meal”, “bolus”, “finger\_stick”, “sleep” and “exercise” are pretty helpful and bring about explicit improvements in most cases.

Hence, the first experiment is to show whether each of these 6 attributes positively impacts BGLP-RMTS. In the experiment, each time, we remove one attribute, excluding “glucose\_level”, from the 6 attributes. We also run GAM with all these 6 attributes and GRU with only “glucose\_level” for comparisons. If GAM with all these 6 attributes performs the best, we can come to a conclusion that each attributes can positively affect BGLP-RMTS. Meanwhile, if GRU with only “glucose\_level” performs the worst, we can draw a conclusion that the combination of these 6 attributes is successful. The relevant results are in Tables 3.1-3.6.

**Table 3.1:** In terms of RMSE (mg/dL), the impact of selecting attributes ( $W = 6$ ), where 6 attributes are “glucose\_level”, “meal”, “bolus”, “finger\_stick”, “sleep” and “exercise”.

Method	559	563	570	575	588	591	540	544	552	567	584	596	Average
GAM 6 attributes w/o meal	19.505	17.842	16.940	22.521	17.315	21.044	21.201	16.255	16.264	21.570	22.226	16.821	19.125
GAM 6 attributes w/o bolus	19.737	17.996	16.737	22.397	17.084	20.886	21.703	<b>15.620</b>	16.703	21.981	23.133	16.403	19.198
GAM 6 attributes w/o finger_stick	19.951	17.824	16.996	22.461	16.943	21.457	20.988	16.221	16.405	21.978	22.626	16.097	19.162
GAM 6 attributes w/o sleep	<b>19.009</b>	17.905	<b>16.119</b>	22.501	17.172	20.826	21.061	16.124	16.468	<b>21.523</b>	22.282	16.273	18.939
GAM 6 attributes w/o exercise	19.106	17.977	16.988	22.418	17.302	21.002	<b>20.886</b>	16.269	<b>16.186</b>	21.544	<b>21.997</b>	16.017	18.974
GAM 6 attributes	19.415	<b>17.596</b>	16.662	<b>22.279</b>	<b>17.057</b>	<b>20.717</b>	21.008	15.954	16.502	21.582	22.220	<b>16.012</b>	<b>18.917</b>
GRU glucose_level	19.439	18.291	18.604	23.620	18.485	21.832	22.771	18.002	17.367	22.919	23.587	17.203	20.177

**Table 3.2:** In terms of MARD (%), the impact of selecting attributes ( $W = 6$ ), where 6 attributes are “glucose\_level”, “meal”, “bolus”, “finger\_stick”, “sleep” and “exercise”.

Method	559	563	570	575	588	591	540	544	552	567	584	596	Average
GAM 6 attributes w/o meal	8.828	7.753	5.375	9.738	7.548	12.173	10.867	7.740	9.198	10.911	10.913	8.778	9.152
GAM 6 attributes w/o bolus	8.889	7.754	5.374	9.554	7.493	12.033	11.091	<b>7.489</b>	9.358	11.108	11.470	8.592	9.184
GAM 6 attributes w/o finger_stick	8.965	7.725	5.382	9.495	<b>7.365</b>	12.253	10.883	7.715	9.214	11.136	11.198	8.545	9.156
GAM 6 attributes w/o sleep	8.711	7.734	<b>5.205</b>	9.598	7.445	<b>11.845</b>	10.778	7.620	9.235	<b>10.646</b>	10.932	8.481	<b>9.019</b>
GAM 6 attributes w/o exercise	<b>8.615</b>	7.708	5.364	9.483	7.500	11.939	<b>10.748</b>	7.750	<b>9.063</b>	10.850	<b>10.791</b>	8.491	9.025
GAM 6 attributes	8.790	<b>7.648</b>	5.259	<b>9.443</b>	7.416	11.965	10.779	7.606	9.146	10.866	11.029	<b>8.430</b>	9.031
GRU glucose_level	8.992	7.978	5.742	10.268	8.028	12.352	11.583	8.688	9.662	11.235	11.255	8.984	9.564

On the other hand, we also want to show why we did not consider other attributes. Therefore, we incorporate one more attribute at a time when given the 6 attributes. We also use the GAM with all 6 attributes for comparisons. If the new considered attribute cannot surpass the GAM with all the 6 attributes in most cases, we will not take the new attribute into account. The relevant results are in Tables 3.7-3.12.

**Hyperparameter settings:** prediction window is  $W = 6$  or  $W = 12$ ; historical sequence length  $T = 12$ ; GRU hidden size is  $H = 256$ ; no. of heads  $M = 1$ ; no. of GAT layers  $L = 1$ . The training algorithm is based on Algorithm 1, and no. of global training epochs in the first or second training step is  $T^{global} = 10,000$  or  $T^{person} = 800$ ; evaluation interval in the first or second training step is  $T^{eval1} = 1,000$  or  $T^{eval2} = 160$ ; batch size is  $B = 128$ ; learning rate in the first or second training step is 0.001 or 0.00001.

### 3.1.2 Result Analysis

From Tables 3.1-3.6, we have the following observations and conclusions.

Overall, when prediction window  $W = 6$  or  $W = 12$ , in terms of RMSE, MARD and MAE, “GAM 6 attributes” performs the best in most cases. For example, when  $W = 6$ , the average RMSE of “GAM 6 attributes” is 18.917 mg/dL, while RMSE



**Table 3.3:** In terms of MAE (mg/dL), the impact of selecting attributes ( $W = 6$ ), where 6 attributes are “glucose\_level”, “meal”, “bolus”, “finger\_stick”, “sleep” and “exercise”.

Method	559	563	570	575	588	591	540	544	552	567	584	596	Average
GAM 6 attributes w/o meal	13.226	12.445	10.891	14.236	12.667	15.108	15.558	11.676	11.945	14.664	15.955	11.828	13.350
GAM 6 attributes w/o bolus	13.335	12.490	10.818	14.055	12.522	14.885	15.922	<b>11.204</b>	12.267	14.945	16.677	11.539	13.388
GAM 6 attributes w/o finger_stick	13.340	12.422	10.942	13.962	<b>12.387</b>	15.197	15.544	11.636	12.101	14.977	16.268	11.404	13.348
GAM 6 attributes w/o sleep	12.897	12.475	<b>10.503</b>	13.968	12.535	<b>14.812</b>	15.430	11.497	12.052	<b>14.537</b>	15.859	11.390	13.163
GAM 6 attributes w/o exercise	<b>12.683</b>	12.419	10.967	13.924	12.630	14.937	<b>15.370</b>	11.683	<b>11.871</b>	14.676	<b>15.817</b>	11.335	13.192
GAM 6 attributes	12.980	<b>12.268</b>	10.659	<b>13.852</b>	12.471	14.872	15.389	11.489	12.017	14.628	16.005	<b>11.271</b>	<b>13.158</b>
GRU glucose_level	13.292	12.784	11.660	14.927	13.365	15.454	16.702	12.909	12.683	15.361	16.519	12.083	13.978

**Table 3.4:** In terms of RMSE (mg/dL), the impact of selecting attributes ( $W = 12$ ), where 6 attributes are “glucose\_level”, “meal”, “bolus”, “finger\_stick”, “sleep” and “exercise”.

Method	559	563	570	575	588	591	540	544	552	567	584	596	Average
GAM 6 attributes w/o meal	32.818	28.968	28.834	35.662	29.971	<b>32.453</b>	38.750	27.333	28.918	36.931	36.309	27.158	32.009
GAM 6 attributes w/o bolus	32.478	<b>28.876</b>	27.626	<b>33.702</b>	29.275	33.206	39.380	26.211	29.623	37.782	38.082	26.364	31.884
GAM 6 attributes w/o finger_stick	31.454	29.769	28.630	35.333	<b>29.070</b>	33.104	38.265	26.619	28.865	36.954	36.287	<b>25.949</b>	31.691
GAM 6 attributes w/o sleep	32.155	29.707	27.831	35.126	29.509	33.032	38.540	27.721	<b>28.497</b>	<b>36.589</b>	<b>36.027</b>	27.293	31.835
GAM 6 attributes w/o exercise	<b>31.241</b>	29.552	28.289	34.993	29.148	33.043	<b>38.261</b>	<b>26.027</b>	28.762	37.081	36.307	26.014	31.560
GAM 6 attributes	31.282	29.641	<b>27.024</b>	35.095	29.666	32.885	38.445	26.348	28.650	36.861	36.267	26.314	<b>31.540</b>
GRU glucose_level	32.819	29.892	30.052	35.516	30.792	33.810	39.894	31.045	29.569	38.032	38.267	28.524	33.184

of others are higher than this value (see Table 3.1). Only when  $W = 6$ , in terms of MARD, “GAM 6 attributes” is not the best. In this case, the average MARD of “GAM 6 attributes” is 9.031%, while the average MARD of “GAM 6 attributes w/o sleep” is 9.019% (see Table 3.2). We can also see that “GRU glucose\_level” consistently performs the worst in all cases. For example, when  $W = 6$ , the average RMSE of “GRU glucose\_level” is 20.177 mg/dL, while the average RMSE of

**Table 3.5:** In terms of MARD (%), the impact of selecting attributes ( $W = 12$ ), where 6 attributes are “glucose\_level”, “meal”, “bolus”, “finger\_stick”, “sleep” and “exercise”.

Method	559	563	570	575	588	591	540	544	552	567	584	596	Average
GAM 6 attributes w/o meal	15.767	12.758	9.846	17.414	13.015	20.804	20.226	13.506	17.553	21.280	18.911	14.759	16.320
GAM 6 attributes w/o bolus	16.099	<b>12.646</b>	9.692	<b>16.467</b>	12.593	21.117	20.477	12.659	17.255	21.545	19.636	14.240	16.202
GAM 6 attributes w/o finger_stick	15.609	12.996	9.821	16.968	<b>12.582</b>	21.123	<b>19.879</b>	12.741	<b>16.876</b>	21.145	19.007	<b>14.181</b>	16.077
GAM 6 attributes w/o sleep	16.203	12.887	9.744	17.351	12.738	<b>20.566</b>	19.963	13.249	17.270	<b>20.263</b>	<b>18.502</b>	14.725	16.122
GAM 6 attributes w/o exercise	15.588	12.790	9.479	16.965	12.770	20.952	20.006	<b>12.565</b>	17.140	21.074	19.228	14.356	16.076
GAM 6 attributes	<b>15.517</b>	12.851	<b>9.421</b>	16.857	12.762	20.721	20.003	12.655	17.173	20.955	19.039	14.262	<b>16.018</b>
GRU glucose_level	16.836	13.282	10.730	17.990	13.275	21.225	20.801	16.462	17.874	21.111	19.700	15.683	17.081

**Table 3.6:** In terms of MAE (mg/dL), the impact of selecting attributes ( $W = 12$ ), where 6 attributes are “glucose\_level”, “meal”, “bolus”, “finger\_stick”, “sleep” and “exercise”.

Method	559	563	570	575	588	591	540	544	552	567	584	596	Average
GAM 6 attributes w/o meal	23.367	<b>20.481</b>	19.685	25.094	22.017	25.115	29.372	20.064	22.257	27.719	27.541	19.870	23.549
GAM 6 attributes w/o bolus	23.514	20.601	19.284	<b>23.857</b>	21.336	25.233	29.869	<b>18.965</b>	22.345	28.000	28.710	19.049	23.397
GAM 6 attributes w/o finger_stick	<b>22.570</b>	20.965	19.727	24.478	<b>21.289</b>	25.467	<b>28.949</b>	19.337	21.963	27.538	27.572	<b>18.803</b>	23.222
GAM 6 attributes w/o sleep	23.150	21.038	19.433	24.550	21.593	<b>25.085</b>	29.182	20.024	22.038	<b>26.942</b>	<b>26.947</b>	19.632	23.301
GAM 6 attributes w/o exercise	22.745	20.820	19.531	24.259	21.515	25.353	29.016	19.025	22.024	27.667	27.719	18.895	23.214
GAM 6 attributes	22.653	20.901	<b>19.028</b>	24.383	21.678	25.094	29.114	19.300	<b>21.960</b>	27.540	27.488	19.235	<b>23.198</b>
GRU glucose_level	24.299	21.713	20.978	25.520	22.206	25.652	30.234	23.903	22.771	28.026	28.483	20.929	24.560

“GAM 6 attributes” is only 18.917 mg/dL (see Table 3.1). Then, we can draw a conclusion that each one of the 6 attributes are helpful to the BGLP-RMTS, and the combination and utilization of these 6 attributes lead to excellent improvements.

On the other hand, in terms of all these metrics, we can observe that when removing “meal”, “insulin” or “finger\_stick”, the performance of GAM decreases more compared with the one removing “sleep” or “exercise”. Therefore, “meal”, “insulin” and “finger\_stick” are more critical compared with “sleep” and “exercise” in BGLP-RMTS. Hence, when this approach is about to be used in a scenario with limited computational resources, “sleep” and “exercise” can be neglected if the prediction accuracy is relatively not very important.

Besides, we can also find some general observations in these tables, which always appears in the rest of the experiments in this paper, so we only mention these observations once in this part. When the prediction window is larger, i.e.,  $W = 12$ , the BGLP-RMTS gets harder, compared with the prediction window  $W = 6$ , since all metrics are much larger when  $W = 12$ . For example, in Tables 3.1 and 3.4, the average RMSE is consistently less than 21 mg/dL in the previous table, while the average RMSE in the latter table are always higher than 30 mg/dL. The difficulties of BGLP-RMTS are various when facing different participants. For example, in Table 3.1, the RMSE of participant 540 is much larger than the RMSE of participant 544 in all different methods, so modeling patterns for participant 540 is harder compared with participant 544. This observation can further show that using a personalized model is quite essential, since the personal data varies a lot across different participants.

As for other attributes, in Tables 3.7-3.12, we can observe that, in most cases, introducing new attributes will not improve the performance. For example, only when  $W = 6$ , considering “basis\_sleep” can improve the performance in a manner, while it cannot improve the performance obviously when  $W = 12$ . Hence, “basis\_sleep” is not taken into account in the selection of attributes. Similarly, temporal attributes, i.e., “day\_of\_week” and “total\_seconds” cannot bring about obvious improvements in most cases, where “total\_seconds” is the total seconds transformed

**Table 3.7:** In terms of RMSE (mg/dL), the impact of selecting attributes ( $W = 6$ ), where 6 attributes are “glucose\_level”, “meal”, “bolus”, “finger\_stick”, “sleep” and “exercise”.

Method	559	563	570	575	588	591	540	544	552	567	584	596	Average
GAM 6 attributes + basal	19.232	19.756	19.415	22.340	17.556	20.919	<b>20.685</b>	16.058	16.857	21.839	25.066	16.006	19.644
GAM 6 attributes + basis_skin_Temperature	19.270	17.948	<b>16.214</b>	22.706	16.992	21.125	20.960	16.420	16.493	21.742	22.607	16.013	19.041
GAM 6 attributes + basis_gsr	19.397	18.027	16.599	22.448	17.089	21.224	20.774	16.339	16.634	21.717	22.676	16.199	19.094
GAM 6 attributes + basis_sleep	19.061	17.779	16.538	<b>22.074</b>	17.226	20.825	21.275	15.821	16.436	<b>21.448</b>	21.997	15.930	<b>18.867</b>
GAM 6 attributes + acceleration	19.307	17.933	16.419	22.242	17.207	20.709	21.080	15.835	16.685	21.816	22.154	<b>15.894</b>	18.940
GAM 6 attributes + work	19.389	17.780	16.797	22.099	16.944	20.825	21.102	16.061	16.536	21.496	<b>21.754</b>	15.910	18.891
GAM 6 attributes + basis_steps	19.048	17.678	16.432	22.382	17.262	20.769	21.166	15.853	16.358	21.715	22.181	16.036	18.907
GAM 6 attributes + basis_heart_rate	19.669	<b>17.436</b>	16.708	22.573	16.966	<b>20.616</b>	21.132	16.104	16.524	21.651	22.044	16.045	18.956
GAM 6 attributes + basis_air_temperature	19.306	17.675	16.227	22.319	17.181	20.722	21.028	15.975	<b>16.156</b>	21.660	22.062	16.133	18.870
GAM 6 attributes + day_of_week	<b>18.851</b>	17.677	16.743	22.692	16.981	20.725	21.079	<b>15.822</b>	16.229	21.904	22.486	16.315	18.959
GAM 6 attributes + total_seconds	19.238	17.871	16.322	22.328	<b>16.900</b>	21.174	20.899	16.074	16.526	21.881	22.498	16.091	18.984
GAM 6 attributes	19.415	17.596	16.662	22.279	17.057	20.717	21.008	15.954	16.502	21.582	22.220	16.012	18.917

**Table 3.8:** In terms of MARD (%), the impact of selecting attributes ( $W = 6$ ), where 6 attributes are “glucose\_level”, “meal”, “bolus”, “finger\_stick”, “sleep” and “exercise”.

Method	559	563	570	575	588	591	540	544	552	567	584	596	Average
GAM 6 attributes + basal	8.748	8.509	7.151	9.476	7.712	12.045	<b>10.699</b>	7.638	9.399	10.993	13.944	<b>8.361</b>	9.556
GAM 6 attributes + basis_skin_Temperature	8.670	7.681	5.287	9.813	7.382	12.050	10.835	7.764	9.377	10.737	11.099	8.472	9.097
GAM 6 attributes + basis_gsr	8.876	7.762	5.270	9.853	7.509	12.000	10.758	7.651	9.460	10.858	11.158	8.522	9.140
GAM 6 attributes + basis_sleep	8.467	7.706	5.277	<b>9.359</b>	7.458	11.795	10.840	7.589	<b>9.110</b>	<b>10.552</b>	10.961	8.401	<b>8.960</b>
GAM 6 attributes + acceleration	8.664	7.686	5.224	9.488	7.418	11.920	10.714	7.547	9.305	11.033	10.946	8.433	9.031
GAM 6 attributes + work	8.725	7.706	5.311	9.470	<b>7.352</b>	11.926	10.771	7.573	9.283	10.833	<b>10.742</b>	8.395	9.007
GAM 6 attributes + basis_steps	8.644	7.629	5.266	9.492	7.443	11.853	10.768	<b>7.501</b>	9.161	10.871	10.918	8.457	9.000
GAM 6 attributes + basis_heart_rate	8.775	7.666	5.298	9.680	7.418	<b>11.768</b>	10.794	7.562	9.210	10.830	10.887	8.499	9.032
GAM 6 attributes + basis_air_temperature	8.611	7.678	5.419	9.561	7.431	11.865	10.733	7.565	9.123	10.907	10.834	8.535	9.022
GAM 6 attributes + day_of_week	<b>8.591</b>	7.689	5.323	9.538	7.370	11.962	10.833	7.529	9.139	10.994	11.170	8.526	9.055
GAM 6 attributes + total_seconds	8.781	7.703	<b>5.203</b>	9.722	7.401	12.068	10.706	7.567	9.256	10.975	11.072	8.447	9.075
GAM 6 attributes	8.790	<b>7.648</b>	5.259	9.443	7.416	11.965	10.779	7.606	9.146	10.866	11.029	8.430	9.031

from the time of a day. For example, when the time is “5:10:01”, the “total\_seconds” is  $5 * 60 * 60 + 10 * 60 + 1 = 18601$ . Therefore, temporal attributes are also ignored in the final combination of attributes. Hence, except the 6 attributes, no more attributes are considered.

Besides, we can also find an interesting observation. In the 6 attributes, excluding “glucose\_level”, all attributes are self-reported. Meanwhile, other attributes collected by devices, e.g., “basis\_heart\_rate” cannot ensure the improvement of per-

**Table 3.9:** In terms of MAE (mg/dL), the impact of selecting attributes ( $W = 6$ ), where 6 attributes are “glucose\_level”, “meal”, “bolus”, “finger\_stick”, “sleep” and “exercise”.

Method	559	563	570	575	588	591	540	544	552	567	584	596	Average
GAM 6 attributes + basal	12.970	13.845	13.557	13.841	12.905	14.954	<b>15.266</b>	11.497	12.282	14.833	19.037	11.280	13.856
GAM 6 attributes + basis_skin_Temperature	12.838	12.410	10.628	14.316	12.409	15.229	15.534	11.729	12.179	14.660	16.250	11.401	13.299
GAM 6 attributes + basis_gsr	13.069	12.496	10.717	14.243	12.561	15.146	15.359	11.627	12.284	14.781	16.378	11.412	13.339
GAM 6 attributes + basis_sleep	<b>12.691</b>	12.438	10.701	<b>13.796</b>	12.577	14.802	15.654	11.404	11.977	<b>14.343</b>	15.848	11.231	<b>13.122</b>
GAM 6 attributes + acceleration	12.853	12.401	10.599	13.874	12.565	14.855	15.436	11.358	12.142	14.868	15.957	11.274	13.182
GAM 6 attributes + work	13.057	12.440	10.761	13.830	<b>12.377</b>	14.806	15.481	11.437	12.142	14.574	<b>15.640</b>	<b>11.204</b>	13.146
GAM 6 attributes + basis_steps	12.911	12.330	10.598	13.906	12.548	14.766	15.494	<b>11.312</b>	11.954	14.648	15.847	11.351	13.139
GAM 6 attributes + basis_heart_rate	13.368	12.289	10.754	14.185	12.481	<b>14.734</b>	15.495	11.473	12.059	14.612	15.899	11.410	13.230
GAM 6 attributes + basis_air_temperature	12.976	12.399	10.879	14.035	12.560	14.836	15.447	11.418	<b>11.883</b>	14.708	15.828	11.496	13.206
GAM 6 attributes + day_of_week	12.705	12.369	10.691	13.996	12.403	14.901	15.460	11.337	11.925	14.766	16.111	11.476	13.178
GAM 6 attributes + total_seconds	12.988	12.450	<b>10.533</b>	14.152	12.389	15.106	15.375	11.413	12.129	14.873	16.232	11.277	13.243
GAM 6 attributes	12.980	<b>12.268</b>	10.659	13.852	12.471	14.872	15.389	11.489	12.017	14.628	16.005	11.271	13.158

**Table 3.10:** In terms of RMSE (mg/dL), the impact of selecting attributes ( $W = 12$ ), where 6 attributes are “glucose\_level”, “meal”, “bolus”, “finger\_stick”, “sleep” and “exercise”.

Method	559	563	570	575	588	591	540	544	552	567	584	596	Average
GAM 6 attributes + basal	31.749	29.598	29.113	<b>34.662</b>	29.477	32.908	38.907	26.425	28.771	36.682	36.980	27.210	31.874
GAM 6 attributes + basis_skin_Temperature	<b>30.994</b>	29.421	27.942	34.996	29.750	33.113	<b>38.042</b>	<b>25.926</b>	28.865	36.262	35.862	26.007	31.432
GAM 6 attributes + basis_gsr	31.578	29.702	27.457	35.327	29.183	33.516	38.115	26.981	29.408	36.938	35.957	26.027	31.682
GAM 6 attributes + basis_sleep	31.617	29.758	27.975	35.327	29.115	<b>32.444</b>	39.046	26.634	<b>28.505</b>	36.661	36.199	26.028	31.609
GAM 6 attributes + acceleration	31.806	30.187	28.829	35.954	29.277	32.635	38.573	26.543	29.169	37.410	35.972	25.776	31.844
GAM 6 attributes + work	32.879	29.994	28.376	35.563	28.723	32.786	38.535	26.123	29.173	36.920	<b>35.553</b>	26.183	31.734
GAM 6 attributes + basis_steps	31.791	29.614	27.865	35.730	30.153	32.948	39.049	26.413	28.934	37.020	36.332	26.192	31.837
GAM 6 attributes + basis_heart_rate	31.369	29.637	27.707	35.127	30.243	32.515	38.708	26.402	28.720	37.030	35.708	26.351	31.626
GAM 6 attributes + basis_air_temperature	31.416	29.758	28.197	36.478	30.747	32.890	38.837	26.219	28.529	37.075	36.295	26.387	31.902
GAM 6 attributes + day_of_week	31.819	29.536	28.148	35.315	29.253	32.843	38.727	26.291	28.676	37.437	36.418	25.834	31.692
GAM 6 attributes + total_seconds	31.967	<b>29.315</b>	27.563	35.132	<b>28.677</b>	32.827	38.088	25.997	28.867	<b>36.016</b>	36.195	<b>25.537</b>	<b>31.348</b>
GAM 6 attributes	31.282	29.641	<b>27.024</b>	35.095	29.666	32.885	38.445	26.348	28.650	36.861	36.267	26.314	31.540

**Table 3.11:** In terms of MARD (%), the impact of selecting attributes ( $W = 12$ ), where 6 attributes are “glucose\_level”, “meal”, “bolus”, “finger\_stick”, “sleep” and “exercise”.

Method	559	563	570	575	588	591	540	544	552	567	584	596	Average
GAM 6 attributes + basal	15.507	13.149	10.424	17.137	12.921	20.759	20.319	12.625	17.299	20.630	18.601	14.260	16.136
GAM 6 attributes + basis_skin_Temperature	<b>14.919</b>	12.853	9.628	17.181	12.817	20.799	19.759	12.283	17.280	19.875	18.601	<b>13.946</b>	15.829
GAM 6 attributes + basis_gsr	15.767	12.905	9.677	17.352	12.718	21.061	19.654	12.588	17.526	20.758	<b>18.447</b>	14.151	16.050
GAM 6 attributes + basis_sleep	15.510	12.972	9.477	16.931	12.649	<b>20.272</b>	20.323	12.886	<b>16.846</b>	20.356	19.120	14.208	15.962
GAM 6 attributes + acceleration	15.682	12.993	9.813	17.081	12.767	20.707	19.894	12.699	17.192	21.329	18.826	14.206	16.099
GAM 6 attributes + work	15.808	13.087	9.781	<b>16.668</b>	12.535	20.956	20.082	<b>12.268</b>	17.204	20.995	18.479	14.249	16.009
GAM 6 attributes + basis_steps	15.729	12.902	9.758	17.201	13.019	20.955	20.282	12.695	17.220	21.197	19.281	14.443	16.223
GAM 6 attributes + basis_heart_rate	15.695	12.988	9.466	17.271	13.243	20.486	20.027	12.654	17.230	21.242	18.677	14.404	16.115
GAM 6 attributes + basis_air_temperature	15.474	12.792	9.933	17.451	13.249	20.822	20.151	12.514	17.165	21.249	19.072	14.352	16.185
GAM 6 attributes + day_of_week	15.603	12.831	9.774	17.117	12.551	20.865	20.487	12.537	16.922	21.288	19.291	14.070	16.111
GAM 6 attributes + total_seconds	15.501	<b>12.774</b>	<b>9.406</b>	16.906	<b>12.423</b>	21.009	<b>19.169</b>	12.361	17.045	<b>20.168</b>	18.907	13.994	<b>15.805</b>
GAM 6 attributes	15.517	12.851	9.421	16.857	12.762	20.721	20.003	12.655	17.173	20.955	19.039	14.262	16.018

formance in most cases. In this scenario, self-reported attributes are more important than the attributes collected by sensors, except “glucose\_level”.

## 3.2 Impact of Hyperparameters

We select four important hyperparameters of GAM to figure out the impact of these hyperparameters, including the hidden size ( $H$ ) of GRU-based memory, no. of heads ( $M$ ) of GAT, no. of layers ( $L$ ) of GAT and historical sequence length ( $T$ ).

**Table 3.12:** In terms of MAE (mg/dL), the impact of selecting attributes ( $W = 12$ ), where 6 attributes are “glucose\_level”, “meal”, “bolus”, “finger\_stick”, “sleep” and “exercise”.

Method	559	563	570	575	588	591	540	544	552	567	584	596	Average
GAM 6 attributes + basal	22.677	21.253	20.745	24.419	21.933	25.173	29.481	19.131	22.084	27.153	27.665	19.916	23.469
GAM 6 attributes + basis_skin_Temperature	<b>22.084</b>	20.806	19.388	24.574	21.814	25.450	28.760	18.827	22.120	26.488	27.008	<b>18.804</b>	23.010
GAM 6 attributes + basis_gsr	22.954	20.900	19.430	24.580	21.476	25.652	28.640	19.406	22.438	27.231	<b>26.930</b>	18.950	23.216
GAM 6 attributes + basis_sleep	22.813	21.104	19.103	<b>24.333</b>	21.392	<b>24.780</b>	29.487	19.447	<b>21.713</b>	26.866	27.524	18.903	23.122
GAM 6 attributes + acceleration	22.989	21.166	19.923	24.653	21.518	25.049	28.988	19.269	21.959	27.990	27.282	18.811	23.300
GAM 6 attributes + work	23.426	21.306	19.551	24.343	21.137	25.340	29.078	<b>18.694</b>	22.234	27.641	26.874	19.061	23.224
GAM 6 attributes + basis_steps	22.953	20.964	19.545	24.707	22.111	25.355	29.460	19.192	22.082	27.663	27.695	19.243	23.414
GAM 6 attributes + basis_heart_rate	22.570	21.064	19.202	24.719	22.224	24.985	29.155	19.144	22.056	27.671	27.149	19.258	23.266
GAM 6 attributes + basis_air_temperature	22.750	20.876	19.880	25.250	22.529	25.317	29.282	19.004	21.875	27.678	27.435	19.162	23.420
GAM 6 attributes + day_of_week	22.740	20.760	19.549	24.580	21.337	25.259	29.446	19.096	21.777	28.126	27.810	18.679	23.263
GAM 6 attributes + total_seconds	22.889	<b>20.696</b>	<b>19.017</b>	24.531	<b>20.985</b>	25.190	<b>28.347</b>	18.772	21.917	<b>26.465</b>	27.298	18.655	<b>22.897</b>
GAM 6 attributes	22.653	20.901	19.028	24.383	21.678	25.094	29.114	19.300	21.960	27.540	27.488	19.235	23.198

The hidden size ( $H$ ) controls the memory ability of GAM. Within certain limits, the larger the hidden size, the higher the memory ability. We use 5 different hidden sizes in this experiment, as  $H \in \{64, 128, 256, 512, 1024\}$ .

Changing the no. of heads ( $M$ ) can vary the representation ability of GAM. A larger  $M$  enables GAM to have multiple groups of attention weights, and graph embeddings have more ways to be merged with each other. For example, if the “glucose\_level” node and “meal” node are activated, they can generate and send messages to each other. If  $M = 1$ , in terms of “glucose\_level” node, it may only summarize the messages from “glucose\_level” node and “meal” node via a group of weights (0.8, 0.2). If  $M = 2$ , in terms of “glucose\_level” node, apart from the group of weights (0.8, 0.2), the “glucose\_level” node may have one more group of weights, e.g., (0.6, 0.4) to aggregate messages that it has received. As for node  $i$ , it will generate  $M$  new tensors after aggregating messages, and these tensors will be further aggregated to one tensor based on Equation 2.4. We use 5 different no. of heads, as  $M \in \{1, 2, 3, 4, 5\}$ .

Varying no. of layers ( $L$ ) of GAT can also change the representation ability of GAM from another perspective. A larger  $L$  makes the GAM more powerful. For example, if  $L = 1$ , in terms of “glucose\_level” node, the node can only receive messages from the adjacent nodes. If  $L = 2$ , in the first layer, the message sending and receiving are the same as the process of  $L = 1$ . In the second layer, even though the “glucose\_level” node still continuously receives messages from the adjacent nodes, the messages are not the original graph embedding. The received messages have been mixed from the previous layer before aggregating, so deeper layer make graph messages merge with each other more times in a complicated way, similar to extending the no. of layers of convolution neural networks (CNNs). We use 5 different no. of layers in this experiment, as  $H \in \{1, 2, 3, 4, 5\}$ .

The historical length  $T$  of RMTS decides how much past information is considered in the prediction. A larger  $T$  means more historical records are leveraged. We use 5 different historical length  $T$  in this experiment, as  $T \in \{6, 12, 24, 32, 48\}$ .

**Hyperparameter settings:** prediction window is  $W = 6$  or  $W = 12$ . When

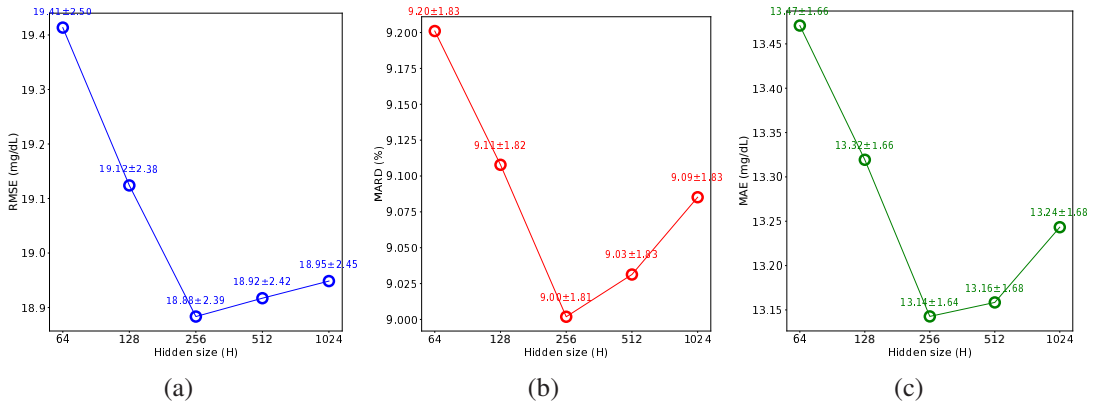


Figure 3.1: The impact of changing hidden size ( $H$ ) when  $W = 6$ .

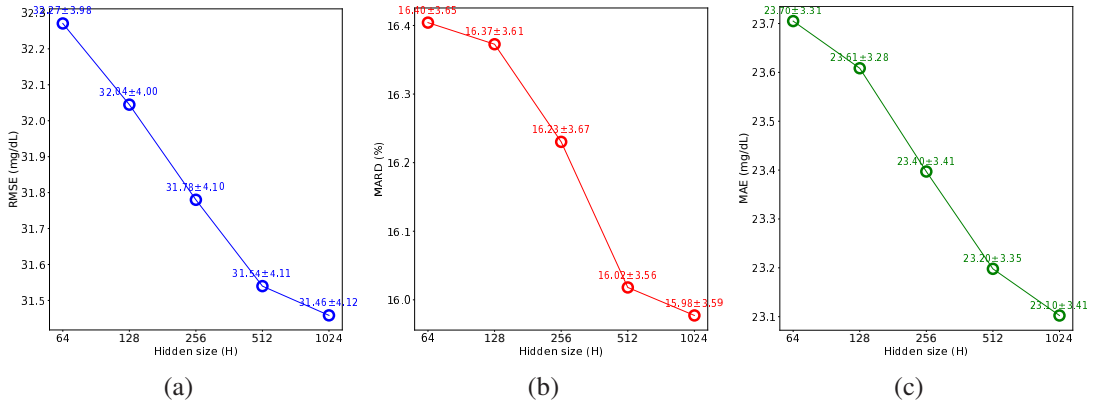


Figure 3.2: The impact of changing hidden size ( $H$ ) when  $W = 12$ .

hidden size  $H$  changes, other hyperparameters are fixed, as  $M = 1$ ,  $L = 2$  and  $T = 24$ . When no. of heads  $M$  varies, other hyperparameters are fixed, as  $H = 512$ ,  $L = 2$  and  $T = 24$ . When no. of layers  $L$  changes, other hyperparameters are fixed, as  $H = 512$ ,  $M = 1$  and  $T = 24$ . When the length of the historical time series ( $T$ ) changes, other hyperparameters are fixed, as  $H = 512$ ,  $M = 1$  and  $L = 2$ . The training algorithm is based on Algorithm 1, and no. of global training epochs in the first or second training step is  $T^{global} = 10,000$  or  $T^{person} = 800$ ; evaluation interval in the first or second training step is  $T^{eval1} = 1,000$  or  $T^{eval2} = 160$ ; batch size is  $B = 128$ ; learning rate in the first or second training step is 0.001 or 0.00001.

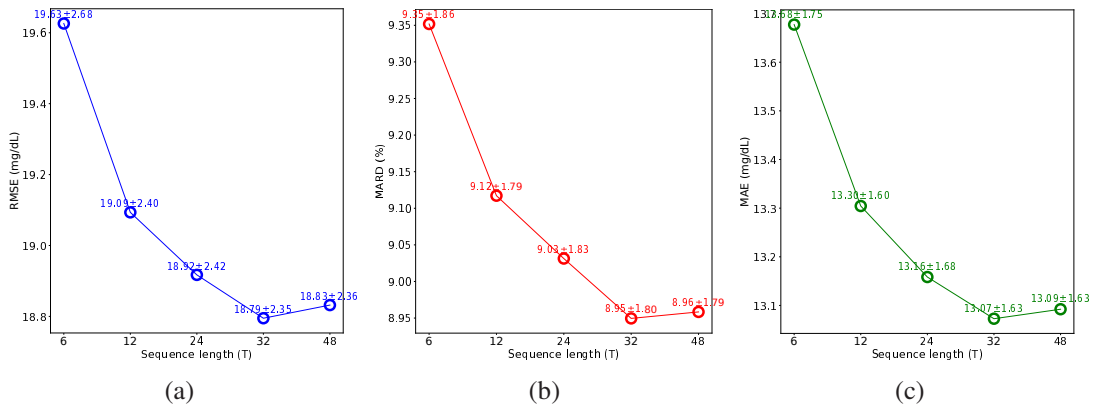


Figure 3.3: The impact of changing sequence length ( $T$ ) when  $W = 6$ .

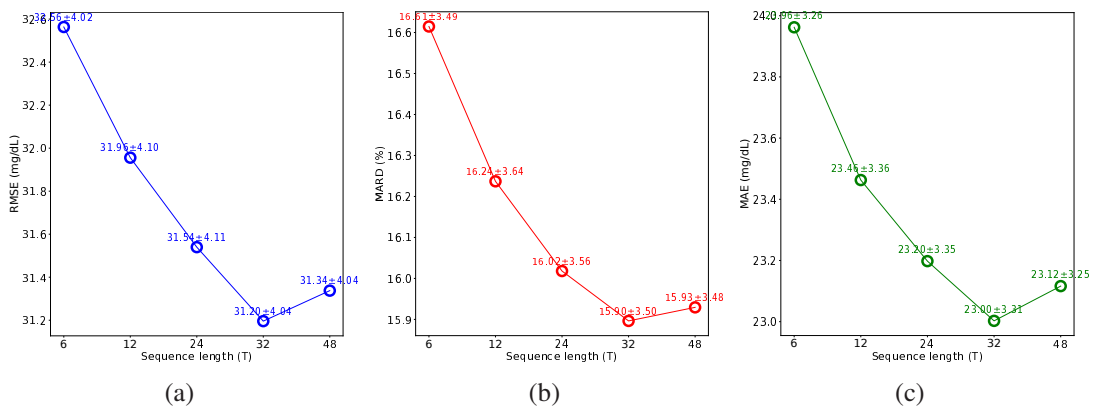


Figure 3.4: The impact of changing sequence length ( $T$ ) when  $W = 12$ .

### 3.2.1 Experiment Settings

### 3.2.2 Result Analysis

The impact of hidden size ( $H$ ) can be seen in Figures 3.1-3.2. We can find that if  $W = 6$ , GAM achieves the best performance when  $H = 256$ . Larger  $H$ , i.e.,  $H = 512$  and  $H = 1024$ , will not lead to better performance. Interestingly, when  $W = 12$ , the performance is obviously improved when increasing  $H$  from 64 to 1024. This is because when the prediction window  $W$  gets larger, the prediction is more challenging, and more historical information is needed to refer to. Larger  $H$  enables GAM to memorize more past information. When the prediction window is not very large, i.e.  $W = 6$ , more history, i.e.,  $H > 256$ , brings more unnecessary information, contributing to relatively worse performance. On the other hand, we can hold the view that the hidden size ( $H$ ) can obviously affect the whole performance. For



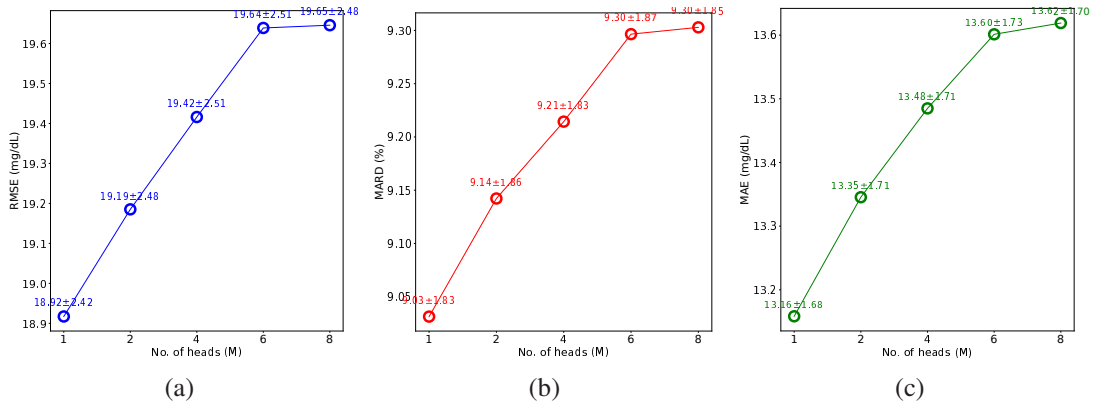


Figure 3.5: The impact of changing no. of heads ( $M$ ) when  $W = 6$ .

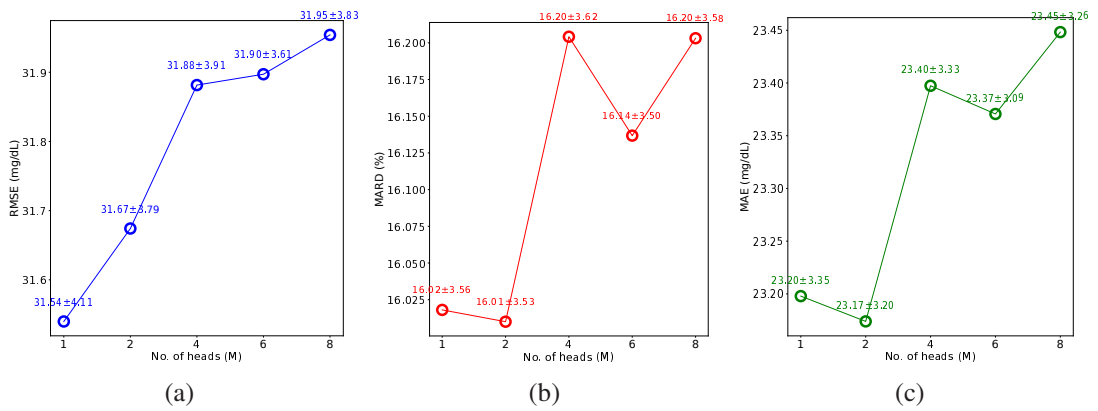


Figure 3.6: The impact of changing no. of heads ( $M$ ) when  $W = 12$ .

example, when  $W = 6$  and  $H = 256$ , the average RMSE is 18.88 mg/dL, while the average RMSE changed to 19.41 mg/dL when  $H = 64$  (see Figure 3.1(a)). Similarly, in Figures 3.3-3.4, we can also find that within a certain range, increasing  $T$  can obviously and positively affect performance. For example, in Figure 3.3(a), when increase  $T$  from 6 to 32, the average RMSE decreases from 19.63 mg/dL to 18.79 mg/dL. This is because larger  $T$  provides GAM with more useful historical information.

The sensitivity of no. of heads  $M$  can be viewed in Figures 3.5-3.6. We can draw a conclusion that more heads cannot enable better performance in this scenario. Meanwhile, from Figure 3.7-3.8, within certain ranges, increasing  $L$  only brings minor improvements. For example, in terms of RMSE, when increase  $L$  from 1 to 4, the average RMSE is improved from 19.02 mg/dL to 18.85 mg/dL (see Figure 3.7(a)). Hence, we can hold the view that compared with  $H$  and  $T$ , increas-



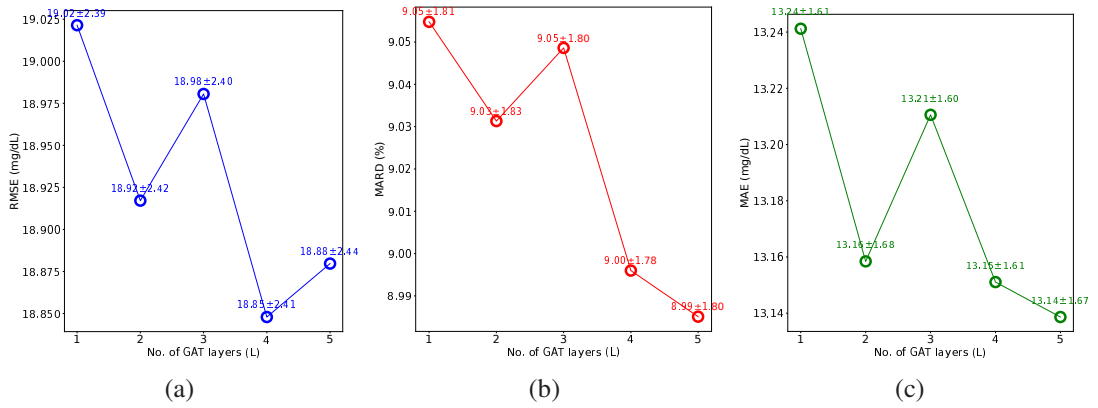


Figure 3.7: The impact of changing no. of layers ( $L$ ) when  $W = 6$ .

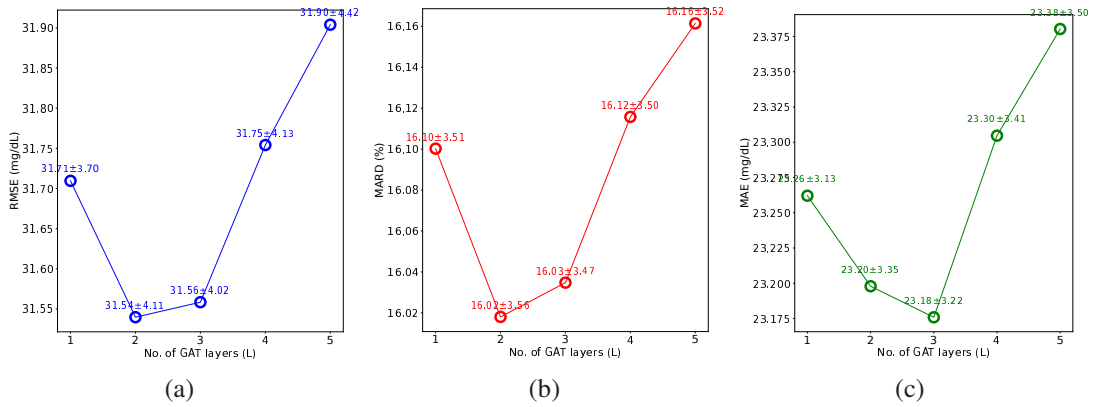


Figure 3.8: The impact of changing no. of layers ( $L$ ) when  $W = 12$ .

ing the ability of GAT, i.e.,  $M$  and  $L$ , cannot bring about obvious improvements in this scenario. This is because the correlations among these attributes are not very complex, so it does not need a very powerful GAT. More powerful GAT to model simple correlations might cause overfitting, increasing RMSE, MARD and MAE.

In summary, temporal hyperparameters  $H$  and  $T$  are relatively more important in this scenario. They control the storing ability and the amount of historical information infused into the neural networks. They can significantly affect the model's performance. However, increasing the hyperparameters, i.e.,  $M$  and  $L$ , of GAT cannot obviously improve the prediction accuracy, and it may even worsen the performance in some cases since the correlations among the attribute are not very complex.

## 3.3 Impact of FL

### 3.3.1 Experiment Settings

Introducing FL can keep the privacy of participants in a great manner. However, it may sacrifice some prediction accuracy. This experiment tries to figure out how much prediction ability is lost when considering FL in the training process. Hence, we directly compare the performance of “GAM + 6 attributes” with “GAM + 6 attributes + FL”. In order to show that the reduction in performance is not caused by our proposed model when incorporating FL. We also introduce LSTM [Hochreiter and Schmidhuber, 1997] and use the same training algorithm to figure out whether leveraging FL will worsen the model performance. Hence, we also compare the performance of “LSTM + 6 attributes” with “LSTM + 6 attributes + FL”. Besides, we leverage LSTM to show whether using FL will reduce the bonus of other attributes excluding “glucose\_level”. Therefore, we need to compare the performance of “LSTM + glucose\_level + FL” with “LSTM + 6 attributes + FL”.

The reason why we introduce LSTM rather than other methods for comparisons is that LSTM is relatively more lightweight, which is suitable and applicable to mobile devices. Given that the target of FL is to leverage the computational resources in mobile devices and to utilize the data generated in the mobile devices directly, how many computational resources the model need should be concerned carefully. This is why we did not use N-BEATS [Oreshkin et al., 2020] based method for comparisons, even though an N-BEATS based method [Rubin-Falcone et al., 2020] achieved first place in the BGLP 2020 challenge, but N-BEATS based method needs very deep layers to improve the performance. On the contrary, only one layer of LSTM can still achieve a satisfying performance [Bevan and Coenen, 2020].

LSTM is a self-gated recurrent neural network, as:

$$\mathbf{i}_t = \sigma(\mathbf{W}_{xi}\mathbf{x}_t + b_{xi} + \mathbf{W}_{hi}\mathbf{h}_{t-1} + b_{hi}), \quad (3.1a)$$

$$\mathbf{f}_t = \sigma(\mathbf{W}_{xf}\mathbf{x}_t + b_{xf} + \mathbf{W}_{hf}\mathbf{h}_{t-1} + b_{hf}), \quad (3.1b)$$

$$\mathbf{j}_t = \tanh(\mathbf{W}_{xj}\mathbf{x}_t + b_{xj} + \mathbf{W}_{hj}\mathbf{h}_{t-1} + b_{hj}), \quad (3.1c)$$

$$\mathbf{o}_t = \sigma(\mathbf{W}_{xo}\mathbf{x}_t + b_{xo} + \mathbf{W}_{ho}\mathbf{h}_{t-1} + b_{ho}), \quad (3.1d)$$

$$\mathbf{c}_t = \mathbf{f}_t * \mathbf{c}_{t-1} + \mathbf{i}_t * \mathbf{j}_t, \quad (3.1e)$$

$$\mathbf{h}_t = \mathbf{o}_t * \tanh(\mathbf{c}_t), \quad \forall t \in \{1, \dots, T\}, \quad (3.1f)$$

where  $\mathbf{W}_{xi}, \mathbf{W}_{xf}, \mathbf{W}_{xj}, \mathbf{W}_{xo} \in \mathbb{R}^{E \times H}$  and  $\mathbf{W}_{hi}, \mathbf{W}_{hf}, \mathbf{W}_{hj}, \mathbf{W}_{ho} \in \mathbb{R}^{H \times H}$  are learnable weights;  $\mathbf{x}_t$  is defined in section 2.1. First of all, the current input  $\mathbf{x}_t$  and previous hidden state  $\mathbf{h}_{t-1}$  will be mapped to an input gate  $\mathbf{i}_t$ , forget gate  $\mathbf{f}_t$ , new information  $\mathbf{j}_t$  and output gate  $\mathbf{o}_t$ , as Equation (3.1a)-(3.1d). In Equation (3.1e), when forget gate  $\mathbf{f}_t$  is activated ( $\mathbf{f}_t$  is close to  $\mathbf{0}$ ), all historical information of the previous cell state  $\mathbf{c}_{t-1}$  is ignored, and it is not passed to the current cell state  $\mathbf{c}_t$ . When the input gate  $\mathbf{i}_t$  is activated ( $\mathbf{i}_t$  is close to  $\mathbf{1}$ ), all the new information of  $\mathbf{j}_t$  can be infused to the current cell state  $\mathbf{c}_t$ . Hence, with the help of the input gate  $\mathbf{i}_t$  and forget gate  $\mathbf{f}_t$ , LSTM can decide how much historical information and new information should be aggregated to the current cell state  $\mathbf{c}_t$ . Comparably, the output gate  $\mathbf{o}_t$  can decide how much information of the current cell state  $\mathbf{c}_t$  can be passed to the current hidden state  $\mathbf{h}_t$ . The self-gated mechanism helps LSTM to avoid gradient descent problems by leveraging an accumulator  $\mathbf{c}_t$ . Finally, we use Equation (2.1e) to estimate the future blood glucose level  $\hat{y}_{T+W}$ .

**Hyperparameter settings:** prediction window is  $W = 6$  or  $W = 12$ ; historical sequence length  $T = 48$ ; both GRU and LSTM hidden size are  $H = 512$ ; no. of heads  $M = 1$ ; no. of GAT layers  $L = 2$ . The training algorithm of ‘‘GAM + 6 attributes’’ and ‘‘LSTM + 6 attributes’’ are based on Algorithm 1, and no. of global training epochs in the first or second training step is  $T^{global} = 15,000$  or  $T^{person} = 1,600$ ; evaluation interval in the first or second training step is  $T^{eval1} = 1,000$  or  $T^{eval2} = 160$ ; batch size is  $B = 128$ ; learning rate in the first or second training step

**Table 3.13:** In terms of RMSE (mg/dL), the impact of FL ( $W = 6$ ), where 6 attributes are “glucose\_level”, “meal”, “bolus”, “finger\_stick”, “sleep” and “exercise”.

Method	559	563	570	575	588	591	540	544	552	567	584	596	Average
LSTM + glucose_level + FL	20.357	18.556	19.789	23.682	18.912	22.589	23.261	18.332	17.746	23.366	23.876	18.312	20.732
LSTM + 6 attributes + FL	20.590	18.654	19.495	26.110	18.139	22.079	21.990	18.083	17.059	22.931	24.275	18.195	20.633
LSTM + 6 attributes	18.664	18.117	17.166	23.804	17.083	21.130	21.568	16.512	16.842	21.969	22.372	16.765	19.333
GAM + 6 attributes + FL	20.156	18.589	18.988	25.059	17.890	22.030	21.960	17.376	17.543	23.269	24.708	18.300	20.489
GAM + 6 attributes	19.222	17.926	16.337	21.677	17.010	20.833	20.816	15.784	16.463	21.619	21.486	15.864	18.753

is 0.001 or 0.00001.

The training algorithm of “GAM + 6 attributes + FL”, “LSTM + 6 attributes + FL” and “LSTM + 6 attributes + FL” are according to Algorithm 2, and no. of FL training epochs in the first training step (FL) are  $T^{total} = 50$  and  $T^{client} = 80$ ; no. of FL training epochs in the second training step is  $T^{person} = 1,600$ ; evaluation interval in the first or second training step is  $T^{eval1} = 2$  or  $T^{eval2} = 160$ ; batch size is  $B = 128$ ; learning rate in the first or second training step is 0.001 or 0.00001.

### 3.3.2 Result Analysis

In Tables 3.13-3.18, we can find that “GAT + 6 attributes” is consistently much better than “GAT + 6 attributes + FL”. For example, when  $W = 6$ , the average RMSE of “GAT + 6 attributes” is 18.753 mg/dL, while the average RMSE of “GAT + 6 attributes + FL” is 20.489 mg/dL (see Table 3.13). We will have a similar observation when comparing “LSTM + 6 attributes” with “LSTM + 6 attributes + FL”. For instance, the average RMSE of “LSTM + 6 attributes” is 19.333 mg/dL when  $W = 6$ , while the average RMSE of “LSTM + 6 attributes + FL” is 20.633 mg/dL. Accordingly, we can conclude that introducing FL sacrifices some prediction accuracy, and it is not caused by the unstable of our proposed model.

Furthermore, “GAM + 6 attributes” is consistently better than “LSTM + 6 attributes”. “GAM + 6 attributes + FL” is better than “LSTM + 6 attributes + FL” in most cases. It shows that our proposed model, GAM, is better than LSTM. Besides, when comparing “LSTM + 6 attributes + FL” with “LSTM + glucose\_level + FL”, there is a minor improvement when considering other attributes, excluding “glucose\_level”, in FL. We suppose that FL worsens the model performance by reducing the benefits of considering other attributes.

**Table 3.14:** In terms of MARD (%), the impact of FL ( $W = 6$ ), where 6 attributes are “glucose\_level”, “meal”, “bolus”, “finger\_stick”, “sleep” and “exercise”.

Method	559	563	570	575	588	591	540	544	552	567	584	596	Average
LSTM + glucose_level + FL	9.404	8.086	6.124	10.747	8.306	12.676	11.730	8.882	10.002	11.594	11.625	9.427	9.883
LSTM + 6 attributes + FL	9.150	8.101	6.046	11.297	7.942	12.601	11.133	8.125	9.395	11.399	11.938	9.368	9.708
LSTM + 6 attributes	8.479	7.856	5.456	10.240	7.452	12.109	10.865	7.664	9.219	10.765	10.809	8.724	9.136
GAM + 6 attributes + FL	9.121	8.099	5.901	10.904	7.842	12.356	10.991	8.050	9.836	12.064	12.181	9.333	9.723
GAM + 6 attributes	8.709	7.700	5.267	9.330	7.387	11.853	10.412	7.437	9.077	10.746	10.459	8.343	8.893

**Table 3.15:** In terms of MAE (mg/dL), the impact of FL ( $W = 6$ ), where 6 attributes are “glucose\_level”, “meal”, “bolus”, “finger\_stick”, “sleep” and “exercise”.

Method	559	563	570	575	588	591	540	544	552	567	584	596	Average
LSTM + glucose_level + FL	14.054	12.900	12.430	15.391	13.781	15.995	16.889	13.091	13.008	15.718	16.951	12.852	14.422
LSTM + 6 attributes + FL	13.897	12.946	12.412	16.681	13.222	15.658	15.909	12.358	12.361	15.415	17.473	12.569	14.242
LSTM + 6 attributes	12.662	12.612	11.011	14.880	12.426	15.091	15.689	11.680	12.129	14.644	16.024	11.649	13.375
GAM + 6 attributes + FL	13.826	12.918	11.929	15.989	13.034	15.560	15.835	12.005	12.891	16.072	17.805	12.599	14.205
GAM + 6 attributes	12.921	12.449	10.713	13.499	12.452	14.915	14.995	11.312	11.963	14.600	15.415	11.100	13.028

## 3.4 Impact of Time-Aware Attention

### 3.4.1 Experiment Settings

According to the results of section 3.1.2, we can find that temporal features, i.e., “day\_of\_week” and “total\_seconds” cannot obviously improve the performance of our model. However, in section 2.5.2, we can find some apparent temporal features which are relevant to the variations of “glucose\_level”, when we analyze the processed “glucose\_level” data. Given that we use zero padding to make adjacent tensors, i.e.,  $\mathbf{x}_t$  and  $\mathbf{x}_{t+1}$ , of RMTS have equal time intervals, i.e., 5 minutes. Hence, maybe our proposed model can infer some temporal features from RMTS directly, which is already enough for the predictions, and no more temporal features are

**Table 3.16:** In terms of RMSE (mg/dL), the impact of FL ( $W = 12$ ), where 6 attributes are “glucose\_level”, “meal”, “bolus”, “finger\_stick”, “sleep” and “exercise”.

Method	559	563	570	575	588	591	540	544	552	567	584	596	Average
LSTM + glucose_level + FL	34.438	30.795	32.335	37.425	31.505	34.621	43.097	31.124	30.504	38.700	38.626	29.905	34.423
LSTM + 6 attributes + FL	34.052	30.581	30.928	39.173	30.774	33.938	41.058	31.602	32.694	38.883	38.722	29.322	34.310
LSTM + 6 attributes	31.428	29.078	29.238	34.465	29.380	33.414	38.641	28.268	29.433	37.275	36.547	27.067	32.019
GAM + 6 attributes + FL	35.751	29.722	30.567	39.775	29.666	34.028	40.754	28.391	30.598	39.585	40.051	28.198	33.924
GAM + 6 attributes	31.616	29.578	26.776	33.806	28.416	32.911	38.348	26.916	28.410	37.073	36.098	25.352	31.275

**Table 3.17:** In terms of MARD (%), the impact of FL ( $W = 12$ ), where 6 attributes are “glucose\_level”, “meal”, “bolus”, “finger\_stick”, “sleep” and “exercise”.

Method	559	563	570	575	588	591	540	544	552	567	584	596	Average
LSTM + glucose_level + FL	17.770	13.860	11.030	18.578	13.900	21.424	21.996	16.689	17.952	21.872	19.849	16.591	17.626
LSTM + 6 attributes + FL	17.254	14.113	10.477	19.025	13.426	21.120	21.346	14.558	19.185	22.008	20.299	15.578	17.366
LSTM + 6 attributes	16.230	12.922	10.287	16.981	12.654	20.850	20.526	13.981	17.013	21.051	18.640	14.930	16.339
GAM + 6 attributes + FL	17.473	13.202	10.335	19.321	13.012	21.737	21.345	13.360	18.559	22.629	21.054	15.740	17.314
GAM + 6 attributes	15.658	12.857	9.819	16.701	12.166	20.668	19.812	12.739	16.994	20.837	18.759	13.822	15.903

**Table 3.18:** In terms of MAE (mg/dL), the impact of FL ( $W = 12$ ), where 6 attributes are “glucose\_level”, “meal”, “bolus”, “finger\_stick”, “sleep” and “exercise”.

Method	559	563	570	575	588	591	540	544	552	567	584	596	Average
LSTM + glucose_level + FL	25.717	22.508	22.347	26.522	23.092	26.257	32.182	24.032	23.046	28.775	28.989	22.148	25.468
LSTM + 6 attributes + FL	25.169	22.593	21.394	27.618	22.764	25.474	30.626	22.097	24.849	28.600	29.226	21.020	25.119
LSTM + 6 attributes	23.063	21.018	20.527	23.997	21.381	25.074	29.473	21.077	22.309	27.453	27.281	19.880	23.544
GAM + 6 attributes + FL	26.123	21.363	20.888	27.969	21.991	25.761	31.136	20.321	23.648	29.232	30.220	20.934	24.966
GAM + 6 attributes	22.763	20.872	19.400	23.913	20.883	25.008	28.947	19.523	21.853	27.455	27.161	18.501	23.023

needed. For example, given  $[\mathbf{x}_1, \dots, \mathbf{x}_{12}]$ , the model can infer that the total period of this RMTS is 1 hour, and the model can also infer the time interval between any  $\mathbf{x}_t$  ( $t > 1$ ) and  $\mathbf{x}_1$ . Maybe the inference of temporal features is enough, or our proposed model cannot leverage temporal features.

In order to find the answers to the above questions, we firstly compare “LSTM + 6 attributes” with “LSTM + 6 attributes + total\_seconds”. If “LSTM + 6 attributes + total\_seconds” is also worse than “LSTM + 6 attributes”, which is the same as the observation in section 3.1.2, we can hold the view that bad performance caused by introducing temporal features is not the problem of our proposed model. Otherwise, the problem may be attributed to our proposed model. On the other hand, we want to add time-aware attention (TA, Liu et al. [2022]) to GAM so as to find whether the temporal features can be utilized by introducing a new module. Therefore, we need to compare “GAT + 6 attributes” with “GAT + TA + 6 attributes + total\_seconds”, and the time-aware attention is as follows ( $t, t' \in \mathcal{T}$ ):

$$\beta_t = \frac{\exp(\mathbf{f}^{time}(d_t)^\top \mathbf{W}^{TA} \mathbf{f}^{time}(d_{T+W}))}{\sum_{t'} \exp(\mathbf{f}^{time}(d_{t'})^\top \mathbf{W}^{TA} \mathbf{f}^{time}(d_{T+W}))}, \quad \forall t \in \mathcal{T} \quad (3.2a)$$

$$\mathbf{h}'_T = \sum_t \beta_t \mathbf{h}_t, \quad (3.2b)$$

where  $d_t \in \mathbb{R}^1$  is the “total\_seconds” of the time slot  $t$ , and “total\_seconds” is explained in section 3.1.1;  $\mathbf{f}^{time}(\cdot)$  maps a scalar  $d_t$  to a tensor, as  $\mathbf{f}^{time}(d_t) \in \mathbb{R}^{E'}$ ;  $\mathbf{W}^{TA} \in \mathbb{R}^{E' \times E'}$  is learnable parameters;  $\mathbf{h}_t$  is the hidden state of Equation (2.1d).

$\mathbf{f}^{time}(d_t)^\top \mathbf{W}^{TA} \mathbf{f}^{time}(d_{T+W})$  calculates a similarity score between  $d_t$  and  $d_{T+W}$ , where  $\forall t \in \mathcal{T}$ . The normalized score is the time-aware attention weight  $\beta_t$  (see Equation 3.2a). In terms of time slot  $t$ , if the temporal feature of  $t$  is more relevant with  $T + W$ , the time-aware attention weight  $\beta_t$  is larger. Then, more information

**Table 3.19:** In terms of RMSE (mg/dL), the impact of TA ( $W = 6$ ), where 6 attributes are “glucose\_level”, “meal”, “bolus”, “finger\_stick”, “sleep” and “exercise”.

Method	559	563	570	575	588	591	540	544	552	567	584	596	Average
LSTM + 6 attributes + total_seconds	18.555	17.606	17.496	22.419	17.075	20.720	21.778	16.292	16.594	21.860	22.538	16.359	19.108
GAM + TA + 6 attributes + total_seconds	19.704	20.303	17.941	22.811	18.176	21.580	23.184	16.859	17.311	22.856	23.032	17.544	20.108
LSTM + 6 attributes	18.664	18.117	17.166	23.804	17.083	21.130	21.568	16.512	16.842	21.969	22.372	16.765	19.333
GAM + 6 attributes	19.222	17.926	16.337	21.677	17.010	20.833	20.816	15.784	16.463	21.619	21.486	15.864	18.753

**Table 3.20:** In terms of MARD (%), the impact of TA ( $W = 6$ ), where 6 attributes are “glucose\_level”, “meal”, “bolus”, “finger\_stick”, “sleep” and “exercise”.

Method	559	563	570	575	588	591	540	544	552	567	584	596	Average
LSTM + 6 attributes + total_seconds	8.370	7.745	5.545	9.852	7.349	12.008	10.706	7.579	8.962	10.796	10.909	8.622	9.037
GAM + TA + 6 attributes + total_seconds	9.162	8.656	6.137	10.300	7.768	12.375	11.881	7.896	9.737	12.012	11.513	9.202	9.720
LSTM + 6 attributes	8.479	7.856	5.456	10.240	7.452	12.109	10.865	7.664	9.219	10.765	10.809	8.724	9.136
GAM + 6 attributes	8.709	7.700	5.267	9.330	7.387	11.853	10.412	7.437	9.077	10.746	10.459	8.343	8.893

of  $\mathbf{h}_t$  is passed to  $\mathbf{h}'_T$  (see Equation 3.2b). This mechanism enables the estimation to leverage the information from  $\{\mathbf{h}_1, \dots, \mathbf{h}_t, \dots, \mathbf{h}_T\}$  with the time-aware attention weights rather than only utilizing  $\mathbf{h}_T$ . The focus of the time-aware attention weights is decided by the temporal features of the target time slot, i.e.,  $T + W$ . Compared with only using the information of  $\mathbf{h}_T$ , this mechanism may further leverage some distant historical information which has been forgotten by the GRU memory. In this way, GAM can explicitly leverage temporal features.

**Hyperparameter settings:** prediction window is  $W = 6$  or  $W = 12$ ; historical sequence length  $T = 48$ ; both GRU and LSTM hidden size are  $H = 512$ ; no. of heads  $M = 1$ ; no. of GAT layers  $L = 2$ . The training algorithm is based on Algorithm 1, and no. of global training epochs in the first or second training step is  $T^{global} = 15,000$  or  $T^{person} = 1,600$ ; evaluation interval in the first or second training step is  $T^{eval1} = 1,000$  or  $T^{eval2} = 160$ ; batch size is  $B = 128$ ; learning rate in the first or second training step is 0.001 or 0.00001.

### 3.4.2 Result Analysis

From Tables 3.19-3.24, we have some observations. Compared with “LSTM + 6 attributes”, after including temporal features, “LSTM + 6 attributes + total\_seconds”

**Table 3.21:** In terms of MAE (mg/dL), the impact of TA ( $W = 6$ ), where 6 attributes are “glucose\_level”, “meal”, “bolus”, “finger\_stick”, “sleep” and “exercise”.

Method	559	563	570	575	588	591	540	544	552	567	584	596	Average
LSTM + 6 attributes + total_seconds	12.675	12.421	11.164	14.313	12.326	14.915	15.619	11.524	11.851	14.644	16.097	11.431	13.248
GAM + TA + 6 attributes + total_seconds	13.759	14.214	12.058	14.695	13.316	15.455	17.169	11.948	12.692	15.962	16.688	12.219	14.181
LSTM + 6 attributes	12.662	12.612	11.011	14.880	12.426	15.091	15.689	11.680	12.129	14.644	16.024	11.649	13.375
GAM + 6 attributes	12.921	12.449	10.713	13.499	12.452	14.915	14.995	11.312	11.963	14.600	15.415	11.100	13.028



**Table 3.22:** In terms of RMSE (mg/dL), the impact of TA ( $W = 12$ ), where 6 attributes are “glucose\_level”, “meal”, “bolus”, “finger\_stick”, “sleep” and “exercise”.

Method	559	563	570	575	588	591	540	544	552	567	584	596	Average
LSTM + 6 attributes + total_seconds	32.550	29.456	29.255	34.727	29.044	32.738	38.774	27.057	29.716	36.582	36.972	27.267	32.011
GAM + TA + 6 attributes + total_seconds	34.653	33.940	29.479	33.819	32.195	34.490	43.031	29.283	30.606	39.103	38.528	27.596	33.893
LSTM + 6 attributes	31.428	29.078	29.238	34.465	29.380	33.414	38.641	28.268	29.433	37.275	36.547	27.067	32.019
GAM + 6 attributes	31.616	29.578	26.776	33.806	28.416	32.911	38.348	26.916	28.410	37.073	36.098	25.352	31.275

**Table 3.23:** In terms of MARD (%), the impact of TA ( $W = 12$ ), where 6 attributes are “glucose\_level”, “meal”, “bolus”, “finger\_stick”, “sleep” and “exercise”.

Method	559	563	570	575	588	591	540	544	552	567	584	596	Average
LSTM + 6 attributes + total_seconds	16.403	13.237	10.164	17.072	12.663	20.650	19.974	13.109	17.546	19.933	18.955	14.903	16.217
GAM + TA + 6 attributes + total_seconds	17.394	14.533	10.963	17.814	13.949	22.338	22.278	13.673	18.591	22.813	20.167	15.176	17.474
LSTM + 6 attributes	16.230	12.922	10.287	16.981	12.654	20.850	20.526	13.981	17.013	21.051	18.640	14.930	16.339
GAM + 6 attributes	15.658	12.857	9.819	16.701	12.166	20.668	19.812	12.739	16.994	20.837	18.759	13.822	15.903

is consistently better. For example, in Table 3.19, the average RMSE of “LSTM + 6 attributes + total\_seconds” is 19.108 mg/dL, while the average RMSE of “LSTM + 6 attributes” is 20.108 mg/dL. In Table 3.22, the average RMSE of “LSTM + 6 attributes + total\_seconds” is 32.011 mg/dL, while the average RMSE of “LSTM + 6 attributes” is 33.893 mg/dL. Hence, introducing temporal features do helpful for the BGLP-RMTS.

However, even though the temporal features can positively affect the prediction tasks, our proposed model still failed to leverage temporal features (see section 3.1.2). In this experiment, when explicitly utilizing temporal features by adding time-aware attention to GAM, “GAM + TA + 6 attribute + total\_seconds” is consistently worse than “GAM + 6 attribute”. For example, in Table 3.19, the average RMSE of “GAM + TA + 6 attribute + total\_seconds” is 19.333 mg/dL, while the average RMSE of “GAM + 6 attribute” is 18.753 mg/dL. In Table 3.22, the average RMSE of “GAM + TA + 6 attribute + total\_seconds” is 32.019 mg/dL, while the average RMSE of “GAM + 6 attribute” is 31.275 mg/dL. Explicitly modeling temporal features by GAM still cannot improve the performance.

Hence, according to the above observations and some guesses (see the first

**Table 3.24:** In terms of MAE (mg/dL), the impact of TA ( $W = 12$ ), where 6 attributes are “glucose\_level”, “meal”, “bolus”, “finger\_stick”, “sleep” and “exercise”.

Method	559	563	570	575	588	591	540	544	552	567	584	596	Average
LSTM + 6 attributes + total_seconds	24.249	21.358	20.127	24.358	21.278	24.742	29.211	19.918	22.572	26.254	27.626	19.823	23.460
GAM + TA + 6 attributes + total_seconds	25.543	24.167	21.509	24.517	23.782	26.610	32.683	21.115	23.899	29.167	29.235	20.162	25.199
LSTM + 6 attributes	23.063	21.018	20.527	23.997	21.381	25.074	29.473	21.077	22.309	27.453	27.281	19.880	23.544
GAM + 6 attributes	22.763	20.872	19.400	23.913	20.883	25.008	28.947	19.523	21.853	27.455	27.161	18.501	23.023



paragraph of section 3.4.1), we further guess that maybe GAM can extract temporal features directly from the RMTS without “total\_seconds”, and more extra temporal features can be seen as redundancy, which might negatively affect the prediction performance.

## 3.5 Answers to the Research Questions

The research questions raised from the research proposal are answered as follows.

Question 1: can the correlations among multiple variables, e.g. glucose level, meal, insulin, sleep, etc., be modeled by graph neural networks?

The answer to Question 1: according to the observations and conclusions of section 3.1.2, we find that there are 6 attributes, i.e., “glucose\_level”, “meal”, “bolus”, “finger\_stick”, “sleep” and “exercise” are helpful for the BGLP-RMTS when leveraging graph attention based sequential neural network, i.e., GAM. Besides, in section 3.3.2, we can obviously observe the benefits when using a graph-based structure compared with a purely LSTM-based method. However, in section 3.2.2, we can find that the benefits are limited because we guess the correlations among these attributes are not very complex, and the graph structure should not be very sophisticated, i.e., very large no. of heads  $M$  or layers  $L$ .

Question 2: can a time-aware attention mechanism directly deal with time series whose adjacent items have different time intervals?

The answer to Question 2: first of all, we transform IMTS into RMTS via zero padding. Then, based on the results of section 3.4.2, we find that a time-aware attention mechanism cannot further improve the performance of GAM when incorporating temporal features, i.e., “total\_seconds”. This may be because that RMTS has equal time intervals between the adjacent items, and some temporal features might be directly inferred (see the first paragraph of section 3.4.1). Besides, the memory of GAM is based on GRU which is good at dealing with RMTS rather than IMTS.

Question 3: in order to protect patient privacy, can a non-personalized model be trained with fully decentralized local data aided by federated learning?

The answer to Question 3: in section 3.3.2, we can observe the performance of FL in two different models, i.e., an LSTM-based model and a graph-based model. We can find that the two models sacrifice some prediction accuracy when introducing FL. Meanwhile, the benefits of considering more attributes are also reduced. Note that we do not use non-personalized models but use personalized models which are generated by fine-tuning the non-personalized model after FL. This is because we find that the body conditions and behaviors vary a lot among the participants in section 2.4.

## Chapter 4

# Discussion

In this chapter, we compare our proposed model with the methods in Ohio 2020 Challenge [Bach et al., 2020] in section 4.1. Then, we further analyze the selected 6 attributes, figuring out whether these attributes are helpful (see section 4.2). Next, we visualize the GAM and testing samples, showing that our proposed model is explainable (see section 4.3). Then, we discuss the convergence and training time of our proposed method (see section 4.4). Finally, we make a brief conclusion, discussing the advantages and limitations of this work, and we also talk about future work and research directions in section 4.5.

### 4.1 Compare with Other Methods

We compare our proposed method, GAM, with the top 8 methods in Ohio 2020 Challenge (see Table 4.1). These methods are also briefly explained as follows.

- **N-BEATS [Rubin-Falcone et al., 2020]:** this method was based on N-BEATS [Oreshkin et al., 2020]. They utilize OhioT1DM’18 (6 participants) and Tidepool data (100 participants) to pretrain the models. Then, they use 80% of the training data of OhioT1DM’20 for training and 20% of the training

**Table 4.1:** Compare with other methods in Ohio 2020 challenge.

Author	Method	RMSE (mg/dL, $W = 6$ )	MAE(mg/dL, $W = 6$ )	RMSE(mg/dL, $W = 12$ )	MAE(mg/dL, $W = 12$ )	Overall
Rubin-Falcone et al. [2020]	N-BEATS	18.22	12.83	31.66	23.60	86.31
Hameed and Kleinberg [2020]	RNN	19.21	13.08	31.77	23.09	87.15
	<b>GAM</b>	<b>18.77</b>	<b>13.39</b>	<b>32.04</b>	<b>23.86</b>	<b>88.06</b>
<b>Proposed model</b>	<b>GAM</b>	<b>18.77</b>	<b>13.39</b>	<b>32.04</b>	<b>23.86</b>	<b>88.06</b>
Zhu et al. [2020b]	GAN (GRU; CNN)	18.34	13.37	32.21	24.20	88.12
Yang et al. [2020]	Multi-Scale LSTM	19.05	13.50	32.03	23.83	88.41
Bevan and Coenen [2020]	LSTM+Attention	18.23	14.37	31.10	25.75	89.45
Sun et al. [2020]	Latent-Variable-based Model	19.37	13.76	32.59	24.64	90.36
Joedicke et al. [2020]	Genetic Programming	19.60	14.25	34.12	25.99	93.96
Ma et al. [2020]	Residual compensation network	20.03	14.52	34.89	26.41	95.85

data for validation. They leverage 5 attributes for the predictions, including “glucose\_level”, “bolus”, “meal”, “finger\_stick”, “time\_of\_day”.

- **RNN [Hameed and Kleinberg, 2020]:** this approach was based on an RNN. They use OhioT1DM’18, excluding the last 20% of the data, to pretrain the models. Next, they use 100% of the training data of OhioT1DM’20 for training and the last 20% of the training data of OhioT1DM’18 for validation. They only use “glucose\_level” as the input.
- **GAN (GRU; CNN) [Zhu et al., 2020b]:** this model was based on GAN. They utilize OhioT1DM’18 to pretrain the models. Then, they use 80% of the training data of OhioT1DM’20 for training and 20% of the training data for validation. They consider 3 attributes for the predictions, i.e., “glucose\_level”, “bolus”, and “meal”.
- **Multi-Scale LSTM [Yang et al., 2020]:** this work was according to LSTM. They do not mention whether they pretrain the models. They use 90% of the training data of OhioT1DM’20 for training and 10% of the training data for validation. They consider 4 attributes for the predictions, and the attributes are “glucose\_level”, “bolus”, “meal” and “basal”.
- **LSTM + Attention [Bevan and Coenen, 2020]:** this work was also based on LSTM. They leverage OhioT1DM’18 to pretrain the models. They use 90% of the training data of OhioT1DM’20 for training and 10% of the training data for validation. They only consider “glucose\_level” for the predictions.
- **Latent-Variable-based Model [Sun et al., 2020]:** this work was based on latent variables. They do not mention whether they pretrain the models. They use 90% of the training data of OhioT1DM’20 for training and 10% of the training data for validation. They consider 3 attributes for the predictions, and the attributes are “glucose\_level”, “bolus” and “basal”.
- **Genetic Programming [Joedicke et al., 2020]:** this work was according to genetic programming. They consider many variables, e.g., “glucose\_level”,

“bolus”, “bolus\_type”, “basal”, “basis\_gsr” and “basis\_skin\_temperature”. Besides, they take some future attributes, including “bolus” and “basal”. The future attributes appear within  $[T + 1, T + W]$ , because they hold the view that the values of “bolus” and “basal” are predictable for the participants.

- **Residual compensation network [Ma et al., 2020]:** this work was based on the residual compensation network. They only consider “glucose\_level” as the input during the predictions.

In order to compare our proposed model with the baselines above, our model is also pretrained by OhioT1DM’18, followed by fine-tuning in OhioT1DM’20, based on Algorithm 1. We do not compare “GAM + FL” with the above baselines because FL obviously worsens the performance, and we mainly want to show the performance differences among these deep models. The hyperparameters are the same as the ones in section 3.4.1.

Overall, we can observe that our proposed model ranks third place. However, it cannot prove that our proposed model is worse than the top 2 models. This is because the N-BEATS-based model is pretrained by a super huge dataset which contains a hundred participants. In comparison, other methods are only pretrained/trained by relatively small datasets which contains 12 participants in total. On the other hand, the N-BEATS uses some special tricks. For example, they trained several models at a time with different hyperparameters, and they used the median of the predictions of these models as their final output. Even though they have an excellent performance, they cannot prove that such performance is caused by the model or the tricks. Similarly, the second method in Table 4.1 also leverages special tricks. For instance, they use the first 80% of data of OhioT1DM’18 to pretrain the models. Next, they use 100% of the training data of OhioT1DM’20 for training and the last 20% of the training data of OhioT1DM’18 for validation. Such cross validation method is much different from others. Different cross validations can affect the performance obviously since we can observe that 80%-20% cross validation methods (N-BEATS, RNN, GAM and GAN (GRU; CNN)) all perform better than 90%-10% cross validation methods (Multi-Scale LSTM, LSTM+Attention

## 4.2. DISCUSSION OF SELECTED ATTRIBUTES CHAPTER 4. DISCUSSION

**Table 4.2:** Distributions of “glucose\_level” and “finger\_stick” in hyperglycemia, normal, hypoglycemia and all samples.

PID	glucose_level (hypo)	glucose_level (normal)	glucose_level (hyper)	glucose_level (all)	finger_stick (hypo)	finger_stick (normal)	finger_stick (hyper)	finger_stick (all)
559	59.90±7.76	124.73±30.93	237.74±48.41	167.23±69.91	108.36±70.97	123.75±56.18	280.47±88.02	194.69±108.09
563	62.56±6.59	128.42±29.14	215.00±32.07	149.80±49.75	75.80±32.12	133.51±37.98	228.06±50.16	166.32±64.47
570	63.00±5.06	133.52±30.89	237.76±38.81	192.95±64.10	63.38±15.13	132.54±35.90	240.72±43.86	196.51±69.61
575	58.31±8.07	122.56±29.29	228.68±43.27	143.34±60.40	67.92±25.90	120.24±38.98	246.89±70.40	154.67±78.95
588	59.81±8.64	136.67±27.18	219.32±32.55	166.82±50.33	88.56±28.70	131.79±35.23	212.74±48.11	153.33±55.21
591	58.39±9.53	126.44±29.71	222.62±33.26	153.75±56.94	68.97±18.19	133.84±44.21	233.82±41.77	161.75±67.97
540	60.18±7.65	120.58±30.50	226.76±38.71	141.35±58.21	68.24±21.77	123.23±34.87	245.74±54.35	155.83±73.33
544	63.06±5.49	130.55±29.28	229.99±41.09	163.44±58.87	69.80±10.45	119.33±30.75	238.55±45.97	140.12±58.23
552	61.70±5.71	124.38±29.61	224.30±35.86	145.47±54.23	85.25±27.48	127.85±32.66	228.85±56.39	150.69±59.01
567	58.11±7.92	129.12±29.74	227.28±40.60	152.46±59.97	52.12±12.80	137.99±31.98	231.05±48.13	187.09±64.75
584	56.96±8.83	139.97±26.62	240.41±50.25	188.50±65.19	199.67±12.22	167.90±36.24	246.32±66.97	213.25±66.82
596	62.56±6.53	127.31±29.09	217.29±30.57	147.33±49.52	134.29±48.56	131.86±33.78	197.22±41.67	141.35±42.74

and Latent-Variable-based Model). Without the help of such tricks (or other tricks that we do not find), We do not think it is reasonable that a simple RNN-based method can exceed many advanced LSTM-based models, i.e., Multi-Scale LSTM and LSTM + Attention.

Another observation is that neural networks (N-BEATS, RNN, GAM, GAN (GRU; CNN), Multi-Scale LSTM and LSTM+Attention) are better than other methods, where most of these top methods are based on neural networks. In terms of attributes, there are 3 methods (RNN, LSTM + Attention and residual compensation network) that only use “glucose\_level” as the input. Apart from the non-neural methods (residual compensation network) and the methods using special tricks (RNN), LSTM + Attention ranks the last one in these neural network-based methods. It means considering other attributes will bring extra benefits during the prediction, which is the same as our results in section 3.1.2. In terms of the neural-based methods which leverage multiple attributes, we can find that “bolus” and “meal” are very popular, which is in accord with our findings in section 3.1.2, as ‘bolus’, “meal” and “finger\_stick” can bring more benefits compared with other attributes excluding “glucoses.level”.

Note that among all these methods, we are the only ones who successfully leverage “sleep” and “exercise” as a part of the input, contributing to some improvements. We are also the only one that proposed an explainable model, which can explain the feature importance by graph attentions. An example of the explanation will be discussed in section 4.3.

## 4.2. DISCUSSION OF SELECTED ATTRIBUTES CHAPTER 4. DISCUSSION

**Table 4.3:** Distributions of “meal” and “bolus” in hyperglycemia, normal, hypoglycemia and all samples.

PID	meal (hypo)	meal (normal)	meal (hyper)	meal (all)	bolus (hypo)	bolus (normal)	bolus (hyper)	bolus (all)
559	25.17±12.50	35.19±14.90	37.46±17.99	35.55±15.95	4.70±1.13	3.44±1.62	4.25±1.71	3.92±1.71
563	36.50±12.48	29.21±15.83	31.47±18.28	29.95±16.33	10.90±3.25	6.94±4.22	9.16±3.73	8.00±4.14
570	76.43±38.05	109.75±40.05	104.70±43.63	105.70±42.15	2.96±1.21	8.17±3.78	7.50±3.58	7.62±3.74
575	31.94±18.88	41.42±23.75	48.54±24.55	40.56±23.43	3.15±1.61	4.60±2.30	5.68±3.10	4.78±2.55
588	25.00±14.72	35.69±35.74	25.71±14.63	32.73±31.37	4.95±0.07	5.00±2.35	3.30±1.94	4.31±2.33
591	26.84±12.78	30.83±13.04	37.05±17.44	31.43±14.20	3.32±1.15	3.06±1.53	3.39±2.10	3.20±1.76
540	58.11±36.10	55.13±28.49	54.00±32.66	55.32±29.37	4.25±2.04	4.14±2.51	3.58±2.39	3.99±2.48
544	52.20±33.77	75.98±38.36	66.33±31.67	73.32±37.18	14.13±4.04	12.99±4.95	9.45±5.45	12.49±5.16
552	39.86±23.18	58.76±33.35	36.60±28.51	53.23±32.88	5.30±0.00	4.31±3.88	3.22±2.18	3.84±3.29
567	None	75.76±22.75	70.60±21.52	74.77±22.19	5.90±0.00	11.14±4.87	12.98±5.89	12.23±5.57
584	20.00±0.00	56.00±10.80	53.75±13.62	54.76±12.42	None	7.39±2.60	7.53±2.95	7.48±2.81
596	30.50±11.84	25.40±13.39	21.70±15.24	25.28±13.60	3.54±1.00	3.02±1.49	3.03±1.35	3.03±1.44

**Table 4.4:** Distributions of “sleep” and “exercise” in hyperglycemia, normal, hypoglycemia and all samples.

PID	sleep (hypo)	sleep (normal)	sleep (hyper)	sleep (all)	exercise (hypo)	exercise (normal)	exercise (hyper)	exercise (all)
559	1.91±0.49	2.26±0.54	2.32±0.61	2.25±0.56	5.00±0.00	5.18±1.06	5.16±0.93	5.17±0.99
563	2.05±0.22	2.57±0.50	2.74±0.44	2.60±0.49	4.22±1.00	4.51±1.28	4.72±0.59	4.52±1.23
570	2.09±0.29	2.18±0.62	2.10±0.43	2.13±0.51	4.89±0.31	5.20±0.61	4.79±0.87	5.02±0.74
575	1.87±0.50	2.74±0.48	2.75±0.54	2.71±0.53	7.00±0.00	5.45±1.02	None	5.53±1.05
588	2.15±0.36	2.78±0.41	2.80±0.40	2.78±0.41	5.00±0.00	5.30±0.48	5.14±0.44	5.22±0.46
591	2.35±0.48	2.71±0.47	2.74±0.53	2.71±0.49	5.67±0.98	4.90±1.42	5.00±1.83	4.96±1.48
540	None	None	None	None	None	None	None	None
544	1.74±0.44	1.94±0.47	1.96±0.37	1.94±0.45	None	6.68±0.48	7.00±0.00	6.83±0.38
552	3.00±0.00	2.64±0.64	2.58±0.74	2.64±0.65	None	7.53±1.02	None	7.53±1.02
567	2.00±0.00	1.90±0.86	2.40±0.73	2.01±0.77	None	None	None	None
584	3.00±0.00	2.99±0.10	2.96±0.20	2.97±0.17	None	10.00±0.00	10.00±0.00	10.00±0.00
596	2.14±0.90	2.80±0.46	2.95±0.33	2.82±0.46	5.37±0.59	5.02±1.12	5.05±1.06	5.04±1.08

## 4.2 Discussion of selected attributes

Based on the results of section 3.1.2, we can find that “meal”, “bolus”, “finger\_stick”, “sleep” and “exercise”, apart from “glucose\_level”, are useful during the predictions of future BG levels. Then, we want to further explore whether we can directly observe some patterns from the statistics of these attributes.

According to Table 4.2-4.4, we can observe the distributions of these attributes in terms of hypoglycemia (hypo), normal glucose levels (normal), hyperglycemia (hyper) and all samples (all). Each attribute is aggregated through mean and standard deviation and grouped by these four statuses of “glucose\_level”.

Then, we can find that the variations of “finger\_stick” have similar trends to “glucose\_level” (see Table 4.2). In most cases, when the “glucose\_level” belongs to hypo/normal/hyper, the values of “finger\_stick” are also in the same status. For example, in terms of participant 570, the mean values of “glucose\_level” are 63.00/133.52/237.76 mg/dL respectively in hypo/normal/hyper,

#### 4.2. DISCUSSION OF SELECTED ATTRIBUTES CHAPTER 4. DISCUSSION

while the mean values of “finger\_stick” are 63.38/132.54/240.72, which is in accord with hypo/normal/hyper. However, not all variation trends of “finger\_stick” are consistent with the variation trends of “glucose\_level”. For example, in terms of participant 559, when the mean value, i.e., 59.90 mg/dL, of “glucose\_level” belongs to hypoglycemia, the mean value of “finger\_stick” is 108.36 mg/dL which is normal rather than hypoglycemia. In this case, given that “finger\_stick” can be seen as the actual BG levels, the samples of “finger\_stick” can be used to calibrate the “glucose\_level” collected by CGM, since there might be some delays, estimations and mistakes of CGM, contributing to the inconsistencies with the actual BG levels. Therefore, because of these inconsistencies between “glucose\_level” and “finger\_stick”, it can prove why “finger\_stick” is helpful during the estimations of the future BG levels.

Furthermore, in Table 4.3, we can find that there are 9 participants whose carbohydrate intake, “meal”, is lower during hypoglycemia compared with the mean value of carbohydrate intake of all samples. In other words, “meal (hypo)” is lower than “meal (all)”. This is reasonable since lower carbohydrate intake tends to contribute to lower BG levels. However, other 3 participants tend to eat more food during hypoglycemia in order to increase their BG levels. During hyperglycemia, there are 6 participants who choose to have more or similar to the mean carbohydrate intake of all samples, where the mean values of “meal (hyper)” are larger than or close to “meal (all)”. Other 6 participants try to eat less food during the hyperglycemia so as to reduce their BG levels. Hence, from these observations, we can find that only a relatively small part of participants control their BG levels via actively controlling the carbohydrate intake. This is because the correct action during hypoglycemia/hyperglycemia is to have more/less carbohydrate intake, but actually, only a relatively small part of participants follow this rule.

Comparably, in terms of “bolus”, there are 8 participants whose mean values of “bolus (hypo)” are less than “bolus (all)”. Interestingly, during hyperglycemia, there are 7 participants whose mean values of “bolus (hyper)” are larger than or close to “bolus (all)”. This is because, having less insulin delivery during hypoglycemia can



mildly reduce the BG levels, and delivering more bolus during hyperglycemia can badly decrease the BG levels. Therefore, during hypoglycemia, the correct action is to have lower or no insulin delivery, while participants should have higher insulin delivery during hyperglycemia. Hence, compared with carbohydrate intake, more participants follow the correct rules and well leverage insulin delivery to control their BG levels.

In terms of “sleep” in Table 4.4, it is interesting to find that 9 participants have hypoglycemia when they have poor sleep quality, where “sleep (hypo)” is less than “sleep (all)”. Meanwhile, 10 participants have hyperglycemia when they have good sleep quality, where “sleep (all)” is larger than or close to “sleep (hyper)”. In terms of “exercise”, more people tend to exercise when their BG levels are normal (exercise (normal) is not None). This is also reasonable as people always feel uncomfortable when they have hypoglycemia or hyperglycemia.

In summary, we can find some interesting patterns from the statistics of these attributes in terms of hypoglycemia/normal BG levels/hyperglycemia. Based on these observations, to some degree, we can understand why these attributes are helpful for the BGLP-RMTS problem.

### 4.3 Visualization

We use two examples to visualize the GAM, as Figures 4.1-4.2, where the examples are selected from the testing samples of participant 570 in OhioT1DM’18, given  $W = 6$  and  $T = 12$ . For each node, the summation of the weights of the edges coming into the node is 1, and the weights are attention weights calculated by Equation (2.3a), and the receiving messages are aggregated by these attention weights according to Equation (2.3b).

In Figure 4.1, when  $t \in \{1, \dots, 4\}$ , we can observe that only the node of “glucose\_level” and the node of “exercise” are activated. Hence, only these two nodes send neural messages to each other, generating aggregated messages from these two nodes, respectively. During the aggregation of neural messages, the neural messages from “glucose\_level” account for around 80%, while the neural messages

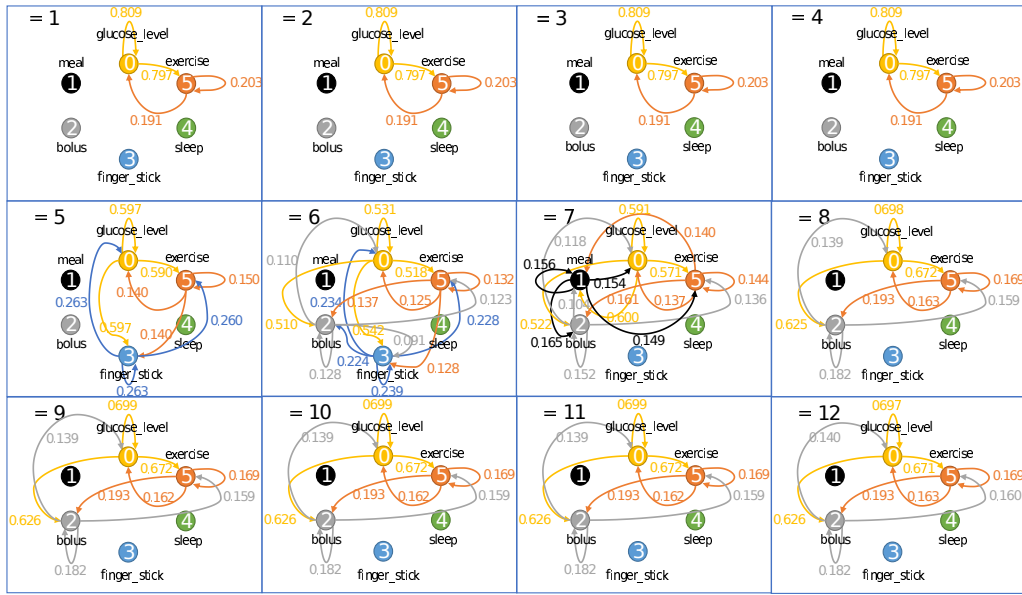


Figure 4.1: Example 1: visualization of graph attentions of participant 570.

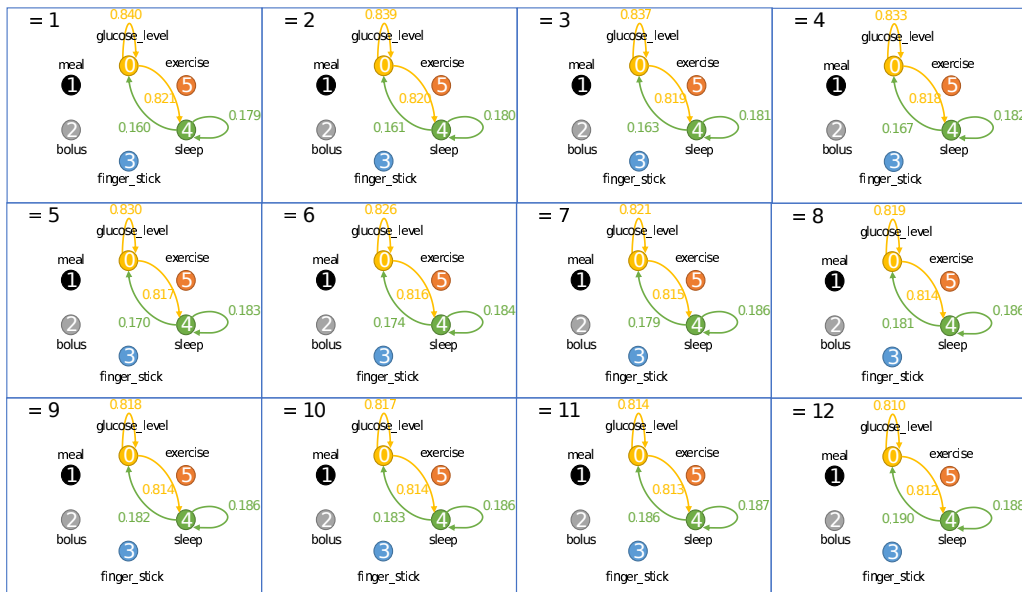


Figure 4.2: Example 2: visualization of graph attentions of participant 570.

from “exercise” account for nearly 20%. According to the proportions of neural messages from different nodes during aggregation, we can get the ranking of attribute importance as “glucose\_level” > “exercise”.

When  $t = 5$ , the node of “finger\_stick” is activated. Then, there are 3 nodes sending neural messages to each other. When aggregating neural messages, the neural messages from “glucose\_level” account for around 60% which is decreased

from nearly 80%, while the neural messages from “exercise” account for nearly 14% which is reduced from around 20%. The neural messages from the node of “finger\_stick” account for about 26%. The attribute importance changes when more nodes are activated. In this case, the ranking of attribute importance is “glucose\_level” > “finger\_stick” > “exercise”. Similarly, when  $t = 6$ , the node of “bolus” is activated, and the attention weights of all nodes change accordingly. The ranking of attribute importance is “glucose\_level” > “finger\_stick” > “exercise” > “bolus”. Then, the node of “finger\_stick” is deactivated, but the node of “meal” is activated, when  $t = 7$ . The ranking of attribute importance is “glucose\_level” > “meal” > “exercise” > “bolus”. Finally, when  $t \in \{8, \dots, 12\}$ , the ranking of attribute importance is stabilized as “glucose\_level” > “exercise” > “bolus”.

In Figure 4.2, when  $t \in \{1, \dots, 12\}$ , there are only two active nodes, i.e., “glucose\_level” and “sleep”, and the ranking of attribute importance is stabilized as “glucose\_level” > “sleep”. However, the values of attention weights change with  $t$ . In terms of “glucose\_level” (see the yellow lines), the attention weight decreases when  $t$  increases. On the contrary, in terms of “sleep” (see the green lines), the attention weight increases when  $t$  increases.

In summary, only activated nodes generate, send, receive and aggregate neural messages. When new nodes are activated, or active nodes are deactivated, the attention weights of all active nodes also change accordingly. In some cases, even though the ranking of attribute importance is stable when increasing  $t$ , the attention weights might still change. Based on these findings, our proposed model is efficient and flexible since not all nodes are active at a time, and the structure of the graph is dynamically changing. Notably, the attention weights give a powerful explanation of our model.

Then, we visualize the testing sample of all participants, as shown in Figures 4.3-4.6. The green curves are the ground truth, and the blue/red curves are the estimated BG levels by “GAM”/“GAM+FL” via sliding windows ( $W = 6$  or  $W = 12$ ). When  $W = 6$  (see Figures 4.3-4.4), there is no noticeable difference among “GAM”, “GAM+FL” and “Ground truth”. When  $W = 12$  (see Figures 4.5-4.6), there is also

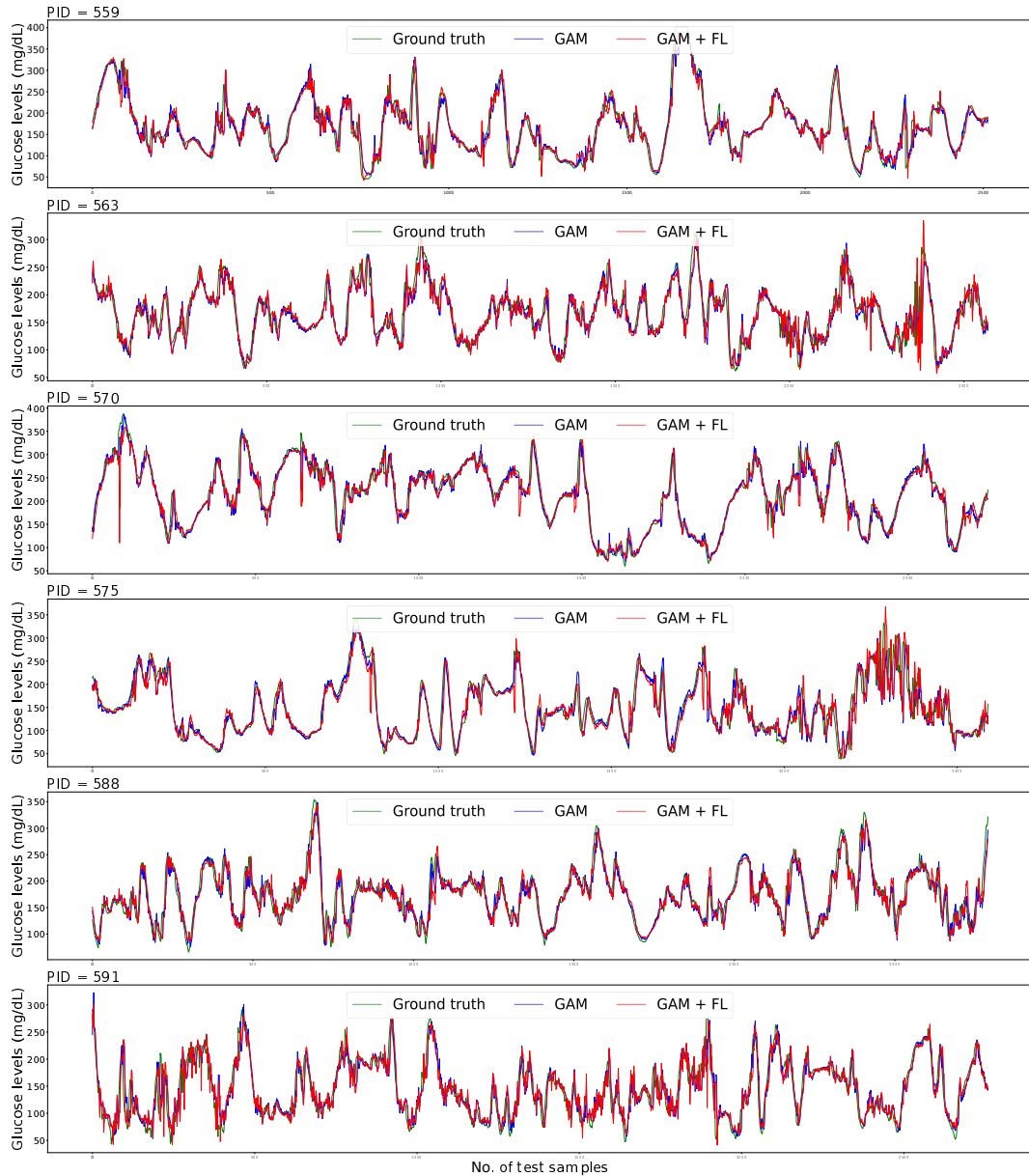


**Figure 4.3:** Example 1: visualization of predictions of GAM ( $W = 6$ ).

no visible difference between “GAM” and “GAM+FL”, but there is a massive gap between “GAM”/“GAM+FL” and “Ground Truth”. Hence, even though there are distinct differences in Tables 3.13-3.18 when comparing “GAM” with “GAM+FL”, the visual differences are minor. The huge gap between “GAM”/“GAM+FL” and “Ground Truth” shows that the task gets much more challenging when  $W = 12$ .

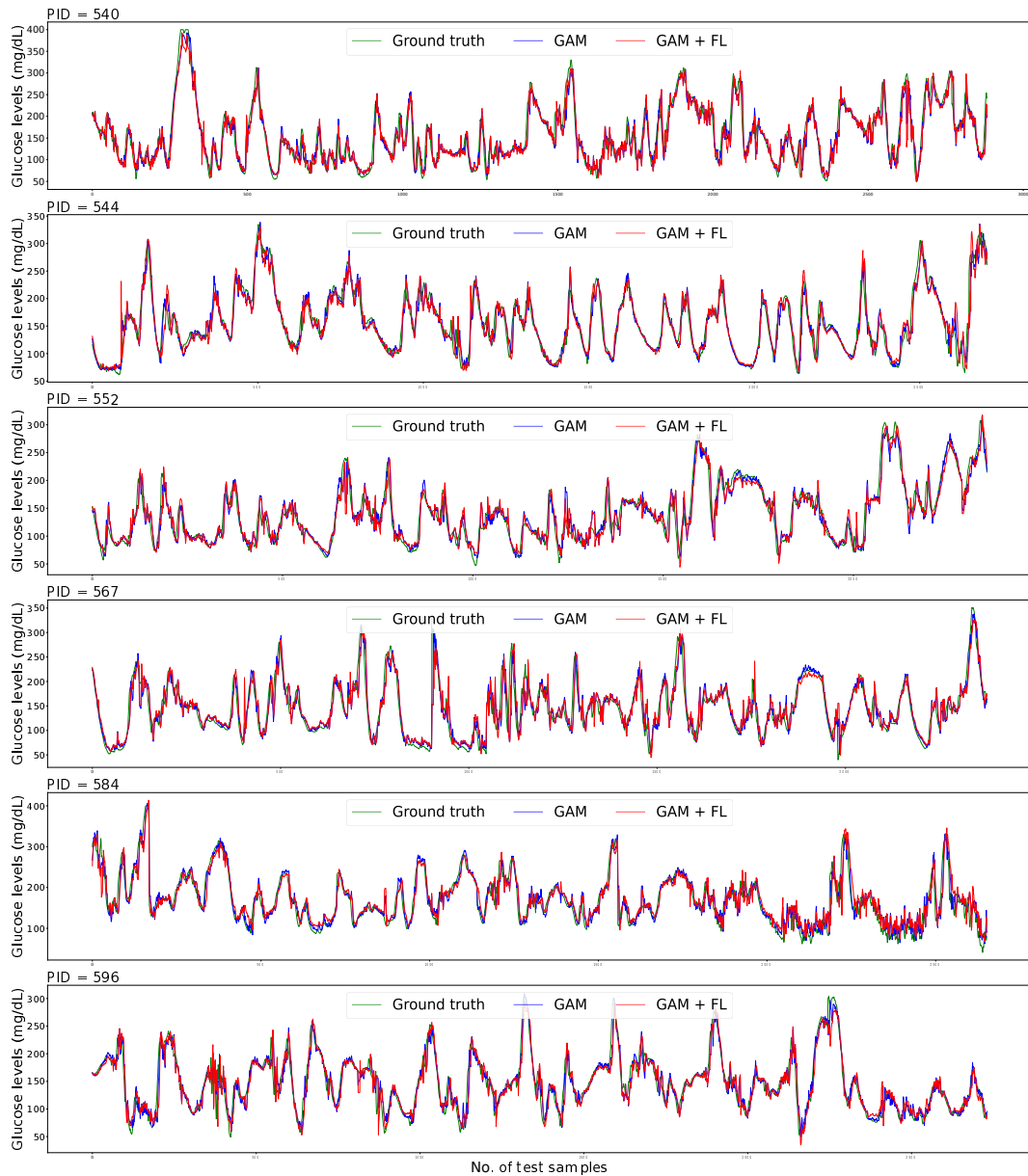


**Figure 4.4:** Example 2: visualization of predictions of GAM ( $W = 6$ ).

## 4.4 Convergence and Training Time

We compare the convergence and training time between “GAM” and “GAM + FL”, where  $W = 6$ ,  $H = 256$ ,  $M = 1$ ,  $L = 1$  and  $T = 12$ . In Figure 4.7, in terms of the RMSE in the validation dataset, we can find that “GAM” converges immediately and maintains a better range compared with “GAM + FL”. When comparing the training time, “GAM + FL (in serial)” is slightly slower than “GAM” (see Figure 4.8). The clients of “GAM + FL (in serial)” run one by one, meaning that only when

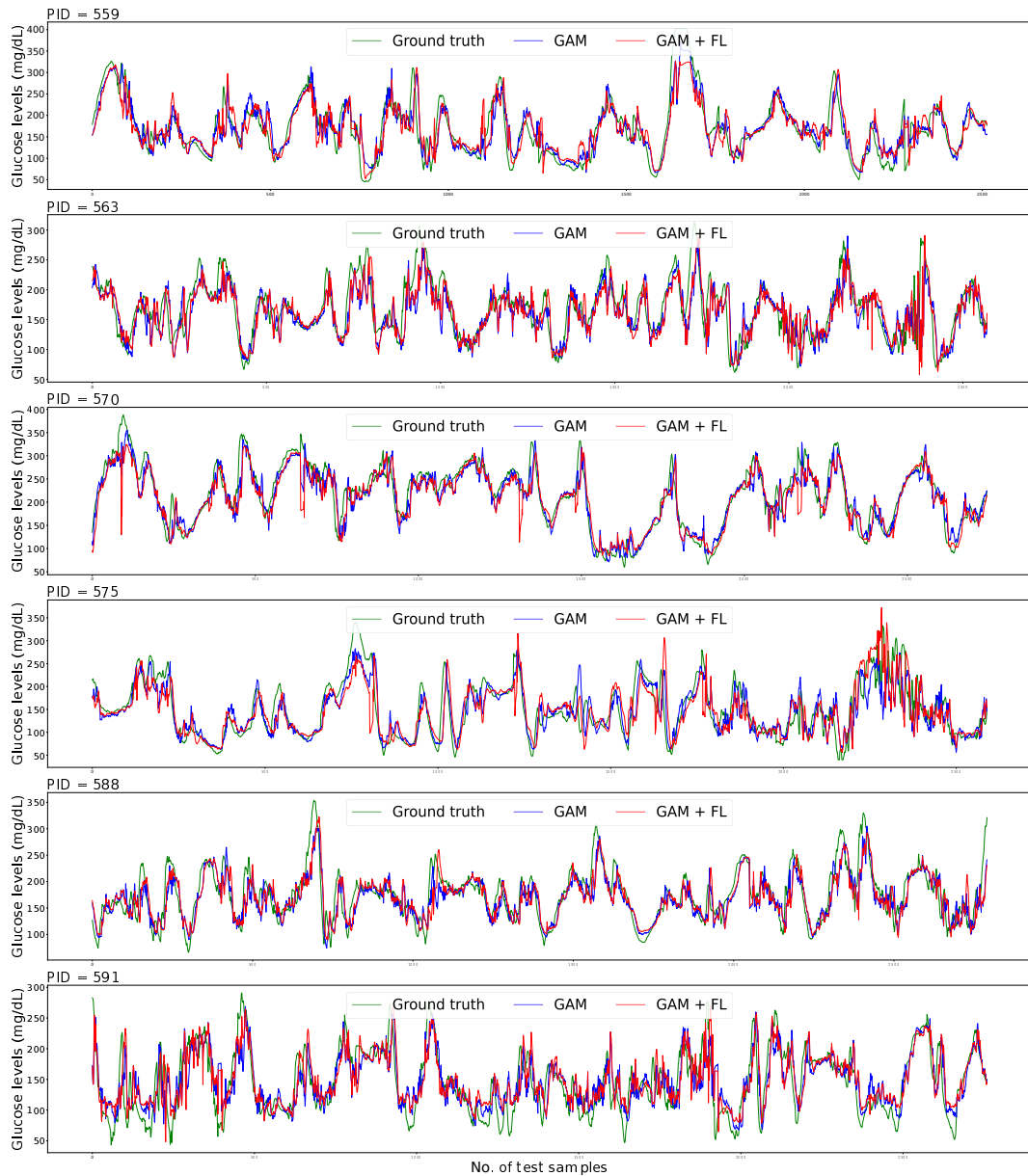


**Figure 4.5:** Example 1: visualization of predictions of GAM ( $W = 12$ ).

a client finishes training does another client start to train. “GAM + FL (in serial)” spends more time collecting, averaging, and sending hyperparameters in the server. In practice, clients run in parallel, and the fastest training time in theoretical is the green line in Figure 4.8, i.e., “GAM + FL (in parallel)”, where all clients start to train at a specific time and finish training together. Hence, even though the performance of “GAM + FL” is worse than “GAM” (see section 3.3.2), the training speed of “GAM + FL” might super fast.

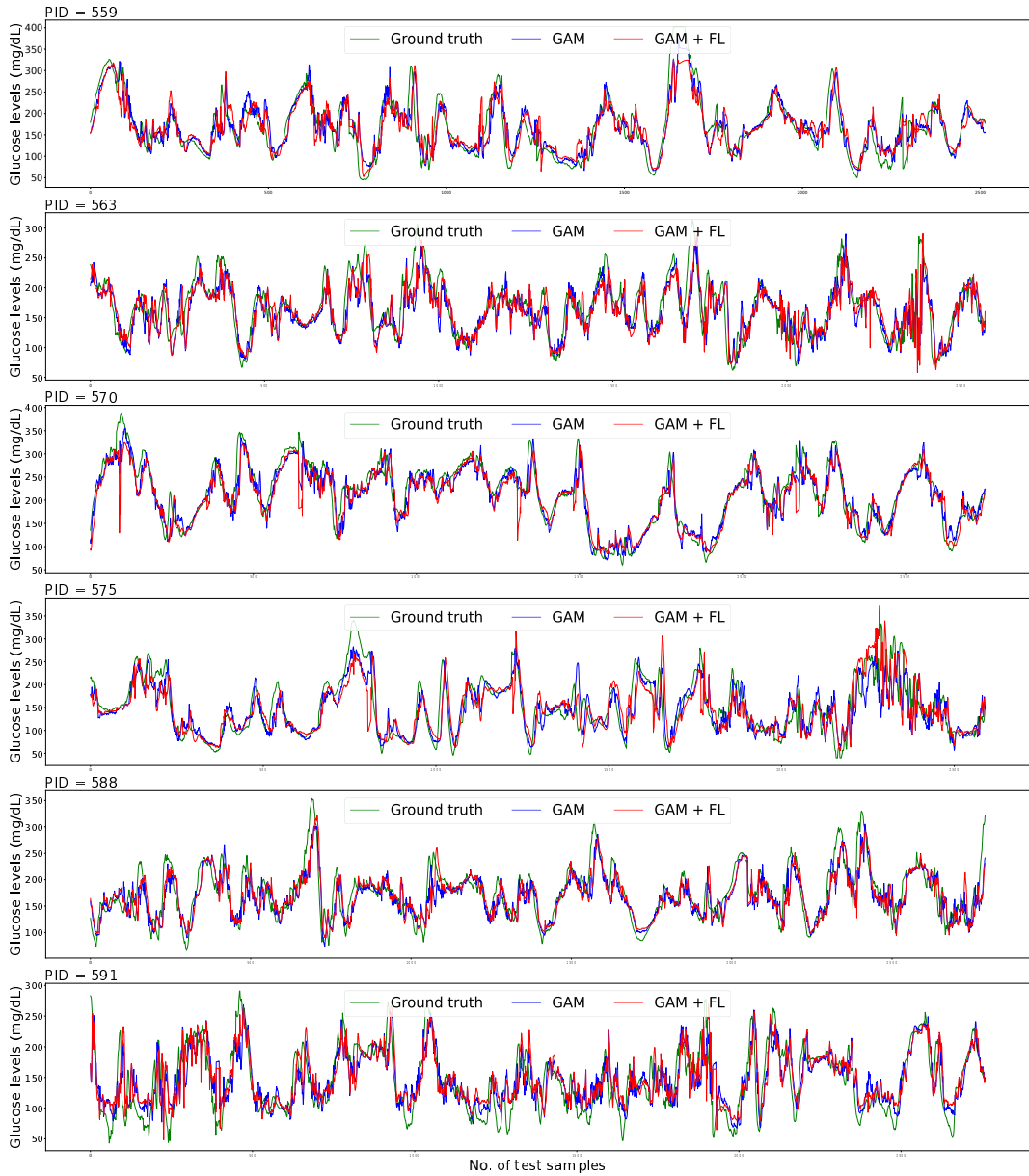


**Figure 4.6:** Example 2: visualization of predictions of GAM ( $W = 12$ ).

## 4.5 Conclusion and Future Work

In this paper, We have comprehensive data analysis, experiments and result analysis to show the selected 6 attributes are reliable and are positively affecting the prediction of the future BG levels. We propose a novel graph attentive memory, called “GAM”. It is explainable, efficient and flexible, given that the attention weights of the graph can be utilized as attribute importance, and the attention weights and the graph structure can dynamically change according to the activated nodes. We



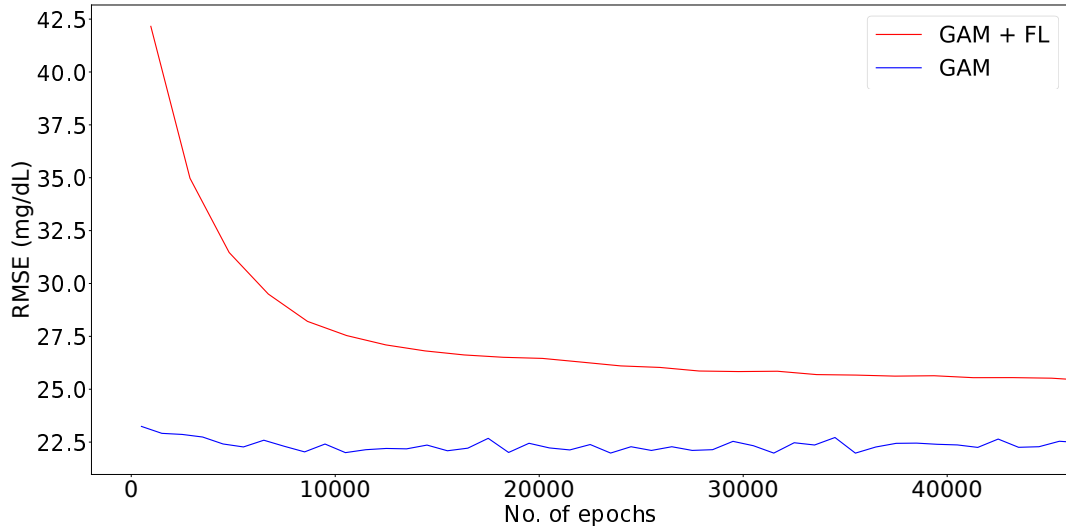


**Figure 4.7:** Training convergence of “GAM” and “GAM + FL”.

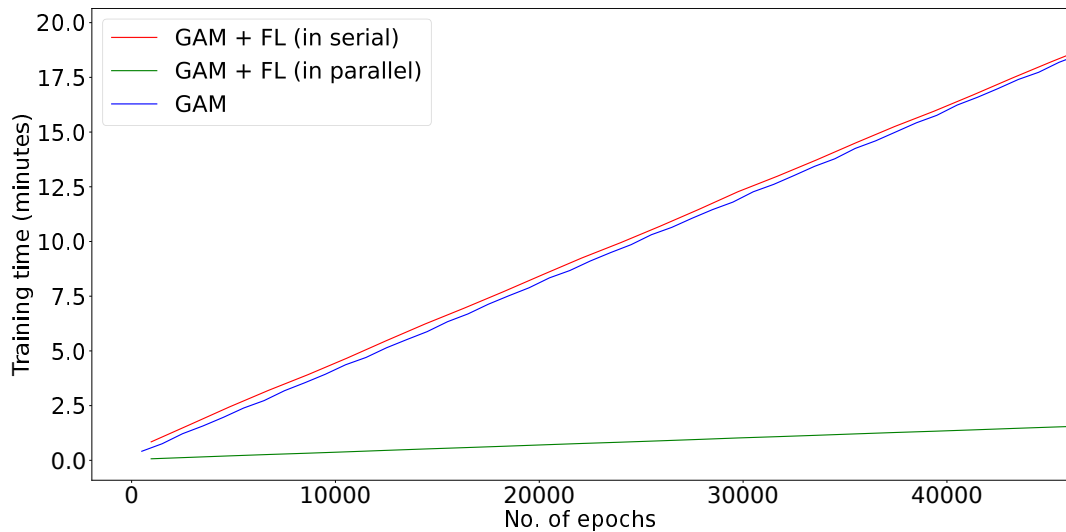


**Figure 4.8:** Training time of “GAM” and “GAM + FL”.

also have related experiments to show the stability and excellence of our GAM. In the discussion, we compare “GAM” with other methods, finding the GAM is quite competitive. We also introduce FL to “GAM”, where FL enables leveraging population patterns without an invasion of the participants’ privacy. Relevant experiments show that the FL algorithm sacrifices some prediction accuracy.

The limitations of this work are: 1) only considering two datasets OhioT1DM’18 and OhioT1DM’20; 2) the GAM is not fully explainable, especially from the temporal perspective; 3) when compared with others, the results of other methods are directly introduced from the published papers, and it exists many



unfair comparisons; 4) the two-step training is not elegant; 5) more advanced FL algorithms should be considered, as there are still obvious gaps between “GAM” and “GAM+FL”.

Based on the limitations, in future work, we will consider larger datasets. Then, we will also find more baselines from the latest top conferences, and run all the baselines by ourselves instead of introducing the results from the published papers. In this case, all methods use the same data which is processed in the same manner, and the comparisons will be fairer because the performance differences are not caused by the differences in the data.

Meanwhile, in terms of the proposed model, we want to add new modules to make it explainable from a temporal view. Furthermore, given that BGLP needs relatively long historical data (see section 3.2.2), we may also take a more sophisticated memory mechanism into account in order to memorize long-term information.

On the other hand, in order to make our model more applicable, more sophisticated and advanced FL algorithms will be introduced or proposed, in order to make the training process asynchronous, personalized and more elegant, only containing one-step training rather than two-step training. We will also try to deploy the FL in real mobile devices instead of only doing simulations. In this case, the computation resources in mobile devices will be utilized, and asynchronous FL is indispensable. This is because maybe sometimes users do not want their mobile devices to attend the training. With the help of asynchronous FL, users can join the training flexibly. Besides, there are no cold starting problems when using FL. If a new user wants to join the FL training, the system can build a personal model immediately, and the model is internalized with the latest learnable parameters of the population model. When the new user generates enough personal data after using CGM, the personalized model will be fine-tuned by the personal data. If the FL is not only asynchronous but also personalized, there will be no fine-tuning process. This is because, in personalized FL, there may be regularization items in the loss, making the personal model decoupled with the population model. Then, the personalized model can keep the specialty, and the population model can remain general.

After achieving all the proposed points, our future model is not only explainable but also can be directly trained and leveraged in mobile devices. The privacy of the participants is well protected. The participants can use their mobile devices to train personalized and explainable models which concurrently leverage population patterns by FL. Then, more participants can attend the training process flexibly and asynchronously. Accordingly, when more participants join the training, the personalized model will be more accurate, attracting more potential participants. The life quality of people with T1D will get better and better.

# Bibliography

Kerstin Bach, Razvan C. Bunescu, Cindy Marling, and Nirmalie Wiratunga, editors. *KDH@ECAI'20*, volume 2675, 2020.

Robert Bevan and Frans Coenen. Experiments in non-personalized future blood glucose level prediction. In *KDH@ECAI'20*, volume 2675, pages 100–104, 2020.

Ananth Reddy Bhimireddy, Priyanshu Sinha, Bolu Oluwalade, Judy Wawira Gichoya, and Saptarshi Purkayastha. Blood glucose level prediction as time-series modeling using sequence-to-sequence neural networks. In *KDH@ECAI'20*, volume 2675, pages 125–130, 2020.

Shaked Brody, Uri Alon, and Eran Yahav. How attentive are graph attention networks? In *ICLR'22*, 2022.

Wenchao Chen, Long Tian, Bo Chen, Liang Dai, Zhibin Duan, and Mingyuan Zhou. Deep variational graph convolutional recurrent network for multivariate time series anomaly detection. In *ICML'22*, volume 162, pages 3621–3633, 2022.

Kyunghyun Cho, Bart van Merriënboer, Çağlar Gülçehre, Dzmitry Bahdanau, Fethi Bougares, Holger Schwenk, and Yoshua Bengio. Learning phrase representations using RNN encoder-decoder for statistical machine translation. In *EMNLP'14*, pages 1724–1734, 2014.

Ran Cui, Chirath Hettiarachchi, Christopher J Nolan, Elena Daskalaki, and Hanna Suominen. Personalised short-term glucose prediction via recurrent self-attention network. In *2021 IEEE 34th International Symposium on Computer-Based Med-*

- ical Systems (CBMS)*, pages 154–159, 2021. doi: 10.1109/CBMS52027.2021.00064.
- John Daniels, Pau Herrero, and Pantelis Georgiou. Personalised glucose prediction via deep multitask networks. In *KDH@ECAI'20*, volume 2675, pages 110–114, 2020.
- John Daniels, Pau Herrero, and Pantelis Georgiou. A multitask learning approach to personalized blood glucose prediction. *IEEE Journal of Biomedical and Health Informatics*, 26(1):436–445, 2022. doi: 10.1109/JBHI.2021.3100558.
- Federico D’Antoni, Lorenzo Petrosino, Fabiola Sgarro, Antonio Pagano, Luca Vollero, Vincenzo Piemonte, and Mario Merone. Prediction of glucose concentration in children with type 1 diabetes using neural networks: An edge computing application. *Bioengineering*, 9(5):183, 2022.
- Ian J. Goodfellow, Jean Pouget-Abadie, Mehdi Mirza, Bing Xu, David Warde-Farley, Sherjil Ozair, Aaron C. Courville, and Yoshua Bengio. Generative adversarial nets. In *NIPS'14*, pages 2672–2680, 2014.
- Hadia Hameed and Samantha Kleinberg. Investigating potentials and pitfalls of knowledge distillation across datasets for blood glucose forecasting. In *KDH@ECAI'20*, volume 2675, pages 85–89, 2020.
- Sepp Hochreiter and Jürgen Schmidhuber. Long short-term memory. *Neural Comput.*, 9(8):1735–1780, 1997.
- Min Hou, Chang Xu, Zhi Li, Yang Liu, Weiqing Liu, Enhong Chen, and Jiang Bian. Multi-granularity residual learning with confidence estimation for time series prediction. In *ACM WWW'22*, pages 112–121, 2022.
- Francesca Iacono, Lalo Magni, and Chiara Toffanin. Personalized LSTM models for glucose prediction in type 1 diabetes subjects. In *MED'22*, pages 324–329. IEEE, 2022. doi: 10.1109/MED54222.2022.9837153. URL <https://doi.org/10.1109/MED54222.2022.9837153>.

- Jingyan Jiang and Liang Hu. Decentralised federated learning with adaptive partial gradient aggregation. *CAAI Transactions on Intelligence Technology*, 5(3):230–236, 2020.
- David Joedicke, Gabriel Kronberger, José Manuel Colmenar, Stephan M. Winkler, José Manuel Velasco, Sergio Contador, and José Ignacio Hidalgo. Analysis of the performance of genetic programming on the blood glucose level prediction challenge 2020. In *KDH@ECAI'20*, volume 2675, pages 141–145, 2020.
- Diederik P. Kingma and Jimmy Ba. Adam: A method for stochastic optimization. In *ICLR'15*, 2015.
- Thomas N. Kipf and Max Welling. Semi-supervised classification with graph convolutional networks. In *ICLR'17*. OpenReview.net, 2017.
- Kezhi Li, John Daniels, Chengyuan Liu, Pau Herrero, and Pantelis Georgiou. Convolutional recurrent neural networks for glucose prediction. *IEEE J. Biomed. Health Informatics*, 24(2):603–613, 2020.
- Chi Harold Liu, Yu Wang, Chengzhe Piao, Zipeng Dai, Ye Yuan, Guoren Wang, and Dapeng Wu. Time-aware location prediction by convolutional area-of-interest modeling and memory-augmented attentive LSTM. *IEEE Trans. Knowl. Data Eng.*, 34(5):2472–2484, 2022.
- Ning Ma, Yuhang Zhao, Shuang Wen, Tao Yang, Ruikun Wu, Rui Tao, Xia Yu, and Hongru Li. Online blood glucose prediction using autoregressive moving average model with residual compensation network. In *KDH@ECAI'20*, volume 2675, pages 151–155, 2020.
- Othmane Marfoq, Giovanni Neglia, Richard Vidal, and Laetitia Kamani. Personalized federated learning through local memorization. In *ICML'22*, volume 162, pages 15070–15092, 2022.
- Cindy Marling and Razvan C. Bunescu. The ohiot1dm dataset for blood glucose level prediction. In *IJCAI-ECAI'18*, volume 2148, pages 60–63, 2018.

- Cindy Marling and Razvan C. Bunescu. The ohiot1dm dataset for blood glucose level prediction: Update 2020. In *KDH@ECAI'20*, volume 2675, pages 71–74, 2020.
- Brendan McMahan, Eider Moore, Daniel Ramage, Seth Hampson, and Blaise Agüera y Arcas. Communication-efficient learning of deep networks from decentralized data. In *AISTATS'17*, volume 54, pages 1273–1282, 2017.
- Christopher Morris, Martin Ritzert, Matthias Fey, William L. Hamilton, Jan Eric Lenssen, Gaurav Rattan, and Martin Grohe. Weisfeiler and leman go neural: Higher-order graph neural networks. In *AAAI'19*, pages 4602–4609, 2019.
- Hoda Nemat, Heydar Khadem, Mohammad R. Eissa, Jackie Elliott, and Mohammed Benaissa. Blood glucose level prediction: Advanced deep-ensemble learning approach. *IEEE Journal of Biomedical and Health Informatics*, 26(6): 2758–2769, 2022. doi: 10.1109/JBHI.2022.3144870.
- Boris N. Oreshkin, Dmitri Carпов, Nicolas Chapados, and Yoshua Bengio. N-BEATS: neural basis expansion analysis for interpretable time series forecasting. In *ICLR'20*, 2020.
- Md Fazle Rabby, Yazhou Tu, Md Imran Hossen, Insup Lee, Anthony S. Maida, and Xiali Hei. Stacked LSTM based deep recurrent neural network with kalman smoothing for blood glucose prediction. *BMC Medical Informatics Decis. Mak.*, 21(1):101, 2021. doi: 10.1186/s12911-021-01462-5. URL <https://doi.org/10.1186/s12911-021-01462-5>.
- Harry Rubin-Falcone, Ian Fox, and Jenna Wiens. Deep residual time-series forecasting: Application to blood glucose prediction. In *KDH@ECAI'20*, volume 2675, pages 105–109, 2020.
- Mona Schirmer, Mazin Eltayeb, Stefan Lessmann, and Maja Rudolph. Modeling irregular time series with continuous recurrent units. In *ICML'22*, volume 162, pages 19388–19405, 2022.

- M. Schuster and K.K. Paliwal. Bidirectional recurrent neural networks. *IEEE Transactions on Signal Processing*, 45(11):2673–2681, 1997. doi: 10.1109/78.650093.
- Aviv Shamsian, Aviv Navon, Ethan Fetaya, and Gal Chechik. Personalized federated learning using hypernetworks. In *ICML’21*, volume 139, pages 9489–9502, 2021.
- Wei Shao, Zhiling Jin, Shuo Wang, Yufan Kang, Xiao Xiao, Hamid Menouar, Zhaofeng Zhang, Junshan Zhang, and Flora D. Salim. Long-term spatio-temporal forecasting via dynamic multiple-graph attention. In *IJCAI’22*, pages 2225–2232, 2022.
- Xiaoyu Sun, Mudassir M. Rashid, Mert Sevil, Nicole Hobbs, Rachel Brandt, Mohammad-Reza Askari, Andrew Shahidehpour, and Ali Cinar. Prediction of blood glucose levels for people with type 1 diabetes using latent-variable-based model. In *KDH@ECAI’20*, volume 2675, pages 115–119, 2020.
- Ilya Sutskever, Oriol Vinyals, and Quoc V. Le. Sequence to sequence learning with neural networks. In *NIPS’14*, pages 3104–3112, 2014.
- Canh T Dinh, Nguyen Tran, and Josh Nguyen. Personalized federated learning with moreau envelopes. *Advances in Neural Information Processing Systems*, 33:21394–21405, 2020.
- Ashish Vaswani, Noam Shazeer, Niki Parmar, Jakob Uszkoreit, Llion Jones, Aidan N. Gomez, Lukasz Kaiser, and Illia Polosukhin. Attention is all you need. In *NIPS’17*, pages 5998–6008, 2017.
- Petar Velickovic, Guillem Cucurull, Arantxa Casanova, Adriana Romero, Pietro Liò, and Yoshua Bengio. Graph attention networks. In *ICLR’18*, 2018.
- Felix Wu, Amauri H. Souza Jr., Tianyi Zhang, Christopher Fifty, Tao Yu, and Kilian Q. Weinberger. Simplifying graph convolutional networks. In *ICML’19*, volume 97, pages 6861–6871, 2019.

- Haibo Yang, Xin Zhang, Prashant Khanduri, and Jia Liu. Anarchic federated learning. In *ICML'22*, volume 162, pages 25331–25363, 2022a.
- Tao Yang, Ruikun Wu, Rui Tao, Shuang Wen, Ning Ma, Yuhang Zhao, Xia Yu, and Hongru Li. Multi-scale long short-term memory network with multi-lag structure for blood glucose prediction. In *KDH@ECAI'20*, volume 2675, pages 136–140, 2020.
- Tao Yang, Xia Yu, Ning Ma, Ruikun Wu, and Hongru Li. An autonomous channel deep learning framework for blood glucose prediction. *Appl. Soft Comput.*, 120: 108636, 2022b.
- Xiang Zhang, Marko Zeman, Theodoros Tsiligkaridis, and Marinka Zitnik. Graph-guided network for irregularly sampled multivariate time series. In *ICLR'22*, 2022.
- Taiyu Zhu, Kezhi Li, Jianwei Chen, Pau Herrero, and Pantelis Georgiou. Dilated recurrent neural networks for glucose forecasting in type 1 diabetes. *J. Heal. Informatics Res.*, 4(3):308–324, 2020a.
- Taiyu Zhu, Xi Yao, Kezhi Li, Pau Herrero, and Pantelis Georgiou. Blood glucose prediction for type 1 diabetes using generative adversarial networks. In *KDH@ECAI'20*, volume 2675, pages 90–94, 2020b.
- Taiyu Zhu, Lei Kuang, Kezhi Li, Junming Zeng, Pau Herrero, and Pantelis Georgiou. Blood glucose prediction in type 1 diabetes using deep learning on the edge. In *2021 IEEE International Symposium on Circuits and Systems (ISCAS)*, pages 1–5, 2021. doi: 10.1109/ISCAS51556.2021.9401083.
- Taiyu Zhu, Lei Kuang, John Daniels, Pau Herrero, Kezhi Li, and Pantelis Georgiou. Iomt-enabled real-time blood glucose prediction with deep learning and edge computing. *IEEE Internet of Things Journal*, pages 1–1, 2022a. doi: 10.1109/JIOT.2022.3143375.



Taiyu Zhu, Kezhi Li, Pau Herrero, and Pantelis Georgiou. Personalized blood glucose prediction for type 1 diabetes using evidential deep learning and meta-learning. *IEEE Transactions on Biomedical Engineering*, pages 1–12, 2022b. doi: 10.1109/TBME.2022.3187703.